ALMA MATER STUDIORUM
UNIVERSITÀ DI BOLOGNA

DOTTORATO DI RICERCA IN

MECCANICA E SCIENZE AVANZATE DELL'INGEGNERIA

Ciclo 37

Settore Concorsuale: 09/A3 - PROGETTAZIONE INDUSTRIALE, COSTRUZIONI MECCANICHE E METALLURGIA

Settore Scientifico Disciplinare: ING-IND/15 - DISEGNO E METODI DELL'INGEGNERIA INDUSTRIALE

VIRTUAL SURGICAL PLANNING AND PATIENT-SPECIFIC DESIGN DRIVEN BY EMERGING TECHNOLOGIES

Presentata da: Giulia Alessandri

Coordinatore Dottorato

Lorenzo Donati

Supervisore

Leonardo Frizziero

Co-supervisore

Alfredo Liverani

Giovanni Trisolino

Esame finale anno 2025

Abstract

In recent years, the integration of emerging technologies in surgery has facilitated the development of innovative approaches to improve preoperative planning and surgical performance. This dissertation provides a comprehensive investigation into the application of emerging engineering technologies – such as computer-aided design, 3D printing, and extended reality – to develop patient-specific models and instruments, addressing the increasing demand for precision and personalization in surgical treatment.

The methodology involved the development of a structured workflow that combines engineering and medical expertise, integrating advanced imaging technologies – including computed tomography and magnetic resonance imaging – with 3D segmentation and 3D modeling software. Furthermore, the study explored additive manufacturing technologies, including fused deposition modeling, stereolithography, and laser powder bed sintering, as well as a range of 3D printing materials. These ranged from basic polymers, such as polylactic acid and thermoplastic polyurethane, to more advanced materials like polyether-ether-ketone and titanium alloy.

The findings of this research have been successfully translated into clinical scenarios, enabling continuous refinement of both the workflow and surgical techniques to achieve increasingly patient-specific and innovative design. The results highlight the effectiveness of technology integration in surgical planning, demonstrating a significant reduction in operative time and intraoperative fluoroscopy exposure. The use of custom-made instruments has proven to be reliable and safe, offering economic and operational advantages. In addition, experimental research has led to promising developments, such as the design of lattice structures for bone grafts and implants with improved osseointegration properties.

Looking beyond the present, this research underscores the growing trend towards novel paradigms, including the establishment of in-hospital 3D laboratories for virtual surgical planning and the point-of-care fabrication of patient-specific devices. These advancements are poised to drive a transformative evolution in surgical care, fostering a new era of precision medicine and personalized treatment strategies.

To the ones who are curious, learn and adapt with grace.

Preface

This dissertation represents the culmination of a three-year doctoral program dedicated to the study, analysis, and application of advanced technologies in virtual surgical planning and patient-specific design. The main objective is to propose an innovative approach that integrates emerging engineering technologies within a hospital setting, to improve clinical processes, personalizing the treatment experience, and optimizing surgical outcomes. The work presents a methodology for developing a complex, integrated workflow that combines engineering and medical expertise to address clinical complexities and reduce the limitations of traditional methodologies.

This doctoral project was conducted at the Department of Industrial Engineering of the University of Bologna, in collaboration with the Rizzoli Orthopaedic Institute in Bologna. Furthermore, six months of foreign research was conducted at the Department of Materials Science and Engineering, in the Division of Biomedical Engineering at the University of Uppsala in Sweden. This experience has contributed significantly to the acquisition of advanced methodologies and the expansion of knowledge in the design and fabrication of implants in lattice structures. In addition, it provided a solid foundation in cellular analysis, concerning the interaction between cells and 3D-printed structures to assess cellular behavior and anticipate their response to implant osseointegration. This allowed for international comparison of methods and approaches.

The dissertation not only delineates sophisticated methodologies and technologies for preoperative surgical planning but also provides a framework for the establishment of intrahospital units that prioritize patient-centric care. It includes an in-depth study of innovative techniques and materials, the development of anatomical models, and the design of customized instruments, such as cutting guides, implants, and grafts. The entire work reflects a unique perspective derived from my background as an industrial designer, which allowed me to combine technical and practical aspects with a design- and function-oriented approach.

During this research, several clinical contexts were investigated, with a particular focus on pediatric orthopedic surgery and, to a lesser extent, the cardiovascular and maxillofacial fields. Three-dimensional model reconstruction methodologies were developed in an academic and

research context, with an emphasis on accessible and cost-effective techniques, rather than on the commercialization of a service. A range of technologies and software, open-source, concerning image segmentation, 3D modeling, design, and additive manufacturing had been followed to evaluate diverse 3D printing solutions for materials and processes.

Thanks to this Ph.D. program, I have expanded my network of international knowledge, encouraging professional and especially personal growth. Collaborations with research institutions and participation in international conferences have enriched my skills, allowing me to develop a comprehensive and integrated view of the field of surgical planning and personalized design. With the hope that the results of this work will lay the foundation for future developments in patient-specific medicine, I hope that my contributions will support a technological revolution that benefits patients and the engineering and medical community.

Contents

List of figures

List of tables

1. Introduction

The development of advanced technologies has significantly changed the landscape of modern medicine, particularly in surgical planning and personalized patient design. In this context, this dissertation aims to explore and apply these technological innovations to improve the effectiveness and precision of surgical interventions.

The healthcare industry is increasingly moving towards the use of advanced technologies to optimize clinical procedures and improve patient outcomes. Surgical planning and custom device design are key areas where engineering can provide innovative solutions. The integration of technologies such as computer-aided design (CAD) systems, 3D printing, and extended reality enables the development of accurate anatomical models and customized surgical instruments, improving preoperative preparation and the performance of surgeries.

This has led to the need to create a workflow that is increasingly integrated with existing diagnostic technologies, to speed up the production time of these devices and to manage activities directly, suggesting the development of dedicated intra-hospital units with specialized staff.

1.1. Research objectives

The objective of this dissertation is to investigate the application and integration of advanced technologies in surgical planning and custom design, to enhance the effectiveness, safety, and efficiency of surgical procedures. The research focuses on evaluating the accuracy and precision of three-dimensional reconstruction methods derived from medical images in an academic and research context. Additionally, it explores the design of patient-specific instruments, such as cutting guides, bone grafts, and implants, using industrial engineering approaches. The goal is to further personalize surgical treatments and improve clinical outcomes. The study will also examine the potential of accessible and cost-effective solutions, emphasizing the use of open-source technologies, materials, and software that can be seamlessly integrated with cutting-edge technologies such as extended reality and artificial intelligence (AI). The central aim of this research is to develop an optimized surgical planning

workflow that incorporates state-of-the-art engineering technologies, such as additive manufacturing and extended reality technologies. The intention is to create a cost-efficient, in-house solution that can be implemented directly within hospital settings.

A key focus of the research is the synergy between engineering and medical expertise to generate multidisciplinary knowledge that enhances surgical planning processes and the design of patient-specific instruments. Furthermore, the research aims to lay the foundation for the development of new patient-centered points of care, where engineering and medicine converge to offer comprehensive and personalized treatments. The study will highlight low-cost, accessible methods for establishing an innovative intra-hospital service that reduces reliance on external providers. Lastly, it will address the ethical and regulatory implications associated with the use of these technologies and processes in clinical practice, ensuring their responsible and sustainable implementation to improve patient outcomes and overall well-being.

1.2. Challenges

The introduction of emerging technologies has the potential to revolutionize preoperative surgical planning, improving efficiency, accuracy, and overall outcomes. However, the initial cost of equipment, such as 3D printers and specific materials, and the difficulty of immediate purchase by hospitals or research centers must be considered. Implementing a new workflow involves new steps with specific timelines: the creation of anatomical models and custom-made devices can be time-consuming, especially in complex cases, increasing preoperative planning time. Each clinical case has its characteristics, making it difficult to standardize the workflow. In addition, the clinical validity of models depends on factors such as the segmentation of medical images, the resolution of the 3D printer, and the fidelity between the digital model and the printed model. These aspects need to be continuously evaluated by the surgeon to demonstrate their practical utility.

This dissertation wants to analyze, assess, and optimize surgical planning and patient care processes by developing a methodology integrated with advanced engineering technologies. The aim is to optimize resources, ensure accuracy and quality, and assist the surgeon in choosing more informed and precise surgical strategies. The research will explore how the

integration of these technologies can contribute to the improvement of surgical planning processes in the clinical setting.

1.3. Research methodology

Research includes the study of preoperative surgical planning methods, the analysis of applied technologies, and the development of innovative solutions to improve the surgical approach and optimize its processes. The most advanced preoperative planning methods involve the analysis of medical images obtained by radiography, magnetic resonance imaging, or computed tomography, and the creation of three-dimensional anatomical models. These models assist in the evaluation and decision-making of surgical strategies, allowing the surgeon to better understand the patient's anatomy. This increases awareness and confidence in decision-making while reducing the duration and risks of surgery.

This research analyses the technologies currently used in preoperative surgical planning and identifies their limitations. Digital CAD modeling, additive manufacturing, and extended reality technologies will be explored to assess their applicability in the hospital setting, examining the impact and benefits, including planning time, accuracy, and clinical outcomes. Open-source technologies and software for medical image segmentation, digital CAD modeling, and additive manufacturing were used, and their effectiveness and accuracy were analyzed.

The methodical process involves the use of a pipeline that converts the patient's medical information into a digital 3D model. This model can be imported into a digital environment and then 3D-printed. The model can then be used to design the specific instruments needed for the surgery, such as cutting guides, bone grafts, or implants, and to evaluate their impact on surgical procedures. The research is based on the experience gained in the surgical context, thanks to the collaboration with the Pediatric Orthopedics and Traumatology Unit of the Rizzoli Orthopaedic Institute, as well as on the analysis of clinical cases followed personally, for which customized instruments have been designed. The collaboration with the Rizzoli Orthopaedic Institute in Bologna allowed the application of the studied methodologies to real cases, thanks to the activation of an experimental study protocol approved by the Ethics Committee of the Emilia-Romagna Vast Area.

Finally, six months of research abroad were conducted at the Department of Materials Science and Engineering, in the Division of Biomedical Engineering at Uppsala University in Sweden, where advanced selective laser sintering 3D printing technologies of metals such as titanium alloy and biotechnologies for cellular analysis were assessed.

1.4. Expected results

The successful implementation of this research will necessitate the development of professionals with multidisciplinary skills, enabling them to comprehend and integrate both clinical needs and industrial engineering requirements. These professionals will be equipped to propose operational models for hospital centers that combine these skills, enhancing the quality of care and the patient experience. Specifically, the research aims to provide an in-depth understanding of the surgical environment, including orthopedic, cardiovascular, and maxillofacial specialties. It will analyze the methods and equipment used in surgical planning and the design of patient-specific instruments, with a particular focus on selecting materials and geometries that fulfill specific aesthetic, mechanical, and geometric requirements.

This study is expected to demonstrate the efficiency and effectiveness of low-cost approaches for reconstructing three-dimensional models and designing customized instruments. Moreover, it will evaluate their manufacturability and practical use within clinical settings. A major outcome of the research is expected to be a significant contribution to preoperative surgical planning, through the development of an innovative methodology that integrates Computer-Aided Design, 3D printing, and Extended Reality technologies. The results could enhance the accuracy of pediatric orthopedic surgeries, reduce operative time, and improve patient outcomes. In addition, the findings may have broader applicability, potentially extending to other areas of specialized surgery and stimulating further technological advancements.

While the validation of experimental studies, analyses, and processes remains a crucial limitation, requiring significant time and resources, the long-term benefits of this research justify the investment. The processes and methodologies evaluated in this work hold substantial promise for improving clinical practice.

This research will not only explore the application of advanced technologies in surgical planning but also lay the foundation for the establishment of integrated intra-hospital units. These units, which provide personalized and comprehensive care for patients, will enhance synergies between engineering and medicine, contributing to a more collaborative and efficient healthcare delivery system.

1.5. Dissertation structure

The dissertation is divided into chapters. Chapter 1 introduces the dissertation with a brief description of the context, methodology, and expected findings. Chapter 2 delves into the research area, focusing on the literature review of emerging technologies used in the medical field, providing an overview of the most recent and interesting research, current trends, challenges, and opportunities. Chapter 3 describes the research project setting, methods, and materials in the research, focusing on the methodological approach and additive manufacturing technologies and their applications in the medical field. Chapter 4 presents the application of the methodology to real clinical cases, while Chapter 5 examines the experimental research conducted in the final year of the PhD, which opens interesting future developments. Chapter 6 is devoted to future research prospects. Finally, in Chapter 7, conclusions are drawn.

2. Background

The preoperative surgical planning phase is of paramount importance in ensuring the success of surgical procedures, particularly in the context of computer-assisted surgery. This process encompasses the preparation and visualization of surgical procedures, employing a comprehensive understanding of the patient's anatomy to optimize the surgical strategy. The key benefits of this approach include a reduction in operative time, a decrease in intraoperative risks, and a reduction in the number of intraoperative fluoroscopies. These benefits have a positive impact on clinical outcomes when compared with traditional surgical methods [1,2]. The primary data set utilized for surgical planning is derived from advanced medical images, such as computed tomography or magnetic resonance imaging, which facilitate the generation of three-dimensional (3D) models of the patient's anatomy. The 3D model facilitates a more comprehensive understanding of the clinical case, allowing a better perception of its depth compared to two-dimensional (2D) images. Furthermore, it serves as a foundation for more precise surgical predictions [3,4].

The discovery of X-rays by Wilhelm Conrad Röntgen in the late 19th century marked the beginning of a revolution in medicine through the advent of imaging. However, traditional radiographs have inherent limitations in resolution and the ability to distinguish overlapping anatomical structures. The subsequent invention of computed tomography by Godfrey Newbold Hounsfield in the 1970s enabled the construction of 3D images of the human body, facilitating surgical planning and reducing dependence on superimposed 2D images. The field of surgical planning saw further evolution with the advent of computer-assisted surgery in the late 1990s. This innovation resulted in the initial comprehensive virtual planning for osteotomies, which was subsequently translated to the operating room with the assistance of intraoperative navigation systems [5–7].

The integration of technologies such as additive manufacturing, also known as 3D printing, has expanded the potential of this approach, as evidenced by recent developments. 3D printing enables the creation of highly detailed physical models that accurately reflect the patient's anatomy, thereby facilitating personalized surgical planning [8–10]. 3D printing enables the fabrication of patient-specific surgical instruments, such as cutting guides and specific

implants, which enhance the precision and efficacy of surgical procedures [11–15]. This approach, which is tailored to the individual patient, has been demonstrated to reduce the risks of complications, improve surgical accuracy, and accelerate patient recovery. Nevertheless, despite these advantages, the large-scale adoption of virtual surgical planning remains limited, confined to centers of excellence. The establishment of intrahospital "Point-of-Care" facilities represents a promising avenue for the dissemination of these technologies, to enhance accessibility to personalized tools within the hospital setting.

2.1. Literature review

The analysis of the existing literature in the field under review allows the research project to be placed in a broader scientific context, following a focused thematic structure. This structure focuses on specific areas of study that are united using emerging engineering technologies in surgery, with a focus on the custom design of anatomical models, surgical instruments, bone grafts, and patient-specific implants.

In recent years, the integration of advanced engineering technologies has resulted in significant advances in surgical planning and the development of patient-specific instruments. In particular, the combined use of computer-aided design, 3D printing, and extended reality has resulted in remarkable innovations aimed at improving precision, efficiency, and clinical outcomes in various surgical fields, such as maxillofacial surgery, orthopedics, neurosurgery, and cardiology.

2.1.1. Virtual Surgical Planning

Virtual Surgical Planning (VSP) has emerged as a key component in the planning of complex surgical procedures, allowing procedures to be simulated in a 3D immersive (fully immersive virtual reality), or non-immersive (computer simulation) digital environment. This method relies on high-resolution images from Computed Tomography (CT) or Magnetic Resonance Imaging (MRI), allowing the creation of highly detailed 3D models of the patient's anatomical structures. Compared with traditional radiographs, which offer two-dimensional and often insufficient information, VSP offers a more complete 3D view of anatomical structures, which is

particularly useful in complex surgical settings where precision in alignments and movements is critical [16,17].

A principal feature of VSP is its capacity to enhance preoperative diagnosis and planning, facilitating advanced surgical simulations, optimal procedure selection, and prediction of operative outcomes. This approach has been demonstrated to diminish surgical uncertainty, particularly in intricate surgeries such as multi-axial and multi-planar tibial osteotomies, conferring substantial advantages in terms of diminished operative time, minimized risk of complications, and enhanced functional and aesthetic outcomes [18–20]. The integration of VSP with intraoperative navigation systems represents a crucial step in enhancing the precision of surgical procedures. This combination enables a direct correlation between the virtual surgical plan and the actual operation, thereby ensuring greater accuracy through precise alignment of anatomical data and accurate selection of landmarks. This enables an optimal alignment between the virtual surgical plan and the actual surgical procedure. The utilization of robotic systems in surgical care presents additional advantages due to their multiple degrees of freedom, which enhance both the accuracy and customization of the procedure. Nevertheless, the considerable expense of implementation and the steep learning curve continue to represent significant obstacles. Originally utilized in neurosurgery and maxillofacial surgery, VSP has demonstrated favorable outcomes in the precision of landmark placement, thereby encouraging its integration into other surgical specialties. Its incorporation into existing workflows has enabled the expansion of its use in other surgical specialties, including orthopedics, where it has been employed in the planning of shoulder and hip arthroplasty surgeries, and in cardiovascular surgery, where it has facilitated the creation of highly detailed 3D-printable anatomical models [21–23].

2.1.2. 3D Printing

3D printing has transformed the domain of virtual surgical planning and the design of patient-specific instruments, transcending the constraints of conventional surgical techniques. As early as the late 1980s, stereolithography (SLA) was being employed as a means of creating medical models as an alternative to milling and other conventional methodologies. This enabled the production of highly accurate models of bone and soft tissue structures [24]. The

utilization of biocompatible materials established the foundation for the direct fabrication of custom implants, thereby facilitating the advancement of 3D printing in the medical field. In many medical fields, including auxiliary diagnosis and treatment, where intricate and minute anatomical structures cannot be externally observed, 3D printing allows for the replication of anatomical structures and pathological tissues with remarkable precision, though not without inherent error margins typical of mechanical systems. This technology provides a highly detailed representation, but the degree of precision varies depending on the technique employed, with no achieving absolute accuracy. Nonetheless, 3D printing remains a valuable tool for enhancing the comprehension of complex aspects of anatomy and pathology under investigation. For instance, in the context of cardiac surgery, the utilization of 3D-printed anatomical models has enhanced the visualization of data throughout the diagnostic, treatment planning, and surgical phases, with a particularly notable impact in the context of complex congenital pathologies. This technology has contributed to the enhancement of medical devices and instruments, thereby improving clinical outcomes. The current trend is toward the creation of increasingly realistic models that not only replicate the anatomy but also the properties and functionality of the cardiovascular system [25,26]. Anatomical models created through 3D printing are also employed to enhance communication between surgeons and patients, thereby increasing transparency and providing substantial educational value [27,28].

The applications of 3D printing have expanded beyond preoperative planning to encompass the fabrication of patient-specific instruments (PSIs), including cutting guides, implants, and custom bone grafts. These tools, which are molded to the patient's specific anatomical features, enhance the precision and efficacy of surgical procedures, thereby reducing the risk of complications and accelerating the recovery process. The utilization of custom cutting guides enables more accurate targeting of surgical procedures, thereby reducing the likelihood of errors and the overall operative time. In the conventional approach, surgeons assess the diagnosis and plan surgery based on radiographic images and CT scans. However, 2D images do not fully capture the intricacies of the surgical field, and the success of surgical operations hinges on the surgeon's experience, who operates with limited guidance. In contrast, the virtual and physical representation of a 3D model of the patient's anatomy provides concrete support for the formulation of a more detailed diagnosis and the design of tailored surgical instruments.

The safety and accuracy of custom cutting guides in high tibial osteotomies have been demonstrated in numerous studies, with functional improvements observed even years after surgery [29–33]. The design of these guides is closely related to the specific anatomy of the patient and is of particular benefit in complex cases, where a custom design can respond to the complexity of the case. Nevertheless, the utilization of these instruments in routine surgical procedures is less practical due to the financial, temporal, and material resources that are necessary for their implementation. The creation of instruments tailored to each patient also enhances the accuracy and predictability of surgical interventions, offering a highly personalized approach that results in a reduction of complications and a more expedient recovery. In addition to enhancements in surgical methodology, 3D printing has facilitated the implementation of "Point-of-Care" (PoC) units within medical facilities. These units provide custom solutions that enhance VSP, reduce wait times, and improve clinical outcomes, particularly in settings of excellence.

Concurrently with these developments, 3D printing has become a pivotal technology in the fabrication of custom prostheses and tissue engineering scaffolds, significantly influencing surgical planning. One of the most promising applications of this technology is bioprinting, which enables the fabrication of complex organic structures by creating layers of biological materials, biochemicals, and living cells. Nevertheless, considerable obstacles remain, including the challenge of accurately reproducing the extracellular matrix and coordinating diverse cell types to reinstate biological functionality. An additional challenge is the vascularization of bio-printed tissues, which is essential for their survival and integration into the body. In addition to the biological challenges previously discussed, orthopedic surgery presents further difficulties related to the stability and mechanical strength of printed products [34,35]. As the use of these innovative technologies expands and becomes more deeply integrated into clinical practice, it is imperative to ensure their safety and compliance with relevant regulations.

Despite the ongoing advancement of 3D printing in the medical field, its widespread implementation remains constrained. Significant challenges remain in the resolution and accuracy of medical images from which 3D anatomical models are reconstructed, such as those obtained from CT and MRI scans. Although CT provides high-resolution images, it exposes patients to ionizing radiation. In comparison, although MRI is a safer alternative, it

offers less accurate images for 3D reconstruction. The development of combined imaging methods that reduce radiation exposure and improve image quality would be of significant benefit. Furthermore, the financial implications of 3D printing are contingent upon the specific technology and materials employed. Fused Deposition Modeling (FDM) is the most prevalent technique, with polylactic acid (PLA) representing the most common material. In contrast, more sophisticated technologies such as stereolithography (SLA) and selective laser sintering (SLS) necessitate the use of advanced equipment and greater process control, in addition to more expensive materials. Another challenge pertains to the reproduction of soft tissues, such as muscles, tendons, and ligaments, as well as dynamic tissues, such as cardiac tissues. The current limitations of 3D printing technology include an inability to accurately reproduce the motion of certain tissues, such as those that are not clearly visible even in medical images such as CT scans.

2.1.3. Patient-specific Design

The combination of Computer-Aided Design (CAD) and 3D printing has radically changed customization in surgery, with the ability to create specific surgical instruments tailored to the unique characteristics of each patient. In traditional surgical procedures, substantial discrepancies between pre-planned and actual implant sizes are frequently observed, affecting both preoperative planning and the precision of implant placement. Therefore, several studies have analyzed the accuracy of implant placement by integrating preoperative planning with patient-specific instrument design and demonstrated a higher degree of accuracy than control groups with manual placement [36,37]. An important example of technological advancement occurred in cranioplasty, where a process for designing and 3D printing polyether-ether-ketone (PEEK) implants was developed at an academic hospital. These implants, which are compliant with the European Medical Device Directive, are used in cranial reconstruction following traumatic brain injury. This advance has enabled hospitals to offer not only cranioplasty surgery but also additive manufacturing of implants directly at the PoC [38]. The customized approach has now spread to many surgical specialties, including oncologic surgery, where customized cutting guides allow precise removal of bone tissue compromised by tumor or trauma, enabling the replacement of nonviable parts [39]. Ambitious

approaches aim to design implants with a porous lattice structure that serves as a scaffold for the formation of new bone tissue. These implants, reinforced with standard orthopedic instruments, provide adequate mechanical support. In this context, the custom design of Ti-6Al-4V implants has demonstrated significant potential in the reconstruction of substantial bone defects, allowing the replacement of substantial bone segments [40]. In the field of maxillofacial surgery, the use of patient-specific cutting guides and implants has become the standard for the correction of skeletal deformities or post-traumatic reconstruction [41].

2.1.4. Bone tissue engineering

Bone tissue engineering is a rapidly evolving field that aims to overcome the limitations of traditional approaches to repair and regenerate damaged bone tissue. In recent decades, additive manufacturing technologies and the use of advanced biomaterials have opened new frontiers in the treatment of bone disease, trauma, and birth defects. The increase in skeletal disorders associated with an aging population has made these technologies particularly relevant. They offer innovative and tailored solutions to complex problems such as shortage of bone donors and poor geometric compatibility between grafts and the recipient site [42]. Autologous and allogeneic bone grafts, which have traditionally been used, present significant challenges, including limited availability and rejection. Although musculoskeletal tissue banks play a valuable role, they cannot always meet the growing demand or ensure optimal integration with the recipient tissue. In this context, bone tissue engineering has been proposed as a promising alternative solution, allowing the creation of customized 3D scaffolds that mimic the architecture and biomechanical properties of natural bone [43–45]. The scaffolds, made of biocompatible biomaterials such as bioactive ceramics and biodegradable polymers, provide structural support for cell growth and promote osseointegration, the process of fusing the implant with the surrounding bone [46,47]. One of the most significant innovations is the ability to fully customize the scaffold geometry using additive manufacturing (AM) techniques such as stereolithography (SLA), selective laser sintering (SLS), and fused deposition modeling (FDM). These technologies enable the fabrication of complex structures with high geometric precision, which is particularly useful in areas such as orthopedic and maxillofacial surgery, where reproducing the porous architecture of natural bone is critical to

clinical success [48]. In addition to geometric customization, scaffolds can be enhanced by the integration of stem cells or growth factors that accelerate bone regeneration. Mesenchymal stem cells have shown exciting potential in promoting new bone formation when seeded on scaffolds. Their ability to differentiate into osteoblasts and support regeneration has been confirmed in several clinical studies, especially in combination with biocompatible scaffolds such as calcium phosphate ceramics. Similarly, the use of growth factors such as bone morphogenetic proteins is effective in inducing cell differentiation and bone formation [49–51]. Despite significant advances, challenges remain for the clinical application of these technologies. The lack of standardization in implantable biomaterials and the difficulty in reproducing optimal porous microstructures for optimal mechanical, immunological, and biochemical properties. In addition, the design of scaffolds with complex geometries remains an area of active research, as geometry strongly influences cellular interaction and bone tissue regeneration [52,53].

The most innovative approaches are transforming scaffolds from simple mechanical supports to bioactive platforms capable of actively stimulating regenerative processes. The biomaterials used must meet mechanical and biological requirements: they must be stiff enough to support mechanical loads and porous enough to promote vascularization and cellular growth. Among the most promising materials are bioactive ceramics, such as calcium phosphate and hydroxyapatite, which have good compatibility with bone tissue, and biodegradable polymers, such as polylactic acid (PLA), polyglycolide (PGA), and polycaprolactone (PCL), which gradually degrade in the human body and are replaced by regenerated bone tissue [54–56]. A material of growing interest is PEEK, a high-performance polymer that combines excellent mechanical properties with good biocompatibility. PEEK is particularly suitable for implants that must withstand high mechanical loads, such as those used in orthopedic surgery. Because of its properties, PEEK can be used to create implantable scaffolds and customized bone grafts that can withstand mechanical stress and facilitate bone tissue regeneration [57,58].

Despite advances, difficulties remain in designing scaffolds with specific geometries and optimizing biomechanical properties. For example, the complexity of designing scaffolds with specific geometries and optimizing biomechanical properties remain areas of active research. Many studies focus on improving the mechanical properties of scaffolds and their integration

with surrounding tissues [59,60], but research on geometric design and custom shapes is still limited. It is known that scaffolds with lattice-like rather than solid structures offer significant advantages by promoting greater cellular interaction and faster regeneration of bone tissue.
In the future, bone tissue engineering could go even further by creating bioengineered scaffolds that not only have optimal mechanical properties but also could actively stimulate bone regeneration through the controlled release of growth factors and other bioactive substances. These bioactive scaffolds represent the next frontier in regenerative medicine, as they will make it possible to overcome current limitations and offer tailored solutions for the treatment of complex bone defects that go beyond the capabilities of traditional approaches. The development of such technologies will not only significantly improve clinical outcomes, but also reduce patient recovery times, opening new perspectives for the treatment of a wide range of bone diseases.

2.1.5. Extended reality

The innovation of VSP aims to increase surgical accuracy and improve safety by reducing procedure-related complications. The application of Extended Reality (XR) technologies in surgery is revolutionizing both medical education and clinical practice. XR technologies, which include augmented reality (AR), virtual reality (VR), and mixed reality (MR), are rapidly becoming key elements in surgical training and planning. While these technologies have different applications and characteristics, they share some key features: digital interaction, digital and immersive visualization, and the creation of interactive environments. The main application areas of XR technologies include three areas: surgical training, surgical procedure simulation, and intraoperative care. XR can accelerate the learning process, allowing surgeons in training to reach an acceptable level of competence before operating in the operating room. In addition, XR-assisted surgery has significant therapeutic potential, especially in complex cases where conventional methods may lead to unsatisfactory results due to lower accuracy [61].
Augmented reality (AR) allows digital data to be superimposed on a real physical environment, improving the intraoperative visualization of critical data such as radiological images or 3D models of the patient's anatomy. Currently, AR technology requires the acquisition of patient

data and the construction of models compatible with AR visualization. To create virtual images that can be manipulated in real-time in the user's view, a camera, computer vision technology, tracking tools such as markers, and an output screen are required. The user is provided with a display to view both the real mode and the computer-generated images. Potential applications include the integration of preoperative imaging as an intraoperative navigation system. AR-based navigation systems provide a 3D representation of anatomical areas, allowing for more accurate visual guidance during complex surgical procedures such as tumor resection or bone reconstruction [62,63]. This system uses a transparent viewer to project real-time images of the patient's anatomy, providing precise guidance for screw placement and removal of complex tumors. This approach has been shown to significantly improve the accuracy and safety of procedures, with positive outcomes in operated patients. In another study, an AR navigation system was used for pedicle screw placement in spinal surgery, showing 94.1% accuracy, with a significant reduction in instrumentation time as surgeons became more experienced. This technology has proven to be a safe and accurate alternative to traditional surgical navigation methods [64,65]. However, despite its advantages, AR has not yet reached its full potential in the clinical workflow, as significant evaluations of the clinical benefits of AR are lacking. Another limitation stems from the behavior of organs, which deform in response to heartbeat, respiration, and physical manipulation, creating problems with registration and accurate alignment of virtual models with physical reality. Traceability and calibration of surgical instruments are essential in AR applications, and there is currently a need for effective segmentation algorithms and improved imaging methods. Finally, user acceptance of new AR interfaces is often slow, influenced by factors such as usability and limitations of the human perceptual system [66,67].

Virtual reality (VR) offers surgeons the ability to immerse themselves in simulated surgical environments, allowing them to practice complex scenarios without risk to the patient. This training approach enhances learning and surgical confidence, especially for procedures that require high precision. Several studies have evaluated the impact of VR on medical education, particularly during the COVID-19 pandemic, when the adoption of new learning methods became necessary. For example, one study developed a simulated training scenario for infusion placement, demonstrating the immense potential of VR in medical education while highlighting the need for technical improvements to optimize the user experience [68].

Preoperatively, VR helps improve procedural accuracy and surgeon confidence by allowing surgeons to familiarize themselves with the patient's anatomy through the creation and visualization of customized 3D anatomical models. When planning complex surgeries, such as spine or neurosurgery, VR allows surgeons to visualize surgical pathways in greater detail and accuracy, reducing the margin of error [69]. In addition to surgical simulation, VR is also used in the treatment of specific diseases, such as chronic pain, or postoperative rehabilitation [70]. Another interesting aspect to explore is how VR can improve collaboration between surgeons and other healthcare professionals. The ability to create shared simulations in real-time allows groups to work on a common surgical strategy, improving communication and coordination among members. These applications demonstrate how VR can support not only surgical training but also therapeutic effectiveness. However, it remains critical to further develop the technological aspects and improve usability to ensure wider adoption of VR in clinical settings. Key challenges include the excessive cost of equipment and infrastructure, which may limit large-scale adoption. This is compounded by the need for adequate training of surgeons and healthcare personnel, given the learning curve associated with the use of immersive technologies. On the technical side, there are issues related to the accuracy of simulations, with the need to improve real-time rendering and alignment between virtual models and physical reality. In addition, the integration of VR into the clinical workflow is a complex challenge, especially regarding intraoperative use. Finally, device ergonomics and user resistance to adoption, influenced by factors such as comfort and ease of use, remain significant barriers. These barriers, if addressed, could encourage wider adoption of VR in surgical practice, thereby improving the safety and effectiveness of procedures.

Mixed reality (MR), a combination of VR and AR, allows surgeons to interact with 3D virtual models in real-time, improving the accuracy of minimally invasive procedures. It provides an immersive and interactive platform that seamlessly integrates the physical and digital worlds. This allows surgeons to navigate through complex anatomical structures, and practice and plan surgeries with unparalleled detail and realism in a controlled environment. MR technology can be used in the operating room both as a teaching tool and as an aid, giving the surgeon access to specific information. For example, the surgeon can consult annotations, access specific surgical techniques, collaborate with online specialists, and visualize patient information without having to physically touch the equipment. Gestures, voice commands, or

even retinal movement can activate these features. MR is particularly valuable in the operating room, where it offers numerous advantages for medical procedures and interventions, such as surgical tool positioning [71]. It allows the integration of patient-specific data with real-time and real-world observations, presenting all this information in a single visualization [72]. This aspect can improve training, education, and surgical planning. The use of MR has been shown to improve clinical outcomes, accuracy of surgical procedures, and collaboration among surgeons, with a positive impact on patient care [73,74]. However, technical complexity due to the need to maintain aseptic conditions in the operating room, equipment cost, and steep learning curves are significant barriers to the widespread adoption of mixed reality and computer-assisted assessment, and issues of usability, bias, and statistical analysis must be considered. Mixed reality offers significant advantages, but there are still outstanding challenges such as ergonomic issues, limited field of view, and battery life that must be addressed to ensure widespread adoption. Despite the technical and operational challenges, MR represents a promising frontier in modern surgery. The ability to integrate real-time data and virtual models with the physical world has the potential to revolutionize not only surgical procedures, but also preoperative training and planning, improving accuracy, safety, and clinical outcomes. As technology continues to evolve and adoption increases, mixed reality has the potential to redefine standards of care, enabling unprecedented personalization and accuracy for the benefit of both surgeons and patients.

XR technology applied to VSP offers many benefits, depending on the specific technology used. However, this is still very preliminary and broad research, so it is critical to focus on specific objectives to be developed. To personalize the surgical treatment for the patient, it is essential to create immersive and interactive environments where the surgeon takes the lead in digital decision-making and operations. This digital environment should be generated by the surgeon each time and supported by predefined simulation software based on an established surgical technique. It is also important that the user interface design is simple and intuitive so that the operator can easily navigate between distinct functions and applications without frustration.

2.1.6. Predictive modeling

Predictive modeling represents an innovative area in surgical planning and personalized patient treatment, experiencing rapid expansion in recent years. This technology analyzes pre-treatment data to predict post-treatment outcomes, thus contributing to an increasingly individualized approach in surgery. Predictive models, also known as digital twins, represent a significant evolution in the field of surgery due to their increasing adoption in industry, where they optimize organizations' monitoring and operational efficiency.

Originally conceived for the aerospace sector, the idea of digital twins has gained attention in the context of Industry 4.0, attracting interest from various sectors, including manufacturing and transportation [75–77]. In healthcare, digital twins are virtual representations of patients that integrate information regarding tissues, organs, and physiological processes, to improve disease prevention, diagnosis, and treatment. These applications have the potential to revolutionize patient care by promoting increasingly data-driven medicine.

By modeling the complex interactions between genetic and environmental factors, digital twins make it possible to monitor disease progression and optimize treatment plans. In addition, through digital simulations, they facilitate the selection of the most appropriate therapies and provide detailed 3D representations for precision surgical planning. These 3D digital models, continuously updated with clinical data, allow surgeons to simulate virtual scenarios, facilitating constant monitoring and improving the accuracy of care [78]. They can simulate the body's response to different treatments, such as bone reconstruction or prosthetic implantation, providing a powerful decision support tool. In addition, predictive modeling makes it possible to simulate and predict the impact of surgical corrections on final appearance, monitoring the patient's recovery in real time and potential evolution during growth, making changes to the treatment plan, and personalizing postoperative therapies. Building a digital twin involves a complex network of skills, professionals, and technological devices. This includes large-scale biological data repositories, cloud storage and computing, standardized protocols for data acquisition and communication, artificial intelligence-based algorithms, and virtual reality technologies. Multidisciplinary collaboration and the development of legal and ethical frameworks related to informed consent and data ownership are essential [79]. Although comprehensive predictive modeling is still under development, several companies and research institutions are already making digital copies of specific body

parts or physiological systems for targeted applications. These advances facilitate a shift toward personalized medicine, optimizing therapies and predicting the future health needs of individuals and populations, as well as facilitating the planning of public health policies and interventions. By analyzing vast amounts of data, digital twins facilitate personalized screening programs for early diagnosis and identify risk patterns for specific diseases. Remote patient monitoring enhances telemedicine capabilities, enabling timely interventions even in isolated areas. However, implementing digital twins comes with significant challenges, including dependence on accurate data from various sources and a lack of standards to ensure interoperability. Creating accurate models for complex systems is a considerable challenge, and maintaining digital infrastructure requires high investment, posing a barrier for smaller healthcare providers. Addressing these issues requires multidisciplinary collaboration, accompanied by investment in research and development of governance standards [80].

2.2. Current market scenario and trend

In recent years, the field of VSP and patient-specific design has undergone a significant transformation, driven by technological innovation and the emergence of patient-centered approaches. The integration of advanced technologies such as 3D CAD modeling, 3D printing, and XR has enabled unprecedented personalization of surgical procedures. These developments have not only improved the accuracy and efficacy of procedures but have also optimized clinical pathways, reducing recovery time and post-operative complications. The VSP market is increasingly characterized by a growing demand for patient-specific solutions, reflecting a greater awareness of individual needs. Advanced imaging technologies, combined with data analytics and artificial intelligence, have opened new vistas for the creation of customized anatomical models, facilitating the simulation and optimization of surgeries.

Growth is being driven both by developed countries, particularly North America, Europe, and Japan, where adoption of these technologies is highest, and by developing countries, such as China, which are investing heavily in advanced healthcare infrastructure. However, adoption remains uneven due to economic and regulatory factors affecting access to these technologies.

The growing focus on personalized medicine has prompted healthcare providers to invest in systems that enable more accurate and predictive surgical planning, meeting the growing need for an individualized approach to patient care. This evolution in the surgical planning landscape not only has clinical implications but also offers significant growth opportunities for companies in the industry, which are being called upon to innovate and adapt to new market needs. The market is characterized by the presence of global players such as Materialise, 3D Systems, Stryker, Siemens Healthineers, Medtronic, and Stratasys, which offer a combination of software, 3D printing hardware, and integrated solutions for surgery. These companies are investing in research and development to improve the accuracy, efficiency, and accessibility of their technologies. In parallel, innovative startups are emerging, often focused on specific niches, such as 3D printing of organs and tissues, surgical instruments based on biocompatible materials, and augmented reality for robotic surgery. Technological innovation is accelerating, with innovative solutions combining AI, machine learning, and biometrics to improve the accuracy of 3D planning and models. Some companies are already implementing solutions that allow surgeons to visualize critical data in real-time via AR during surgery [81,82]. In this dynamic world that is always looking for the latest advancements, it is important to continually learn and adapt, stay up-to-date, be curious, and embrace the opportunity to integrate all these innovations.

2.3. 3D Point-of-Care and Regulations

Traditionally, commercial vendors have manufactured 3D anatomical models and patient-specific tools. While effective, these providers have various limitations in their ability to customize to specific program needs, typically require extended lead times (several weeks) for model production, and incur significant costs. Therefore, the implementation of an in-house 3D modeling and printing flow that allows for customization to specific program needs, fast lead times for 3D model production, and more affordable costs may be desired in capable institutions. In addition to the potential time and cost savings, creating an in-house workflow also protects patient information by not sending scans and patient data to commercial providers [83].

This landscape includes the proliferation of Point-of-Care (PoC) 3D printing centers, which enable just-in-time production of anatomical models based on patient medical data, blurring the line between healthcare providers, medical centers, and device manufacturers. The applications of 3D printing in medicine are many, including the creation of patient-specific anatomical models, the manufacture of patient-specific instruments such as cutting guides, and the fabrication of custom implants. However, this new scenario raises regulatory issues, as the regulatory classification of such 3D-printed devices is still uncertain, creating ambiguity about their status as medical devices.

Devices printed in PoC centers fall into three main categories: diagnostic anatomical models, specific surgical instruments, and custom implants. While there are significant benefits to creating such devices, PoC centers must maintain ambitious standards of quality and safety. Manufacturers must follow strict procedures for documenting manufacturing processes, including the materials used, the parameters set for 3D printing, and the monitoring of environmental conditions. The manufacturing process, from image segmentation to model creation, must be carefully planned and validated to ensure that the final device meets clinical needs.

Internal regulation of PoC centers is essential to ensure compliance with safety requirements. For example, 3D-printed anatomical models for diagnostic use must be created using approved and validated segmentation software and certified for diagnostic use. To ensure the accuracy of the models, radiologists and surgeons must review and approve each step of the segmentation process. In addition, all materials used in 3D printing must be documented, including certificates of analysis and specific details on post-production processes such as media removal and sterilization. Sterilization is a critical step, as the process can alter the properties of the device. Validation studies must be performed to ensure that devices continue to meet biocompatibility and safety standards. Each device produced in PoC centers must be accompanied by transparent and detailed documentation, including information such as the name and address of the producing healthcare institution, design and manufacturing data, intended use of the device, and post-use clinical outcomes. In addition, a periodic review process should be in place to evaluate the effectiveness of the device and take any necessary corrective action.

In Europe, the 2017 Medical Device Regulation (MDR) has introduced stricter rules for 3D-printed devices, although it is still unclear in some places. The MDR does not appear to apply when devices are manufactured and used exclusively within healthcare institutions, provided that they adhere to an adequate quality management system (QMS), there is a well-justified need for specific devices that cannot be adequately met by an equivalent commercially available alternative, a traceable procedure is in place for their manufacturing, modification, and use, and comprehensive documentation and evaluations on their clinical application are maintained. Hospitals and PoC centers must implement QMS in their 3D printing labs to ensure traceability and regulatory compliance. A QMS structure allows them to optimize device quality, reduce errors, and increase the credibility of PoC facilities. According to the MDR, all 3D-printed devices must be manufactured and used within the same legal entity, such as a hospital. A hospital must then justify the decision to manufacture devices in-house rather than purchase them based on factors such as design flexibility, lead time, cost, or specificity of patient needs [84,85].

2.4. Challenges and opportunities

One of the biggest difficulties in the adoption of these innovative approaches is the lack of clear regulations, particularly for 3D-printed devices and XR technologies. Regulations must determine whether devices produced in 3D printing PoC centers should be considered medical devices, or whether they fall into a new category. The European Union is setting stricter standards in this area through the MDR, but the situation remains complex.

Although 3D and XR printing technologies offer tangible benefits in terms of improved surgical outcomes, initial implementation costs can be high. Adoption of these technologies requires significant investment in infrastructure, staff training, and integration into clinical workflows.

Partnerships between hospitals, universities, and technology companies represent a strategic opportunity to accelerate the development and implementation of innovative solutions. Collaborations in 3D printing and XR technologies are leading to the creation of centers of excellence where surgeons can experiment and adopt the latest innovations.

The future of the personalized surgical planning market, integrated with CAD technologies, 3D printing, and XR, looks promising. Technologies continue to evolve and the increasing

interaction between medicine and engineering will open new horizons, making surgery increasingly precise, safe, and personalized. Market expansion will depend on the ability to overcome regulatory barriers and make these technologies accessible on a scale. In this context, PoC centers will be essential to push the boundaries of personalization in surgery, bringing technology ever closer to the patient.

3. Materials and Methods

This chapter describes in detail the setting of the research project, the methodologies adopted, and the materials used for surgical planning and personalized design in pediatric orthopedic, cardiovascular, and maxillofacial settings. Special emphasis is placed on the need for close collaboration between universities and hospitals, highlighting the importance of the activation of experimental clinical protocols approved by the Ethics Committee of Area Vasta Emilia Centro (CE AVEC). These protocols allow the application of developed technologies to real clinical cases.

During the Ph.D., the main collaboration was with the Pediatric Orthopedics and Traumatology Unit of the Rizzoli Orthopaedic Institute in Bologna, although it included further synergies with other institutions, such as the Department of Cardiac Surgery at the Sant'Orsola-Malpighi Polyclinic in Bologna and the Department of Materials Science and Engineering at Uppsala University, in the context of the research period abroad. This chapter discusses the methods and materials used during the project, regarding those that were directly accessed and integrated into the surgical planning and custom design workflow.

3.1. Collaboration between the University and Hospital and clinical trial protocols

The research group, which I joined during my Ph.D., aimed at improving preoperative surgical planning, was launched in 2017 thanks to a collaboration between the Department of Industrial Engineering (DIN) of the Alma Mater Studiorum University of Bologna and the Pediatric Orthopedics and Trauma Unit of the Rizzoli Orthopaedic Institute (IOR).

The implementation of university research into clinical applications was made possible through the activation of a clinical study approved by the Ethics Committee of Area Vasta Emilia Centro (CE AVEC). This protocol allowed the testing, validation, and implementation of technologies for the simulation, planning, and customization of surgeries aimed at correcting musculoskeletal disorders of the pediatric limbs (3D-MALF clinical study: "3D Printing Models

in Preoperative Planning of the Pediatric Patient with Congenital Malformations. Pilot study". - EC AVEC: 356/2018/Sper/IOR). Following the initial pilot study, preoperative planning using computer-assisted surgical simulation (CASS) and 3D-printing of customized sterilizable models and cutting guides has become an established clinical practice. This has led to the activation of an additional clinical protocol to compare the geometry of manually modeled bone grafts with that of grafts fabricated using specific tools such as cutting guides. The current clinical study aims to validate the feasibility, accuracy, and efficacy of an innovative process to produce customized bone allografts for the correction of pediatric skeletal deformities (3D-MALF II clinical study: "Customized bone grafts by three-dimensional analysis in pediatric skeletal deformities" - CE AVEC: 301/2022/Sper/IOR).

This collaboration has facilitated the introduction of new techniques, methodologies, and technologies in the field of pediatric orthopedic surgery, to create a digital and virtual environment for surgical planning. The activation of clinical protocols is crucial for the application of basic research results in the clinical setting. Without such protocols, the results would remain at the level of academic research without concrete practical application.

This process is also applicable to other areas where research needs to be translated into real-world applications.

During the research period abroad at Uppsala University in Sweden, there was a lack of formal collaboration between the university and the hospital, despite surgeons' interest in technologies developed in academia. This lack of collaboration prevented the clinical application of technologies, in part because of the lack of safety and quality certifications for the 3D-printed objects. However, these were implants, such as mandibular plates for maxillofacial surgery, which must remain in the human body, unlike cutting guides, which are non-permanent, disposable devices. As a result, the level of safety required for implants is higher. The activation of clinical protocols depends strongly on the type of device being developed and can be a complex procedure to concretize.

3.2. Low-cost innovative workflow proposal

The collaboration between the university and the hospital enabled the development of an innovative workflow based on low-cost, internally managed technologies. By integrating an interdisciplinary team of engineers and healthcare professionals, it was possible to create a systematic workflow that could effectively manage the entire process, from patient clinical data management to software and hardware interfaces (Figure 1).

Several studies have identified key criteria for improving communication between engineers and surgeons, with a focus on data management and patient privacy, as well as the development of protocols for studying and analyzing data during the planning and execution phases of surgery [86,87]. The in-house workflow involves the use of open-source software and FDM 3D printing technology to create 3D anatomical models of complex cases, thereby improving preoperative planning (Figure 2). In addition, the use of these advanced technologies allows for more accurate selection of intraoperative instruments, such as implants, plates, and fixation screws. This suggests an optimization of the instrumentation required in preparation for surgery, thereby improving operating room workflow and surgeon efficiency [88]. The growing adoption of in-house 3D printing to produce patient-specific devices shows promising results, suggesting that this technology has reached a level of maturity that can compete with many available commercial systems. However, certification of the entire design, simulation, and 3D printing process remains a key requirement, especially in the European context. This limits the use of open-source software and low-cost 3D printers in the surgical field [89].

To overcome these barriers, it is essential to promote comparative studies and clinical trials that demonstrate the effectiveness and equivalence of open-source solutions compared to commercial ones. One of the main objectives of the research workflow described in this dissertation is precisely to develop and validate such solutions, in collaboration with the Rizzoli Orthopaedic Institute. In parallel, it will be necessary to develop standardized and certified procedures and equipment to consolidate the role of PoC 3D printing as a viable and economically sustainable practice compared to outsourced solutions.

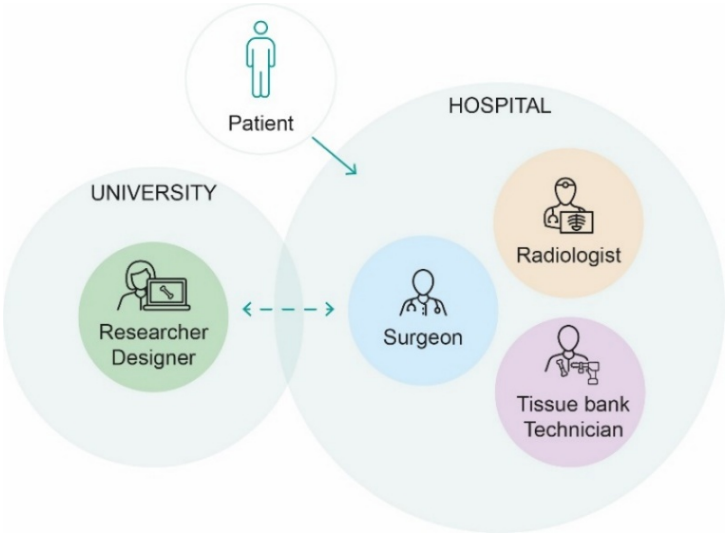

Figure 1. Actors of the new workflow. The researcher designer collaborates closely with hospital professionals, including radiologists, surgeons, and technicians, to develop and implement patient-specific solutions. The patient initiates the process by seeking care from the hospital. A bidirectional arrow between the university and the hospital highlights their continuous and reciprocal collaboration, to integrate research and clinical expertise to optimize surgical planning and outcomes.

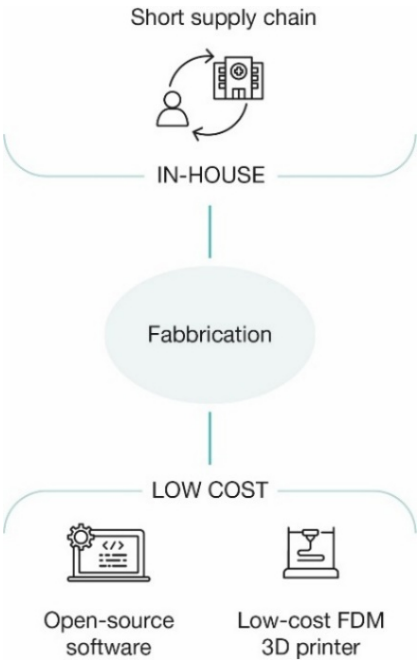

Figure 2. In-house fabrication. This approach integrated efficient, localized manufacturing, minimizing external dependencies. By adopting an in-house model, the process benefits from a short supply chain, reducing lead times and enhancing flexibility. The use of open-source software and low-cost FDM 3D printers ensures cost-effective, precise production. This system facilitated the rapid prototyping and production of customized, patient-specific solutions, optimizing time and resources.

3.3. Methodology

The DIN research group, in collaboration with the Pediatric Orthopedics and Traumatology Unit at the Rizzoli Orthopaedic Institute, has developed a workflow that includes the conversion of medical images into 3D printable anatomical models and the design of specific PSIs in sterilizable materials [90,91].

This process was further optimized during the Ph.D. program by integrating multidisciplinary teams and involving radiologists and bone bank technicians.

Currently, the workflow is being used at the Rizzoli Orthopaedic Institute for real-world clinical case management and will continue to be monitored for updates and refinements (Figure 3).

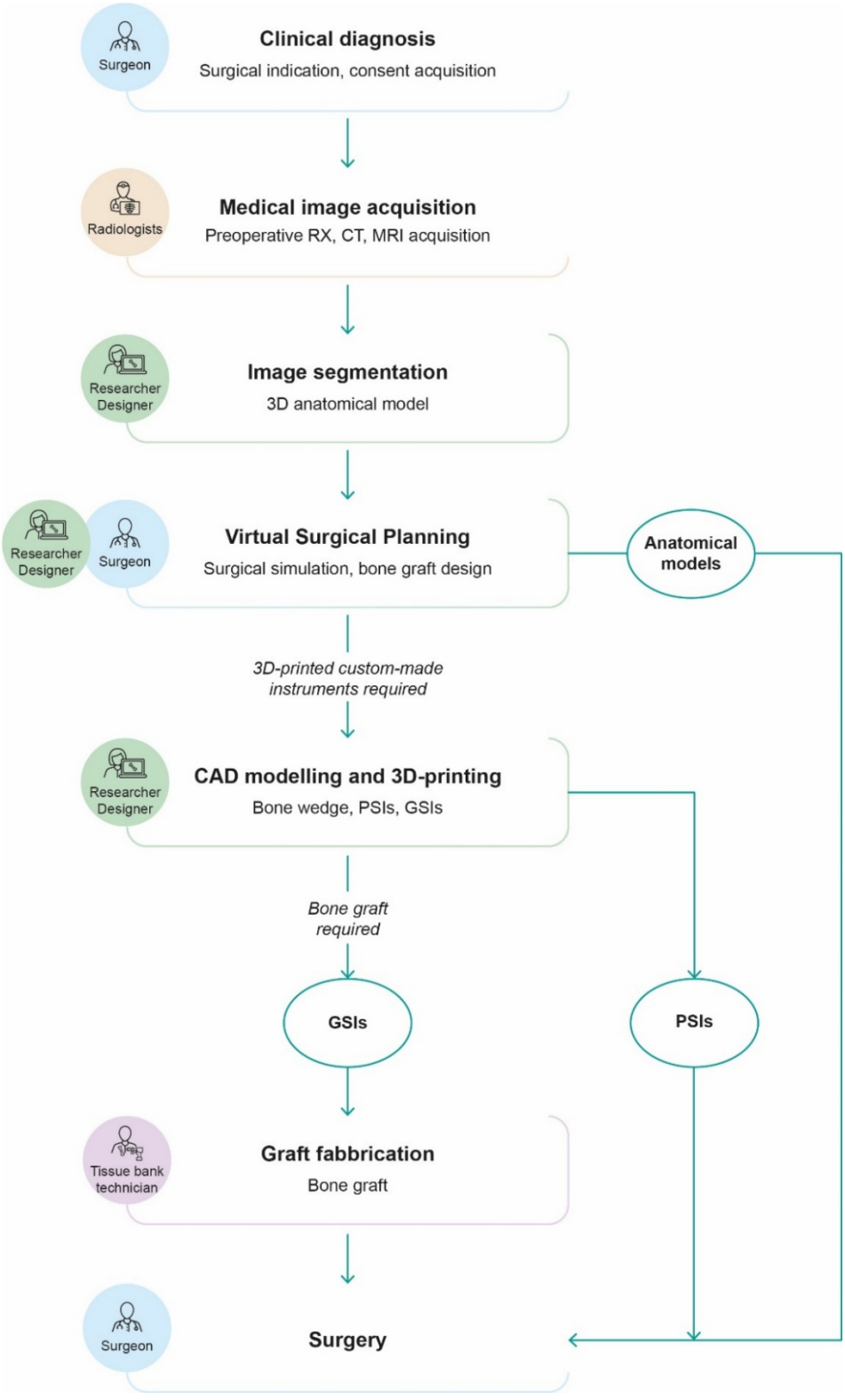

Figure 3. Virtual Surgical Planning and Patient-Specific Design and Fabrication workflow.

Of particular interest is how this process can be increasingly integrated with emerging technologies and approaches, such as the design and fabrication of bone grafts using

biocompatible materials and customized implants. In addition, the use of emerging technologies such as extended reality (XR) and artificial intelligence (AI) offers promising opportunities to further optimize various stages of workflow.

3.3.1. Clinical diagnosis

The workflow begins with the surgeon's selection of the patient. After a clinical evaluation that includes a diagnosis of the underlying pathology and the deformity to be treated, the surgeon explains the procedure to the patient and family to obtain informed consent. Once enrolled, the patient undergoes a radiological study performed by a team of radiologists.

3.3.2. Medical image acquisition

In orthopedic surgery, the first step in clinical practice is to examine the bone segments using panoramic radiographs (X-rays), accompanied by comparisons with the contralateral limb. This is followed by preoperative ultra-low dose CT scans. The acquisition was performed by obtaining scans with 5 mm slice thickness (0.625 mm reconstructions), which allows good accuracy for optimal reconstruction and modeling while reducing the radiation dose ($CTDI_{vol}$ = 13.3 mGy, DLP = 276.4 mGy·cm) [92]. However, a disadvantage of this method is the long processing time required by the software, which takes approximately 30 minutes to display the final images. In the cardiovascular field, the reference examination is Computed Tomography Angiography (CTA), a specific computed tomography scan in which a contrast agent is injected to visualize blood vessels and blood flow in detail, as opposed to standard CT scans, which focus on bone structures and soft tissue without the use of contrast [93]. In maxillofacial surgery, the most used test is Cone Beam CT (CBCT), a three-dimensional imaging technique particularly suited to analyzing dentofacial structures, which provides detailed images of the bones of the jaw and jawbone with a lower radiation dose than conventional CT [94].
The resulting images show body tissues in different shades of grey, with denser structures such as bones appearing lighter (almost white) and less dense tissues such as muscles and organs appearing darker. The data acquired during the scan is stored in the Digital Imaging and Communications in Medicine (DICOM) format, an ISO 12052 standard format for managing and

sharing medical images between different software and clinical systems. Finally, the images are transferred to the 3D printing PoC, appropriately pseudo-anonymized, following the sensitive data protection regulations (GDPR 2016/679). Specifically, the files are renamed with a unique PatientID for each patient.

3.3.3. Image segmentation

Medical imaging is at a pivotal moment in the creation of patient-specific 3D models useful for simulation and surgical planning. Tools such as 3D Slicer (open source) and Materialise Mimics (commercial) allow detailed reconstructions of anatomical structures, improving the accuracy of preoperative preparation. Image segmentation (Figure 4), required to isolate regions of interest (ROIs) corresponding to relevant anatomical structures, can be performed manually or by automated and semi-automated algorithms. The segmentation software has a similar interface with four viewing panels: three two-dimensional views (axial, coronal, and sagittal) and a three-dimensional view for 3D reconstruction of the data. DICOM files are imported by selecting the appropriate option, allowing a choice of image sets. After import, images are displayed in the three 2D planes and segmented using specific tools such as thresholding, which highlights areas based on intensity intervals. For bone structures, an optimal range is between +200 and +3000 HU, but pediatric patients require more care due to lower bone density and the presence of growth cartilage. Once an initial selection has been made, advanced editing tools allow further refinement of the segmentation by removing unwanted areas or adding detail to ROIs. Automatic interpolation algorithms between slices facilitate the selection of ROIs in planes not manually segmented. Accurate segmentation facilitates the creation of functional stereolithography (STL) files for 3D printing and modeling, minimizing post-processing. Segmentation time and model quality depend on the complexity of the anatomical region and the resolution of the CT images.

At the end of the process, models for each identified anatomical segment, such as bones or synthetic tools, can be exported in STL format. This format facilitates further modification of the models for subsequent planning steps.

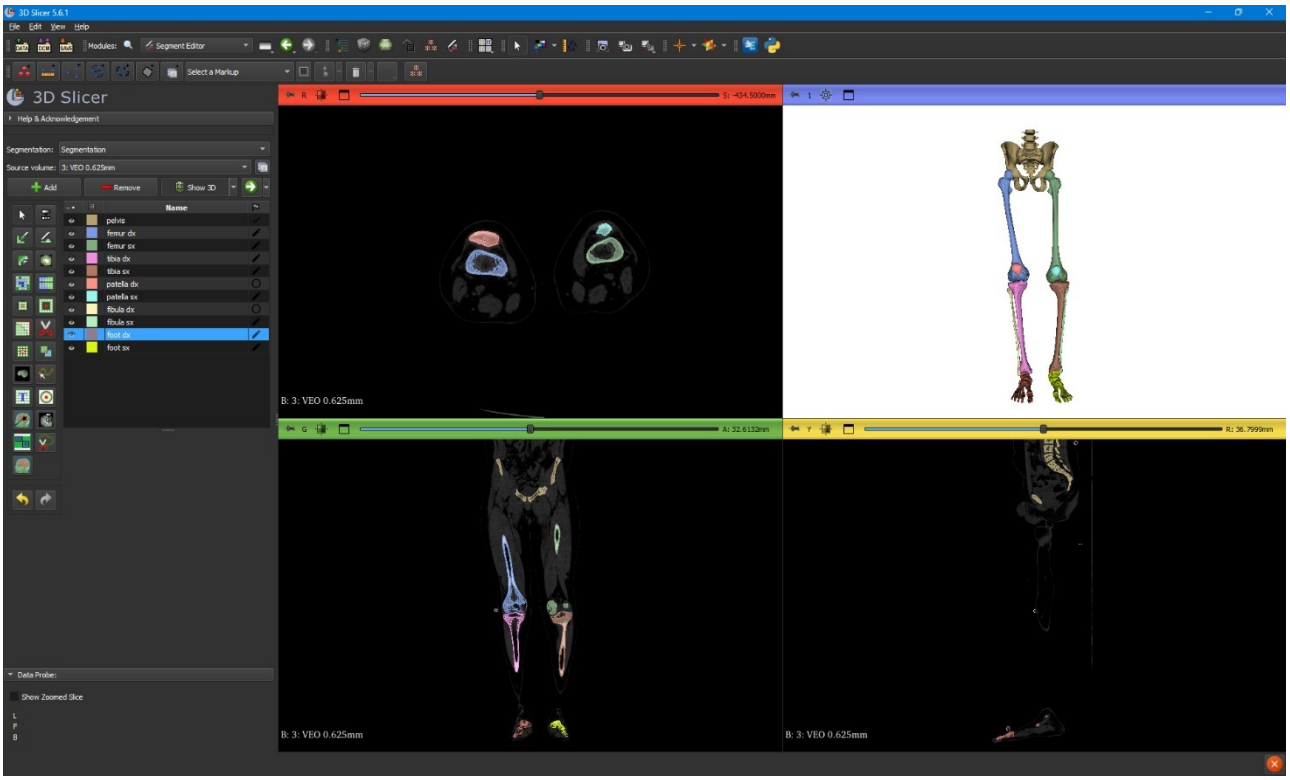

Figure 4. User interface of 3D Slicer during image segmentation. The user interface displays the axial, coronal, and sagittal views alongside the segmented 3D model, providing a comprehensive visualization of the anatomical structure.

Model preparation for surgical planning requires careful optimization of the STL files generated by 3D Slicer, which can be imported into modeling software such as Blender or MeshLab for further editing and refinement. It is critical to obtain an accurate model with a small number of vertices to ensure smooth handling in visualization and editing software, as well as to ensure the quality of the final model, especially if it is intended for 3D printing. MeshLab is an excellent intermediate tool for performing specific mesh editing and repair operations. This application is designed for manipulating STL files and offers a wide range of tools for editing, cleaning, repairing, and correcting polygons. In MeshLab it is possible to "lighten" the outer surface of the mesh, making the inner areas darker. This can be done using a selection defined by a color range. By setting the values of this range to black, you can isolate and eliminate unlit vertices. Alternatively, Blender optimizes the model through decimation or remesh modifiers, to reduce the number of vertices while maintaining good visual quality and reduced computational load. Depending on the level of detail of the imported model, the ratio parameter of the decimation modifier is set between 0.1 and 1 (where 1 corresponds to 100 percent of the original vertices).

This operation aims to obtain several vertices typically between 5,000 and 30,000, without exceeding 100,000 vertices, although this value may vary depending on the complexity and size of the mesh. It is crucial to obtain a triangulated surface that appears visually smooth and continuous, avoiding overly triangulated geometries that do not accurately represent reality, especially regarding the 3D printing of the model. These operations help reduce the computational load on the software and simplify subsequent modeling tasks (Figure 5).

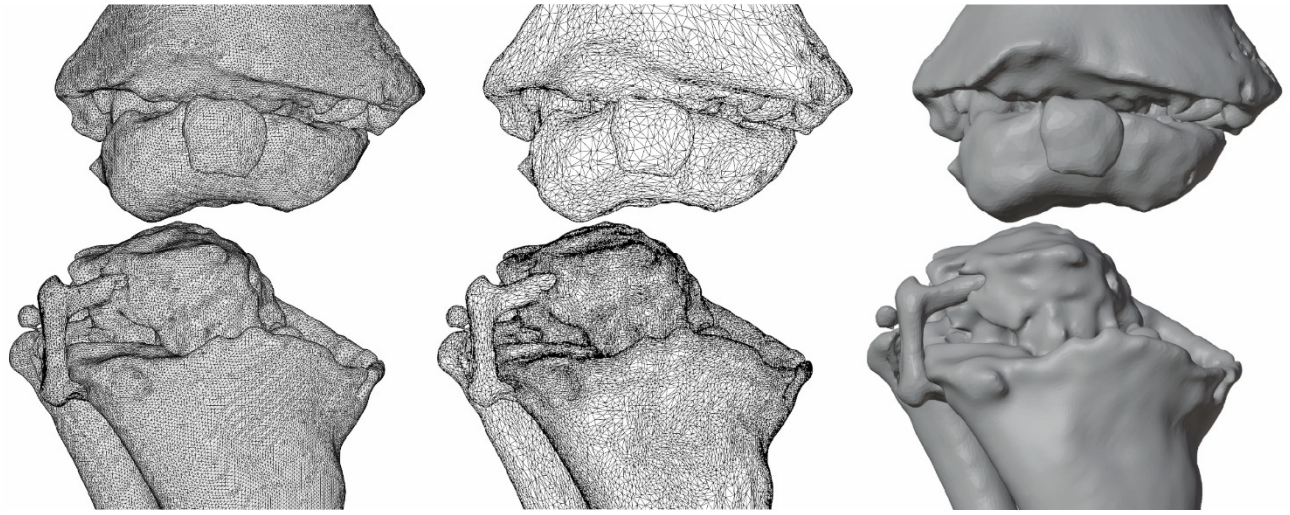

Figure 5. Mesh simplification process in Blender. On the left, the dense mesh generated after segmentation is shown in Edit Mode, displaying a high number of vertices (273,459). In the center, the mesh is visualized after a simplification process, reducing the vertex count to 87,040 while preserving the overall geometry. On the right, the simplified mesh is displayed in Object Mode with solid shading, providing a clear representation of the final lightweight model.

Next, it is important to remove unwanted internal surfaces to ensure a clean and accurate model. This can be done in “Edit Mode” by selecting the surface you want to keep. Then select all vertices connected to it and use the inverse selection function to remove isolated, unconnected vertices (Figure 6).

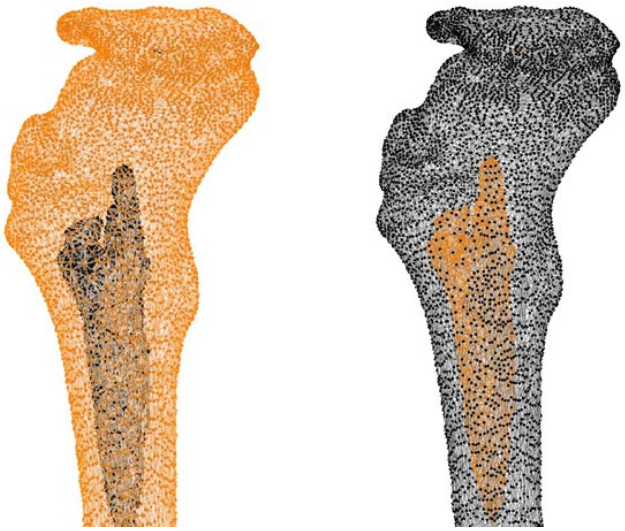

Figure 6. Vertex selection in Blender. The first image shows the selection of the surface to retain (highlighted in orange). By inverting the selection, all hidden and /or disconnected vertices from the main surface are identified in the second image. These vertices can be removed to further reduce the mesh complexity and optimize the model.

3.3.1. Virtual Surgical Planning

VSP enables precise surgical planning by visualizing the expected results of surgery in a digital environment before the actual procedure. After validating the 3D anatomical model, the surgeon and engineer work together to outline the details of the surgery. This phase includes defining surgical access points, osteotomies, correction of deformities, use of bone grafts, and design of specific instruments such as cutting guides and custom implants. In addition, CAD models of available implants, such as distinct types of plates and designed cutting guides, can be imported to verify the accuracy of the surgical plan. The organization of elements into distinct collections within the software facilitates the planning process and ensures more efficient model management.

In orthopedic and maxillofacial surgery, VSP enables accurate planning of the placement and orientation of the cutting planes and the attachment points of the cutting guides to the patient's bone. This approach enables the design of customized bone grafts or scaffolds to replace injured bone segments, correct congenital deformities, or lengthen the bone. Critical parameters such as the correction angle and graft geometry are defined at this stage, with the

ability to create grafts of variable density based on the distribution of bone components such as cortical, trabecular, and medullary.

The planning methodology in Blender begins with importing the clean, simplified anatomical model and positioning it in the workspace to the global reference system along the x, y, and z axes. The "Object Mode" and "Edit Mode" are fundamental to the process: in "Object Mode", elements are treated as unique objects, while in "Edit Mode" the mesh structure, consisting of vertices, edges, and faces, is accessed, allowing detailed manipulation. In this mode, you can select individual parts of the mesh and apply changes such as extrusion or fill. If the imported STL model represents multiple anatomical parts, such as the femur and tibia, you can separate them into independent objects by selecting individual meshes in “Edit Mode” and separating them from the others. The Boolean operations modifier allows operations between objects to obtain the intersection of two objects, to merge them, or to subtract one from the other. These Boolean modifiers are particularly useful for precisely defining the cutting areas of bone structures when simulating osteotomies (Figure 7). The parentage feature also allows objects to be linked together, facilitating coordinated manipulation of complex anatomical structures, such as the bones of a limb, and optimizing surgical simulation. Essential are local and specific reference systems created for individual objects, such as an anatomical axis, for example, the femoral axis, or a plane representing the cutting surface for the osteotomy, around which precise rotations can be performed.

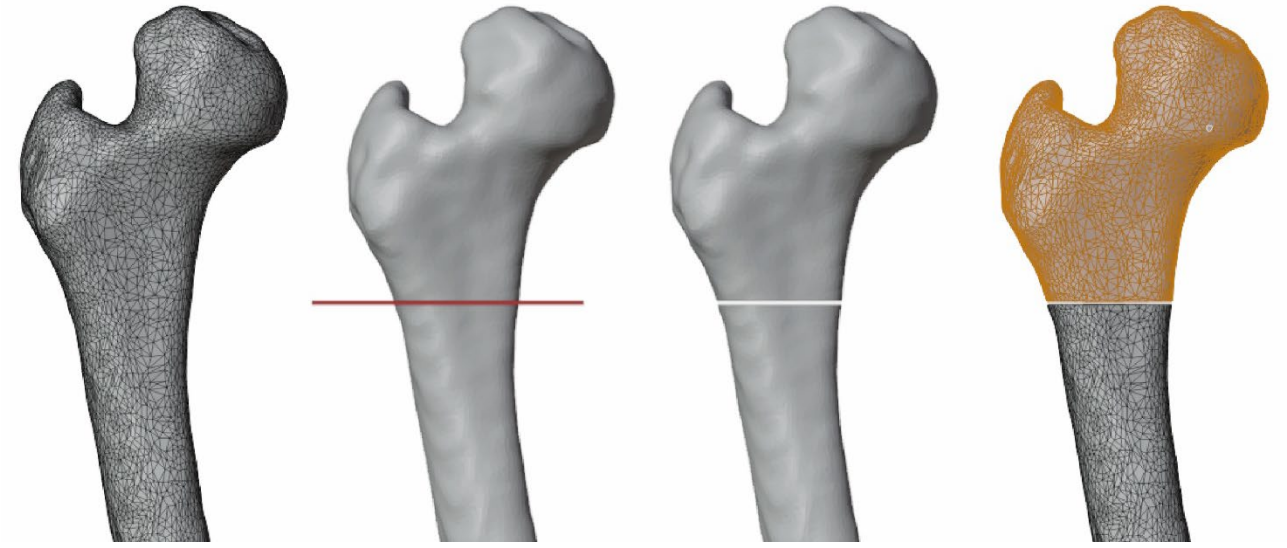

Figure 7. Boolean subtraction operation and mesh separation operation. The first image shows the original triangulate mesh. In the second image, a secondary mesh is positioned as a dividing plane. The third image

illustrates the result of a Boolean subtraction operation, where the dividing plane is used to split the mesh. Finally, the fourth image, displayed in Edit Mode, highlights one of the two resulting surfaces (in orange), which can be separated from the other to create distinct mesh components.

In cardiac surgery, VSP is particularly useful for complex pathologies such as aortic aneurysms, acute aortic syndromes, and congenital coarctation. For example, in aortic dissection, VSP allows precise visualization of the aortic anatomy, identification of pathological channels, and differentiation between true and false lumens. 3D visualization also allows accurate assessment of the surface characteristics of both lumens of the aorta, providing an in-depth view of the pathology under investigation and a valuable aid in planning interventions. This detailed view facilitates the identification of the origin and termination of the false lumen, the measurement of the distance between the two lumens along the aortic arch, and the location of any points of contact between the conduits. Such a realistic and thorough view of the clinical case allows the medical team to plan the most appropriate surgical approach and anticipate any complications associated with the procedure (Figure 8).

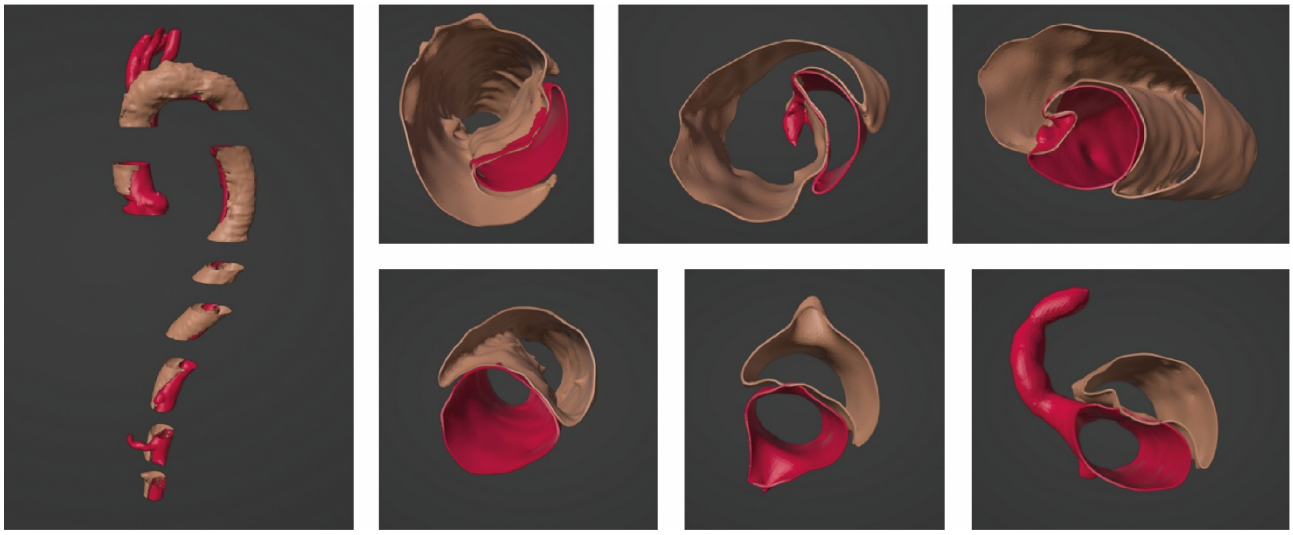

Figure 8. 3D digital representation of the aorta arch for VSP. The false lumen is depicted in red, clearly separated from the true aortic lumen. The digital 3D model enhances the identification of the connection points between the two lumens, improving the accuracy of preoperative planning.

The integration of Virtual Reality (VR), especially in orthopedic surgery, is another way to optimize preoperative planning and make the surgeon's work more autonomous and efficient.

The implementation of VR allows surgeons to interact with the patient's anatomy in a virtual environment, placing landmarks and manipulating three-dimensional objects. These intuitive virtual environments allow them to simulate and evaluate different correction hypotheses, providing the ability to explore and visualize multiple surgical solutions before making a final decision. Unlike traditional simulation systems, where the surgical procedure is often predetermined by software, VR for surgical planning provides direct interaction, giving the user, the surgeon, full control over the planning steps. The surgeon can decide in real-time which steps to follow, where to place landmarks, and how to make necessary corrections, improving the accuracy and effectiveness of surgical planning.
Virtual planning is the basis for the design and fabrication of 3D anatomical models, custom surgical instruments such as cutting guides and implants, and bone grafts.

3.3.2. CAD Modelling

Custom design includes the creation of 3D anatomical models, patient-specific instruments (PSIs), graft-specific instruments (GSIs), and bone grafts, scaffolds, or implants such as plates. Each of these instruments plays a critical role in the success of a surgical procedure. These devices are designed using 3D CAD modeling software such as Blender, PTC Creo Parametric, or nTopology according to the defined preoperative plan. These instruments are designed with the additive manufacturing technology that will be used to manufacture them in mind. Once the design is complete, the digital models are exported in STL format, ensuring a fully accurate export tolerance (approximately 0.1 mm) to ensure the accuracy of the printed model. These models are then sent to the slicing software for 3D printing. It is essential to adopt a CAD-compatible labeling system that clearly identifies the modeled objects and provides indications of use, such as front or back.

Design of 3D anatomical models

The anatomical models processed during VSP are used in preparation for 3D printing, ensuring that the mesh is free of holes and that the export tolerance is appropriate for the complexity of the model. This process ensures that 3D-printed models are accurate.

Design of PSI

PSIs are medical devices designed to improve the precision of osteotomies by guiding the movement of the saw during bone cutting and simplifying surgical procedures. Unlike traditional techniques, which rely heavily on the surgeon's experience, these patient-specific instruments are designed to increase the precision of the surgery and reduce operating time, thereby limiting the use of intraoperative fluoroscopy.

The design process (Figure 9) for the PSIs begins with the identification of skeletal landmarks, which are essential for the accurate positioning of instruments and devices during surgery. A 3D digital model of the bone tissue is then used to create a 0.1 mm offset bearing surface that compensates for inaccuracies resulting from reconstruction from diagnostic images and digital cleaning of the bone surface. The guide does not rest directly on the bone, but on strategic points that provide stability during surgery. The minimum thickness is set at 3 mm to ensure robustness and strength. The design of the guide must consider the specific geometries of the surgical instruments used, such as the saw blade and Kirschner wires. The wires, which range in diameter from 1.6 to 2.5 mm, are used both to orient the bone segments and to fix the screws used to implant the orthopedic plates. To ensure stability, each guide requires at least two guide wires, and their insertion direction is carefully designed to avoid interference during guide application and removal. For example, for fixation in pediatric osteotomies, a 2 mm diameter Kirschner wire is preferred, and for cutting, the saw blade is 0.38 mm thick. Thus, the hole is designed 3 mm. To facilitate blade movement, the closed cutting guides have a slot 1.6 mm wide and 20 mm long, which is sufficient to facilitate blade movement. When bone geometry does not allow for a closed slot, an open guide is used, which provides minimal guidance for cutting, but is less accurate than the closed slot. A reinforcing edge is also provided around both the holes and the slots or invitations for blade insertion. This edge is a minimum of 4 mm.

Finally, the design must consider sterilization requirements. 3D-printed in thermoplastic materials, the cutting devices must be able to withstand thermal stress. For this reason, compact, edge-free shapes with thicknesses greater than 3 mm and calibrated holes to compensate for thermal shrinkage and print accuracy are preferred. Table 1 provides a checklist for designing cutting guides.

Table 1. Checklist of design measures for cutting guides.

Parameters	Value
Offset	> 0.1 mm
Thickness	> 3 mm
Diameter of holes	Wire diameter + 1 mm
Dimensions of saw blade insertion	1.6 mm x 20 mm
Thickness of insert reinforcements	4 mm

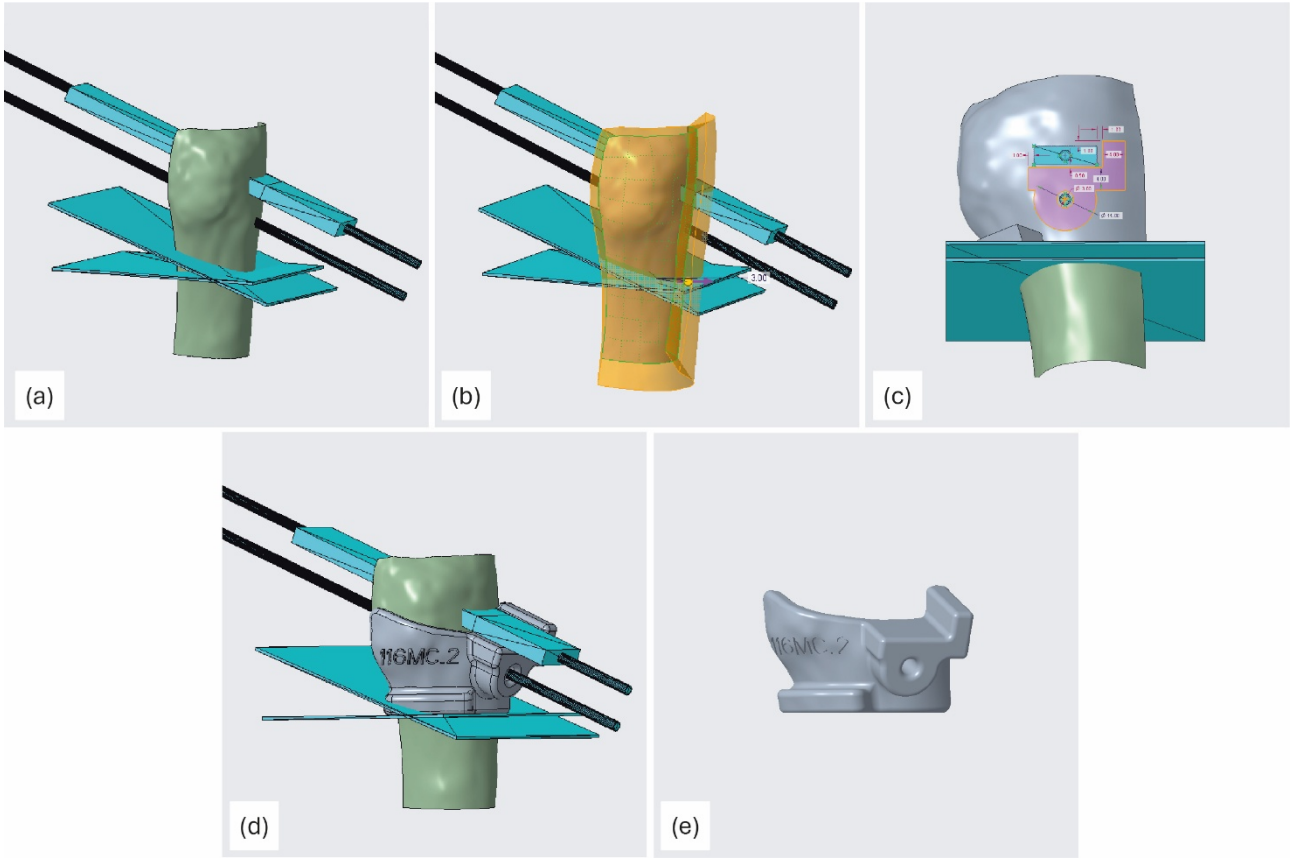

Figure 9. 3D modeling process of a cutting guide. (a) Import geometric references from VSP, (b) apply a 0.1 mm offset and 3 mm thickness, (c) sketch Ø3 mm holes and define blade orientations based on the imported cutting planes, (d) refine the model by adding rounded edges, and (e) export the final model with maximum tolerance accuracy.

Design of GSI

Unlike PSIs, GSIs do not require specific size constraints because they are intended for use with donor tissue that is free of foreign material. However, one of the main challenges in

designing GSIs is the need to avoid perforating the bone tissue with Kirschner wires during fixation of the cutting guide, which makes donor bone manipulation more complex. To maintain alignment between the GSI and the donor bone tissue, musculoskeletal tissue bank (BTM) technicians use a large clamp to secure both the donor bone and the GSI (Figure 10).

Figure 10. Stabilization of GSI by musculoskeletal tissue bank technicians.

Design of bone wedge

Designing bone grafts in Blender begins with placing the bone segments in their final configuration, which is assumed to achieve the desired correction. In “Edit Mode,” select and duplicate the surfaces of the upper and lower bone segments. Next, equalize the number of vertices of the surfaces, making sure that both sides of the wedge have the same number of vertices. To create the side face of the wedge, we connect the vertices of the top face to those of the bottom face using the “Bridge Edge Loops” function. Once modeling is complete, the wedge is exported to STL format for drafting and subsequent 3D printing (Figure 11).

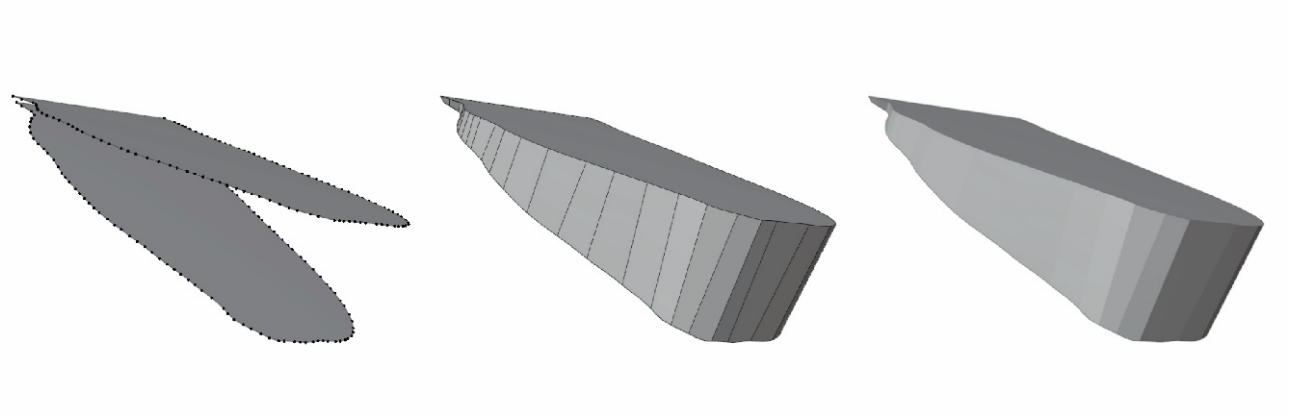

Figure 11. Wedge generation. All vertices of the two surfaces intended for creating a closed surface are selected.

Design of custom scaffolds and implant

A rapidly developing area of research is the design of customized scaffolds that serve as biological or synthetic substitutes to facilitate bone regeneration. These scaffolds, made of biocompatible and inert materials or supplemented with stem cells and growth factors, represent a promising solution for the treatment of complex diseases and trauma, particularly when donor bone tissue is unavailable or incompatible with the required implant. Scaffolds can function as passive scaffolds, colonized by cells from the surrounding tissue, or combined with stem cells to promote regeneration.

The design of scaffolds involves the use of lattice structures that promote cell development and bone regeneration over solid structures. This approach allows the creation of highly biocompatible and geometrically tailored scaffolds that are optimized to promote the formation of new bone tissue, even in areas of significant deficiency. An important advantage of lattice structures is the ability to design scaffolds with different densities based on medical image segmentation that distinguishes different zones of bone tissue (cortical, trabecular, and medullary) using the Hounsfield scale. Correct correlation between bone tissue densities and mesh filling allows for scaffolds with higher density in cortical areas and lower density in trabecular and medullary areas, mimicking the structure of human bone.

Using 3D modeling software such as nTopology, lattice structures are created based on Triply Periodic Minimal Surface (TPMS) structures, such as the gyroid, which are selected for their excellent mechanical and biological properties, making them particularly suitable for implant applications. TPMS lattice structures have the potential to improve osseointegration and

reduce the phenomenon of stress shielding that can cause bone resorption. These structures are particularly promising for applications such as mandibular plates, where uniform distribution of fibers and optimal mechanical properties are critical to prevent implant failure. Although this approach has shown promising results, further specific research is needed before large-scale clinical application.

The specific methodology of this design is described in Experimental Investigations, chapter 5.

3.3.3. 3D printing of custom-made instruments

Custom-made instruments such as anatomical models, PSI, GSI, scaffolds, and implants are manufactured using additive manufacturing techniques (Figure 12).

To produce anatomical PSI and GSI models, FDM technology is used with low- to mid-range printers such as the Bambu Lab and the Qidi Tech i-Mate S, both of which are used to produce objects for medical use. Industrial FDM printers, such as the CreatBot PEEK-300, are used to produce scaffolds from high-performance biocompatible materials. Metal mandibular implants, on the other hand, are produced using Laser Powder Bed Fusion (L-PBF) technology with industrial printers such as the EOS M100. This equipment has been used at several research sites: the Department of Industrial Engineering at the University of Bologna the Pediatric Orthopedics Unit at the Rizzoli Orthopaedic Institute for FDM technologies, and the Department of Materials Science and Engineering at Uppsala University for L-PBF technology.

The designed models are converted into print formats such as G-code, 3mf, or SLI, which can be read by the slicing software of the printers used.

The choice of print materials depends on the technology used and the purpose of the model. For anatomical models, which have a purely aesthetic function, PLA, an inexpensive and easy-to-process material, is used. For PSI and GSI, PLA Crystal is preferred because it can be sterilized in an autoclave, as is done at the Rizzoli Orthopedic Institute. It is important to set a 100% fill density to ensure the robustness of the guides during sterilization and use (Table 2).

Before sterilization, the 3D-printed PSIs undergo a heat treatment to complete the crystallization process of the material. This treatment involves heating in a controlled environment, first at 80°C for 10 minutes, then at 100°C for 50 minutes, according to the heat deflection temperature specified in the material manufacturer's datasheet.

Table 2. 3D printing parameters for PLA and PLA Crystal.

Parameters	**FiloAlfa®** **PLA**	**Fillamentum** **PLA Crystal**
Printing Temperature	200 °C	220 °C
Heated Bed Temperature	60 °C	60 °C
Nozzle Diameter	0.4 mm	0.4 mm
Layer Thickness	0.2 mm	0.2 mm
Printing Speed	60 mm/s	60 mm/s
Travel Speed	200 mm/s	150 mm/s
Infill Density	15 (%)	100 (%)
Flow	100 (%)	100 (%)
Cooling	Yes	Yes
Support	Yes	Yes

Figure 12. 3D-printed custom-made instruments. These include anatomical models, patient-specific and graft-specific cutting guides, fabricated using opaque PLA, and more translucent Crystal PLA.

PEEK, a biocompatible high-performance material, is used to fabricate variable-density scaffolds and requires precise control of the printing parameters to ensure optimal mechanical and thermal properties. Finally, lattice implants are made of powdered titanium alloy Ti6Al4V, which is known for its excellent mechanical properties, biocompatibility, and corrosion resistance, essential characteristics for long-term bone implants. In addition, L-PBF technologies make it possible to produce fine lattice structures that are difficult to achieve with other additive manufacturing technologies. More details on the 3D printing processes of these materials are explained in the Experimental Investigations chapter.

3.3.1. Fabrication of the bone graft

When a bone graft is needed, its geometry is determined based on the VSP, such as a wedge, cortico-spongiosa unit, or diaphyseal segment. Bone tissues used for graft fabrication are harvested from cadaveric donors, processed, and stored in accordance with the National Transplant Center's "Minimum organizational, structural and technological requirements of Tissue Institutes for quality and safety in the donation, procurement, testing, processing, preservation, storage and distribution of human tissues and cells". Musculoskeletal tissues distributed by the Musculoskeletal Tissue Bank (BTM), internal to the Rizzoli Orthopaedic Institute, are always within normal clinical practice, as they are legally classified as transplants and not as medical devices, regardless of the processing performed.

Depending on availability and timing, bone graft processing can follow two different approaches. In the first case, once the main dimensions (length, width, height, and shape) of the required graft are extracted from the VSP, this information is sent to the BTM for manual fabrication of the graft using a two-dimensional dimensional drawing. In this case, there is no specific selection of the graft to be processed; the required graft is simply obtained during normal tissue processing based on the information received. In the second case, BTM provides a set of CT scans of available bone segments for processing, which are then processed for 3D reconstruction. Three-dimensional matching operations are then performed between the desired graft and the available segments, with modifications to the VSP planning based on the selected graft (Figure 13). In this case, graft-specific instruments (GSIs) are also designed and 3D-printed. BTM is responsible for sterilizing the GSIs that will be used in the clean room processing of the graft. Segment processing will be performed using an oscillating saw, taking advantage of the custom models and GSIs.

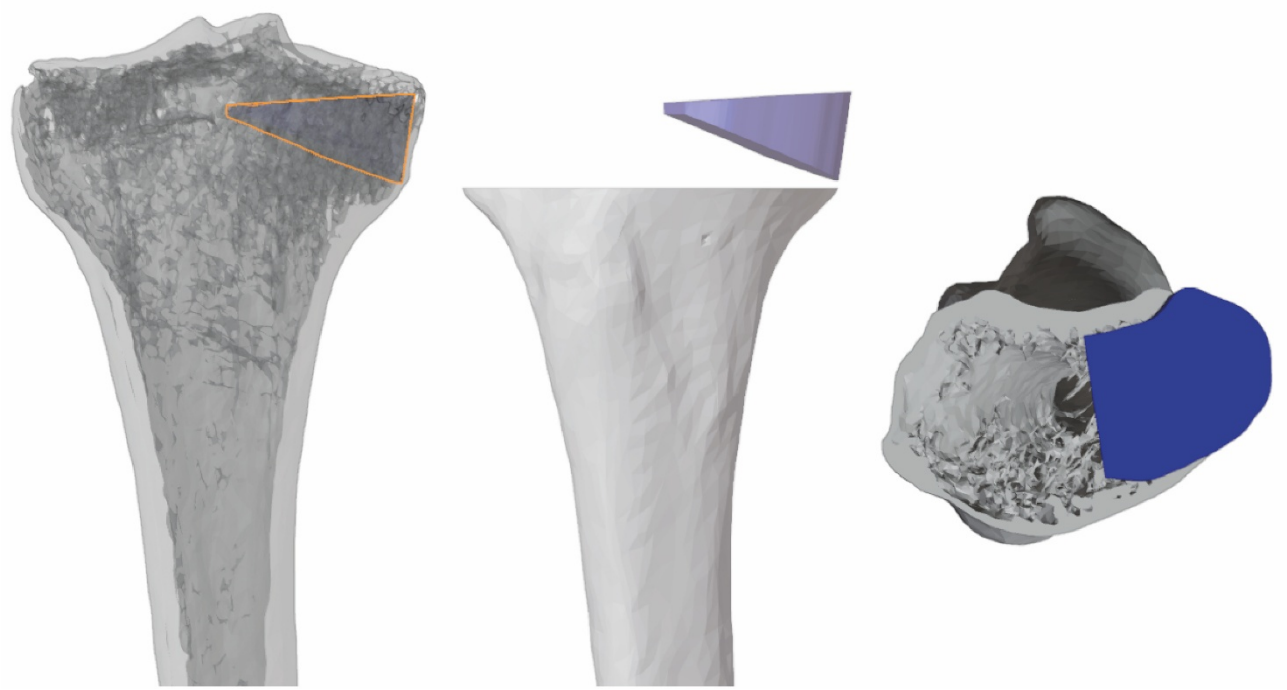

Figure 13. Positioning of the bone wedge planned by VSP. The wedge, derived from the segmented digital model of the donor bone provided by the BTM, is overlayed on the model to analyze its dimensions and geometry, to ensure congruence and suitability for grafting.

In both methods, the design of the allograft and its aseptic processing preserves the cortical portion of the tissue, which is essential to ensure adequate structural support. Graft size and orientation are precisely measured and controlled before sterilization and packaging (Figure 14). A key aspect of this approach is the ability to customize the wedge graft to the patient's unique anatomy. This allows for customized grafts that provide greater construct stability, faster healing, reduced graft failure, and reduced risk of recurrence.

Figure 14. Fabrication and packaging of bone grafts by BTM, compared with respective 3D-printed models.

3.3.2. Sterilization

The sterilization process of 3D-printed surgical instruments, such as surgical cutting guides, is critical to ensure patient safety and prevent infection during surgery. Before being used in the operating room, the instruments must be completely free of contaminants, as any biological or microbial residue could jeopardize the success of the surgery. To achieve this, an autoclave sterilization cycle is used, with alternating phases of vacuum and saturated steam injection.

In the in-house pharmacy of the Rizzoli Orthopaedic Institute, the autoclave cycle begins with temperature and pressure stabilization at approximately 80°C and 94 kPa. Vacuum cycles remove air and reduce pressure to 30 kPa then alternate with high-pressure (180 kPa) saturated steam injection phases. This ensures that the steam penetrates evenly into the most complex surfaces of the cutting guides. After five vacuum-steam cycles, the temperature is gradually raised to approximately 134°C and kept constant during the sterilization phase, in which the pressure reaches 311 kPa. During this phase, the stability of the temperature and pressure parameters ensures the effectiveness of the sterilization process. After sterilization, the slides are thoroughly washed to remove any residues, followed by two drying cycles. The process ends with a final airing step to remove residual moisture. The entire sterilization cycle takes approximately 50 minutes, after which the instruments are packaged and ready to be transported directly to the operating room for scheduled surgery (Figure 15).

Figure 15. 3D-printed PSIs and bone grafts on the operating table.

3.3.3. Visual materials for the surgery

To support the entire surgical planning methodology, a set of visual materials is prepared to guide the surgical steps. Like an instruction manual, these materials illustrate the different steps of the surgical procedure, including the execution of the osteotomies, the correct positioning of the PSIs, the size and specifications of the fixation wires, and the angle corrections to be made. Insertion of the bone graft from the BTM and application of the fixation plate are also detailed, with precise guidance on the screw lengths to be used. These visual aids assist the surgical team in the precise and orderly execution of the planned procedures, helping to optimize operating time and improve patient safety.

3.4. Materials and equipment

During this doctoral research, it was necessary to use a wide variety of materials and equipment, including several pieces of software, each with a specific function. This section aims to detail all the equipment and materials that I had direct access to, highlighting their role in the context of this research.

3.3.4. Software

During the project, several software programs were used, each of which played a crucial role in the various stages of the workflow described above, from segmentation of medical images to 3D design and preparation of files for 3D printing. A key aspect of software selection is the distinction between open-source and commercial solutions, each with specific advantages and limitations. Open-source software, such as inVesalius and 3D Slicer, offers high flexibility and low cost, allowing users to customize functionality according to project needs. However, using open-source software can require a steeper learning curve. In contrast, commercial software such as Materialise Mimics and PTC Creo Parametric offer greater reliability and dedicated technical support at a higher cost. Despite these differences, both types of software produced results of comparable quality during this project, demonstrating that the choice of tool may depend on economic or practical constraints rather than inherent effectiveness.

Medical image segmentation software

Segmentation of medical images is an essential step in the creation of 3D anatomical models. For this purpose, inVesalius, 3D Slicer and Materialise Mimics were used (Figure 16).

The first choice was inVesalius, open-source software with an intuitive interface that facilitates the processing of CT and MRI images. A distinctive feature of inVesalius is its ability to manage multiple file formats, which facilitates integration with other tools.

Next came 3D Slicer, a more advanced open-source platform that is widely used for its versatility. 3D Slicer features a modular architecture that allows users to install only the features and plug-ins they need, making it highly customizable. Thanks to its active community and the wide range of available tools, this software has become standard in both research and clinical practice, especially for manual and automatic segmentation.

In contrast to these open-source solutions, Materialise Mimics is a commercial 3D segmentation and modeling software that is particularly valued for its ISO 13485 certification and CE marking, which attest to its compliance with the safety and quality standards required for clinical applications. In addition, the Food and Drug Administration (FDA) has cleared Mimics for use in clinical decision support. The ability of this software to generate detailed

anatomical models ready for 3D printing makes it an essential tool to produce cutting guides and patient-specific models.

Figure 16. Software used for segmentation.

Virtual Surgical Planning and CAD Modelling software

In the 3D modeling phase required for virtual surgical planning, various modeling software were employed (Figure 17), including Blender, a tool primarily used for graphics and animation. Despite its original use, Blender has shown great versatility in the context of VSP. Because of its advanced modeling capabilities, it was possible to simulate complex surgeries and provide a preliminary view of the expected results, thus improving preparation for surgery.

In addition to Blender, PTC Creo Parametric, a commercial software known for its ability to manage complex geometries and adapt designs to patient anatomy, was used to design specific tools such as cutting guides. Creo Parametric proved particularly effective in managing design changes, providing flexibility and precision in the design of custom surgical instruments.

Finally, nTopology, an innovative software for creating lattice structures and complex geometries, was used for applications requiring weight and performance optimization. nTopology is designed to support generative design, enabling users to develop complex structures that can improve mechanical efficiency and reduce unnecessary material. Its application is particularly useful in the design of custom implants and medical devices where lightweight and strength are critical factors.

Figure 17. Software used for 3D modeling.

3D printing software

A variety of slicing software was used to prepare models for 3D printing, each selected based on the specific printer being used (Figure 18).

For FDM printers, Ultimaker Cura stood out for its ease of use and ability to intuitively configure print parameters, supporting a wide range of 3D printers. The ability to visualize the print path before execution enables the optimization of the final model's quality and reduces the risk of errors during printing.

Another software, Qidi Studio, is specific to the Qidi Tech i-Mate S printer and has similar functionality to Ultimaker Cura but is optimized for optimal performance on this 3D printer manufacturer.

On the other hand, Bambu Studio is an innovative solution that integrates real-time monitoring of the printing process thanks to a camera inside the printer. This feature, combined with the ability to initiate a print remotely via a WLAN connection, allows for more responsive management of operations, improving workflow efficiency.

CreatWare, specific to the CreatBot PEEK-300 printer, facilitates the management of advanced features to optimize the printing of special and complex materials such as PEEK.

For the L-PBF technology used to prepare metal parts for printing, two main software programs were used: Autodesk NetFabb and EOS Print, both of which are compatible with the EOS M100 printer. Autodesk NetFabb is known for its advanced file analysis and repair capabilities, which enable design optimization for 3D printing and improve the quality of the parts produced. It also provides tools for media management and print process simulation, making it easier to identify potential problems before production. EOS Print, on the other hand, specializes in the printing workflow for the EOS system, enabling efficient management of printing processes and easy integration with specific metal materials used in additive manufacturing.

Finally, Lychee Slicer was used to manage printing parameters for SLA technology. This software enables detailed configuration of resin printing parameters to improve the quality and accuracy of final models. Its features include media optimization and media structure density management, ensuring high-quality models and reducing the risk of print defects.

Figure 18. Software used for 3D printing.

3.3.5. 3D printers

The integration of 3D printing into the workflow enabled the creation of custom anatomical models and surgical instruments to facilitate the planning and preparation of surgeries. Throughout the project, a variety of additive manufacturing technologies were used, including fused deposition modeling (FDM), stereolithography (SLA), and laser powder bed sintering (L-PBF). This variety of technologies has allowed the use of different 3D printers, each selected based on specific design requirements and materials needed.

Fused Deposition Modeling (FDM)

One of the most popular and accessible 3D printing methods, FDM technology uses thermoplastic filaments. The process relies on the use of thermoplastic filaments that are heated to a viscous state and then extruded through a nozzle, allowing material to be deposited layer by layer to form the desired three-dimensional object. FDM is popular not only for its ease of use but also for its low cost, making it accessible to a wide audience. One of the key strengths of FDM technology is the wide range of filaments available, including materials such

as PLA (polylactic acid) and TPU (thermoplastic polyurethane). These materials offer different mechanical and thermal properties, making FDM particularly versatile for a wide range of applications, from rapid prototyping to the production of functional components. PLA is known for its ease of printing and biodegradability, while TPU is known for producing objects that are flexible and soft to the touch. However, FDM has several limitations. First, the resolution achieved with this technology tends to be lower than other 3D printing methods, such as SLA or L-PBF. The surface quality of FDM-printed objects may require careful post-processing, such as media removal and surface smoothing, to achieve a smoother and more professional finish. In addition, the final mechanical properties of the product can vary depending on the printer configuration and print settings, affecting the repeatability of the results. Despite these challenges, FDM technology is widely used in the medical field, particularly for creating anatomical models and cutting guides. The ability to rapidly produce customized prototypes and the low cost of FDM 3D printing make it a valuable resource for surgeons and biomedical engineers.

Several FDM 3D printers were used in this research, each selected for its high performance and reliability (Figure 19). The Anycubic Predator is praised for its ease of setup and maintenance, making it ideal for dynamic work environments. The Bambu Lab X1 Carbon was selected for its advanced print monitoring and optimization features, using intelligent sensors and algorithms to continuously improve the printing process. The Qidi i-Mate S, on the other hand, supports a wide variety of materials, allowing for greater flexibility in pattern design. It is important to note that these mid-range printers share some common features, such as a maximum extrusion temperature of around 300°C and a print bed temperature of around 100°C, allowing them to work with a wide range of thermoplastic filaments. The CreatBot PEEK-300, on the other hand, offers excellent performance when printing high-performance materials such as PEEK. This printer is capable of high print temperatures up to 480°C, while the platen can be heated up to 200°C and the hot chamber up to 120°C. This setup creates a highly efficient heat control system, which is essential for processing temperature-sensitive materials and ensuring the dimensional and mechanical stability of printed components. It also features triple thermal insulation and a liquid cooling system to help maintain constant temperatures and prevent distortion during printing.

Figure 19. FDM 3D printers used: (a) Anycubic Predator, (b) Qidi i-Mate S, (c) Bambu Lab X1 Carbon, (d) CreatBot PEEK-300.

Stereolithography (SLA)

SLA technology is based on the use of photosensitive resins that solidify when exposed to an ultraviolet light source. During the printing process, a laser or UV projector hardens the resin layer by layer, allowing for much finer detail than FDM. SLA is particularly suitable for producing high-precision prototypes and detailed models, making it a popular choice in fields such as engineering, medicine, and industrial design. However, SLA printing requires more attention to material handling and post-processing. Printed objects must be washed with appropriate

solvents, such as isopropyl alcohol, to remove uncured resin, and may sometimes require additional treatment, such as curing under UV light, to ensure the strength and durability of the final model. In addition, the resins used in SLA can be expensive and require proper handling to ensure operator safety, as some can be toxic or irritating. Despite these limitations, SLA technology is widely used to create anatomical models where high accuracy and, in some cases, model transparency are required, such as in cardiac surgery applications. In addition, SLA is particularly effective in the production of surgical instruments due to its ability to generate complex details and smooth surfaces.

The Anycubic Photon M3 Max was used as the SLA 3D printer for the research (Figure 20). This advanced model is equipped with a monochrome Liquid Crystal Display that allows for reduced exposure time and longer light source life. The printer supports a variety of resins, including standard resins, high-hardness resins, and transparent resins, increasing application versatility. The printer's robust construction and automatic platen leveling system help ensure high-quality results and ease of use, making it an ideal choice for medical projects.

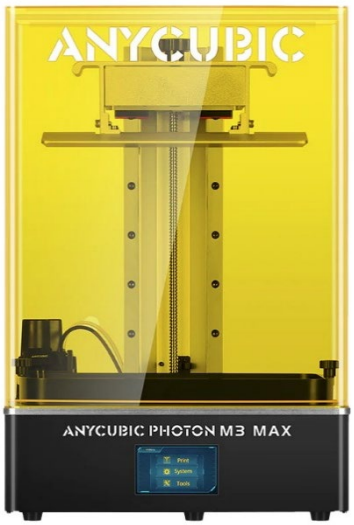

Figure 20. SLA 3D printer used: Anycubic Photon M3 Max.

Laser Powder Bed Fusion (L-PBF)

L-PBF technology is an additive manufacturing process that uses a high-powered laser to selectively fuse powder particles, layer by layer, to create complex three-dimensional objects. This technology is particularly effective when using metal powders, such as titanium alloy, and

enables the creation of complex geometries without the need for substrates, as the un-melted powder acts as a support during printing. One of the main advantages of L-PBF is the strength and durability of the printed objects, which have excellent mechanical properties, making them ideal for industrial and medical applications, such as the manufacture of customized implants and prosthetics. However, L-PBF tends to be more expensive than FDM and SLA, both in terms of machines and materials and requires more attention to dust management.

During research abroad, the EOS M100 was used to print titanium alloy components (Figure 21). The EOS M100 is particularly appreciated for its accuracy and the quality of the finished products, making it ideal for industrial applications. The printer's technical features include a high-power laser system for precise powder fusion, a build chamber optimized for temperature and pressure control, and advanced software for managing and monitoring printing processes.

Figure 21. L-PBF 3D printer used: EOS M100.

3.3.6. Materials for 3D-printing

The choice of materials for 3D printing is primarily determined by the intended use, the required mechanical properties, and the specific applications. Among the wide range of materials available, thermoplastic polymers, resins, and powdered metals are used, each with specific characteristics and distinct advantages. For example, polylactic acid (PLA) and thermoplastic

polyurethane (TPU) are commonly used to visualize and study anatomy, while crystalline PLA, with its resistance to elevated temperatures, is used to make sterilizable cutting guides. Advanced materials such as polyether-ether-ketone (PEEK) and Titanium alloy are used for critical structural applications such as implant and prosthesis manufacturing where high mechanical performance is required.

The relevant printing parameters are determined from the data sheets provided by the manufacturers of each material, which indicate recommended printing temperatures and speeds. Optimizing these parameters requires careful experimentation and verification, especially for unconventional or high-tech materials such as PEEK and titanium.

Biocompatibility is another important consideration when selecting materials for 3D printing, especially in the medical field. Materials such as PEEK and Titanium (Ti6Al4V) are often used to make implants and prostheses because of their excellent biocompatibility, which reduces the risk of adverse reactions in the human body. Scaffold design involves the selection of materials that can withstand specific biological stresses, ensuring that each biomaterial meets stringent mechanical and biological requirements. In addition, some resins can be formulated to have biocompatible properties, expanding their use in the manufacture of surgical instruments.

PLA (Polylactic Acid)

PLA is one of the most widely used polymers in 3D printing due to its ease of use and biodegradability. Made from renewable resources such as cornstarch, PLA offers good surface quality and a wide range of colors, making it a popular choice for prototyping and anatomical modeling. During the research, FiloAlfa® PLA (Figure 22) was used with printing parameters such as an extrusion temperature of 200°C, a hot plate temperature of 60°C, and a printing speed of around 60 mm/s. For the fabrication of anatomical models, a fill density between 10 and 25 percent is set. Depending on the 3D printer used, these parameters vary, such as a higher print speed on the Bambu Lab X1 Carbon.

Figure 22. FiloAlfa® PLA White.

PLA Crystal

A variant of PLA, Fillamentum PLA Crystal (Figure 23), exhibits greater transparency than standard PLA, allowing internal details, such as those of an aortic cross-section, to be visualized and improving the comprehensibility of models during clinical presentations or surgical planning. Increased heat resistance, especially after an annealing process, allows PLA Crystal to withstand temperatures up to approximately 110°C without deformation, making it suitable for more functional applications. Like conventional PLA, PLA Crystal is biodegradable, although it requires industrial composting conditions, and is easy to print with low odor during the printing process. Printing parameters include an extrusion temperature of 220 °C, a plate heated to 60 °C, and a printing speed of 60 mm/s. When used to make PSIs, an infill density of 100% must be set.

Figure 23. Fillamentum PLA Crystal Clear and Emerald.

TPU (Thermoplastic Polyurethane)

TPU is an elastic and flexible material that is particularly suitable for printing anatomical models that require some deformability, such as heart models. In the experiments conducted, clear Recreus Filaflex 82A and TreeD Filaments Pure FT were used to fabricate aortic sections

(Figure 24). Printing parameters included an extrusion temperature of 250°C, a printing plate heated to 50°C, and a printing speed of 60 mm/s. For flexible materials such as TPU, it is critical to optimize retraction, as an inappropriate setting can result in smearing and residual filaments. In this case, retraction was set to 2 mm at a speed of 25 mm/s. Unlike TPU, PLA requires a higher retraction, usually around 4-6 mm, due to its stiffness, to avoid the risk of stringing. Correct configuration of this parameter affects the final quality of printed patterns, improving the sharpness of details in flexible prints.

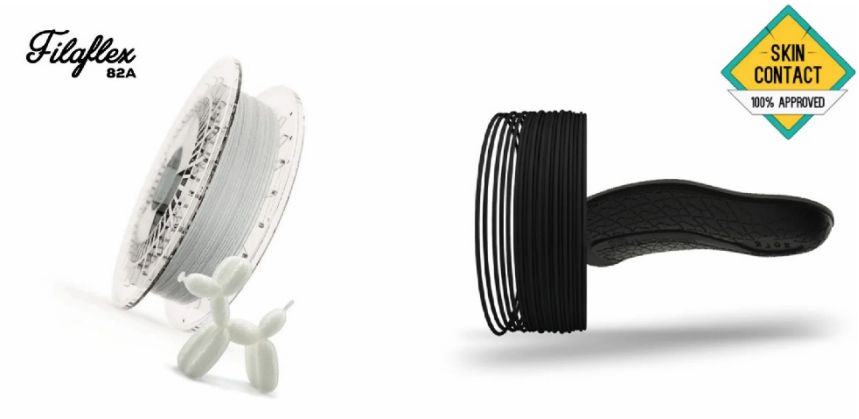

Figure 24. Recreus Filaflex 82A (on the left) and TreeD Filaments Pure FT (on the right).

PEEK (Polyether-ether-ketone)

PEEK is a high-performance polymer known for its mechanical, chemical, and thermal resistance, making it ideal for medical implants and prostheses that require biocompatibility and durability. However, its high melting temperature requires specialized 3D printing equipment. The TreeD Filaments PEEK Nat used in the study (Figure 25) requires careful pre-treatment: due to its sensitivity to moisture, it must be dried at 120°C for 6-8 hours before printing to avoid deformation or print defects. Printing parameters include an extrusion temperature of 440°C, a plate heated to 140°C and a printing chamber maintained at 100°C. It is critical to disable the cooling fan to ensure proper adhesion of the layers and maintain mechanical properties. The recommended print speed is 30 mm/s. In addition, it is essential to use a proper ventilation system to avoid exposure to potentially harmful vapors when printing with PEEK.

Figure 25. TreeD Filaments PEEK Nat.

Resin

Photosensitive resins, commonly used in 3D printing with SLA technology, provide excellent print quality characterized by precise details and smooth surfaces. This study used Anycubic Water-Wash Resin+ (Figure 26), a photosensitive resin that allows for highly detailed models that can be easily washed with water, eliminating the need for chemical solvents. These characteristics make it particularly useful for surgical planning and medical education. However, SLA resins require post-processing to improve the strength of the printed models and must be managed with care due to their toxicity. Printing parameters used included: 3 initial layers (bottom layers) with an exposure time of 25 seconds for each, a lift distance between 4 and 7 mm, and a lift speed of 60-180 mm/min. For the normal layers, the thickness was 50 µm, with an exposure time of 3 seconds, maintaining the same lift and retraction settings. These parameters are essential to achieve the highest accuracy and stability in printed patterns.

Figure 26. Anycubic Water-Wash Resin+.

Titanium alloy Ti6Al4V

Titanium alloy Ti6Al4V is widely used for applications requiring high strength and low weight, such as implants and surgical instruments. Laser powder bed sintering (L-PBF) allows the fabrication of complex geometries that would not be possible with traditional techniques. Titanium is valued for its biocompatibility and corrosion resistance, making it ideal for permanent implants. The printing parameters for Ti6Al4V require high melting temperatures and specific environmental control systems to ensure proper powder sintering. The experiments conducted at the Department of Materials Science and Engineering in Uppsala used Osprey® Ti6Al4V powder (Figure 27) supplied by Sandvik Additive Manufacturing AB (Sandviken, Sweden) with a particle size distribution characterized by d10 = 29.0 µm, d50 = 42.7 µm and d90 = 62.4 µm. The printing parameters used for the alloy included: layer spacing of 0.06 mm, scan speed of 1300 mm/s, laser power of 100 W, beam offset of 0.02 mm, and strip width of 5 mm. The filling (hatching) strategy included alternating scanning along the X and Y axes with rotation at each layer.

Figure 27. Osprey® Ti6Al4V powder.

3.3.7. Extended Reality (XR) platforms

XR technologies were explored to integrate them into virtual surgical planning to assist the surgeon in the decision-making process. This study analyzed a workflow that replaces the traditional use of software such as Blender with an immersive virtual environment in which the surgeon can move and interact with anatomical models in real-time. This approach allows surgical planning tasks traditionally performed by engineers to be performed directly in an

immersive environment, optimizing the workflow from segmentation and image cleaning to surgical planning.

Unity, an advanced graphics engine widely used in the video game industry as well as in simulation and engineering contexts, was chosen for the development of this virtual environment. Unity provides a comprehensive development platform with an intuitive interface and an extensive library of assets and scripts for creating immersive virtual reality (VR) and augmented reality (AR) experiences. These features made it possible to develop a system in which the surgeon can manipulate virtual objects, observe the results of his actions in real-time, and interact fluidly and instantly with the environment.
The implemented system uses several key components to manage interactions with the XR environment. Scripts written in C# and implemented in Unity using Visual Studio Code link user interactions to objects in the virtual scene, enabling operations such as grasping, manipulating, and observing their realistic physical behaviors such as gravity and inertia. In addition, Figma has facilitated the design of user interfaces and interactive prototypes that can be easily imported into Unity (Figure 28).

Figure 28. Software used for XR platform.

The integration of the XR Interaction Toolkit made it possible to easily manage interactions in the XR environment, supporting devices such as VR controllers and motion tracking systems. Specific assets such as the XR Grab Interactable, which allows the user to manipulate virtual objects, and the XR Origin, which synchronizes the real user's movements with those of their virtual avatar, helped to enhance the immersive experience.

Both the Meta Quest 2 visor, due to its widespread use and commercial availability, and the more advanced Meta Quest 3 visor, with its higher resolution, pass-through, wider field of view,

and improved graphics due to the new integrated processor, were used in the research (Figure 29).

Figure 29. Hardware used for XR platform.

The entire system was developed using the OpenXR standard, which provides compatibility with a wide range of XR devices, including Oculus Rift, HTC Vive, Microsoft HoloLens, and AR application frameworks such as ARKit and ARCore. This choice facilitates the scalability of projects and ensures their accessibility on different devices, providing a flexible environment open to future customization and integration.

A key goal of the project was to make the tool accessible to surgeons without advanced training in 3D modeling by focusing on a simple and intuitive interface. In particular, the system has been optimized for pediatric orthopedic applications, with a focus on pediatric musculoskeletal conditions, such as tibia vara, which require precise and individualized surgical planning. The workflow follows the path established during Ph.D. research, from image segmentation to the creation of 3D models of the tibia and the design of customized cutting guides. The implementation of VR technology in surgical planning aims to provide the surgeon with direct and immediate interaction with anatomical models, allowing visualization and simulation of bone deformity correction in an immersive environment, with greater accuracy and autonomy than traditional methods. This system allows the surgeon to manage the correction of bone deformities, reducing the reliance more directly on engineers to manipulate 3D models and improving the overall efficiency of the planning process.

4. Clinical applications at Rizzoli Orthopaedic Institute

Over the course of three years, using the VSP and patient-specific design proposed in the 3D-MALF II protocol, more than 100 clinical cases involving both upper and lower limbs have been treated. This dissertation presents a representative selection of these cases, focusing particularly on lower limb surgeries and specific segments such as the femur and tibia, with varying degrees of complexity and operative approaches. Examples of multi-segmental (involving multiple bone segments) and multi-planar (with corrections in multiple planes) surgeries are given, highlighting the increased complexity and technical challenges faced. Polyfocal cases, in which the same bone segment was treated from different points of intervention, are also presented. Of particular interest was the design of a cutting guide for two bone grafts used on a single donor to meet the need for grafting for two different patients.

All application cases followed the methodology procedure described above, starting with low-dose CT image acquisition, 3D reconstruction of the anatomical model by image segmentation, and mesh lightening to facilitate VSP operations. This chapter will detail VSP operations, the design of PSI and bone grafts, the preparation of material for surgery, and the results of surgery.

The studies were conducted in accordance with the Declaration of Helsinki. Written informed consent was collected from the patient's parents, who also provided consent for the publication of clinical data, including anonymous photos. Parents were informed of the purpose, method, and expected benefits of the study. They were also informed that participation in the research involved no financial benefit and that there was no potential harm that would affect their social status. They were also informed of their full right to refuse to participate in this research, with no consequences for existing or future health care.

4.1. Open-wedge high tibial osteotomy and dome tibial osteotomy

Clinical case description

The first clinical case was a 4-year-old girl with significant knee bowing caused by spondyloepiphyseal dysplasia underwent tibial hemiepiphysiodesis using tension band plates. After two and a half years, her clinical condition had not improved, and radiographic images revealed a slight progression of the deformity (Figure 30). Consequently, an acute correction involving a double osteotomy and structural allograft was planned to use VSP. Two surgeries were performed to correct bilateral deformities. Here is the VSP for the right knee.

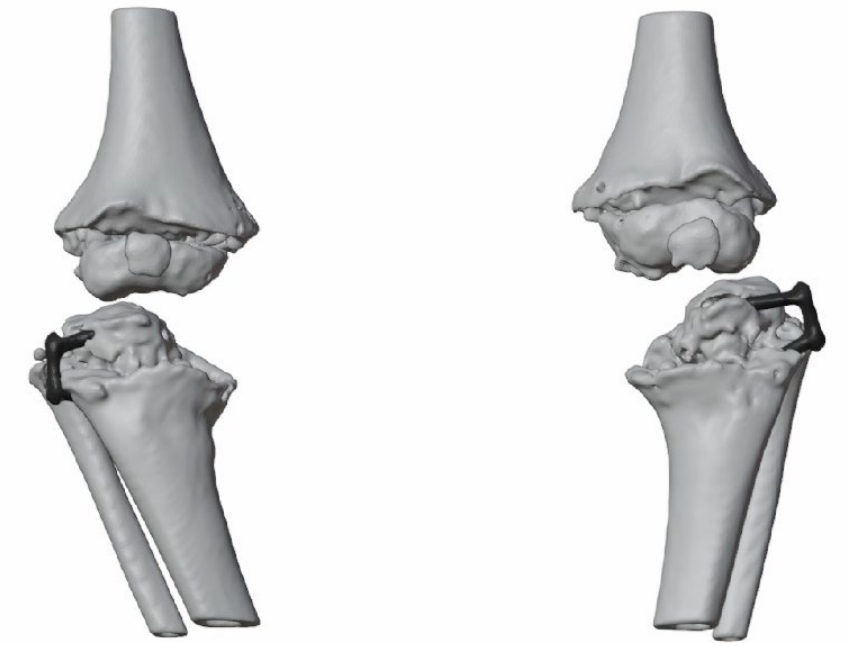

Figure 30. The initial condition of severe genu varum in a 7-year-old girl.

VSP

A double valgus osteotomy was planned: first, a medial open-wedge high tibial osteotomy stabilized with an allograft, and second, a dome osteotomy below the anterior tibial tuberosity. The size and position of the wedge and the placement and radius of curvature of the dome were calculated to achieve a total anatomic tibiofemoral angle (aTFA) correction of 45°.

The proximal osteotomy was simulated by cutting 18 mm from the medial end of the tibia with a 40° inclination to the horizontal axis of the tibia and a depth of 35 mm. The distal osteotomy was simulated as a curved cut 32 mm from the starting point of the proximal osteotomy, with

a radius of 15 mm to ensure a large contact area and low displacement between the osteotomized bone segments (Figure 31). The wedge sizing for the proximal osteotomy was designed and defined to avoid excessive bone stress during insertion, keeping the height below 25 mm and the correction angle below 40° (Figure 32).

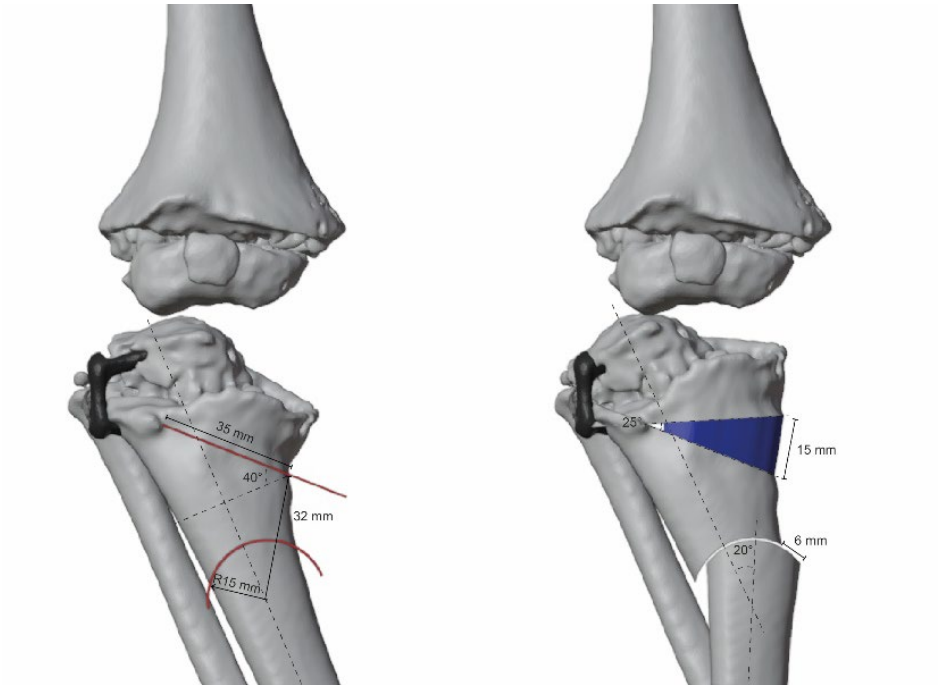

Figure 31. VSP. Definition of cut planes and final planned outcome.

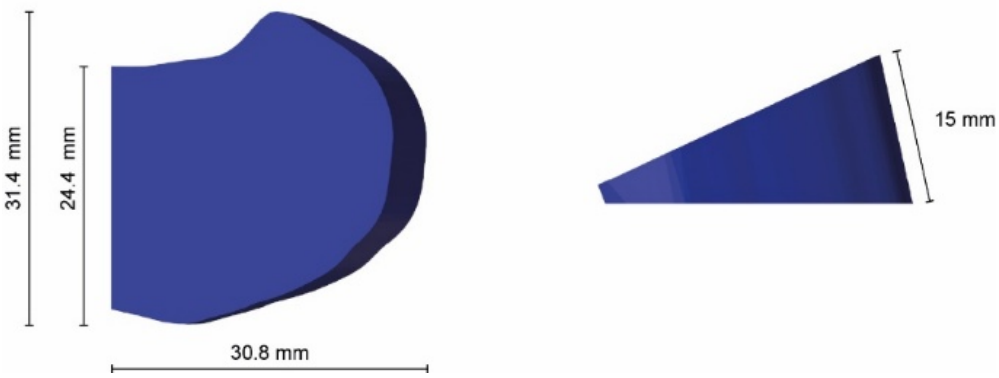

Figure 32. Planned bone wedge.

Fabrication of allograft

VSP allowed the geometry of the allograft to be precisely defined. The Rizzoli Musculoskeletal Tissue Bank was contacted to fabricate the wedge. CT scans of donor bone archived at the

bank were segmented and reconstructed in 3D to manually select the bone segment that best fits the simulated bone wedge, focusing on bone cortical compatibility and wedge curvature. A similar distance between the anterior and posterior portions of the donor tibia was required for good compatibility (Figure 13). The wedge was manually shaped in a clean room according to the bank's standards for processing, preservation, storage, and distribution of bone allografts. Cortical tissue portions were preserved to ensure a load-bearing graft and prepared for implantation before sterilization and packaging (Figure 33).

Figure 33. Fabricated allograft by BMT.

Design of PSIs

Based on the planned correction, two patient-specific PSIs were designed (Figure 34): one for the proximal osteotomy and the other for the curved cut. Both PSIs were designed using PTC Creo Parametric CAD software.

The first cutting guide was designed to ensure geometric stability by conforming to the bone via fixation pins and providing 3 mm diameter holes to ensure proper tolerance during the insertion of 2 mm Kirschner wires and 3 mm thickness. A slot for the saw blade was included, calculated to accommodate its size and to account for lateral oscillations during use. A 15 mm radius was defined for the distal osteotomy to achieve a curved cut that minimizes translational correction while maintaining adequate bone contact after correction. This cutting guide acts as a compass, fixed with a Kirschner wire that is progressively rotated during osteotomy.

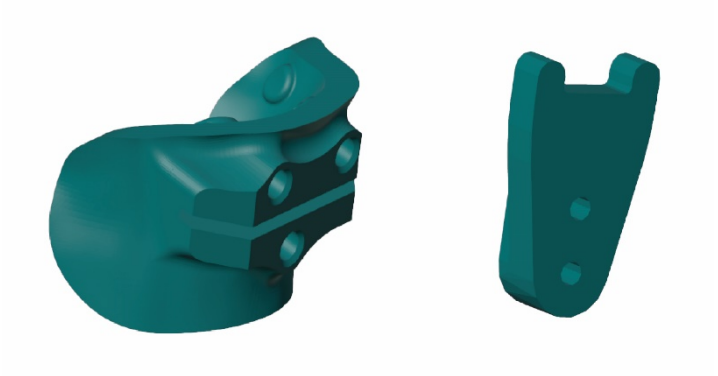

Figure 34. Designed cutting guides, left for proximal osteotomy, right for distal osteotomy.

3D printing of PSIs

Pre-operative and post-operative anatomical models were 3D-printed (Figure 35). This is the first clinical case in which PLA cutting guides were produced using FDM 3D printing technology (Figure 36). The guides were then sent to the sterilization center.

Figure 35. 3D-printed anatomical models.

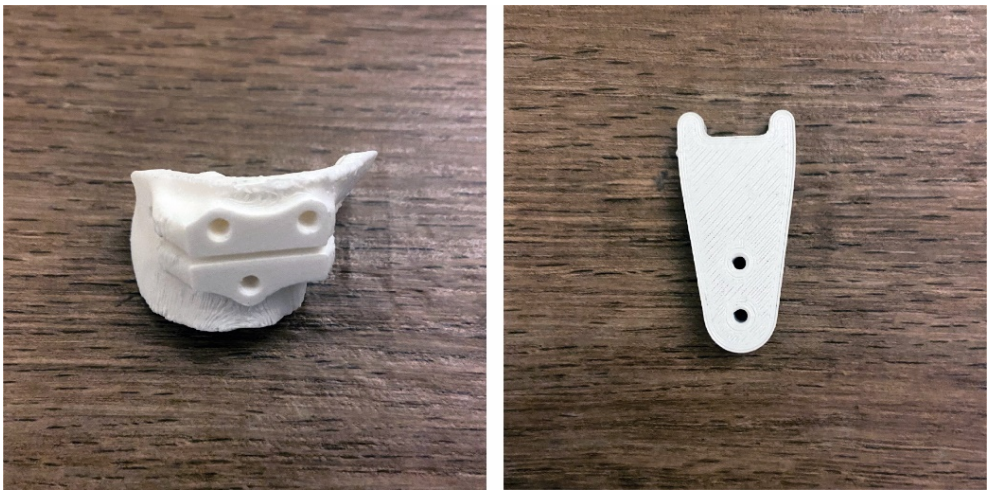

Figure 36. 3D-printed PSIs in PLA.

How to use

The bone at the proximal tibia is skeletonized to place the first cutting guide and secured with three Kirschner wires. The first osteotomy is then performed (Figure 37). A spreader and chisel are used to create space for the allograft (Figure 38). The second cutting guide is then placed 35 mm from the first cut, and the compass guide is fixed in rotation with a Kirschner wire. Using a 10-mm wide blade and rotating the compass, make as many cuts as necessary to complete a dome osteotomy (Figure 39). Finally, the planned angle correction is completed.

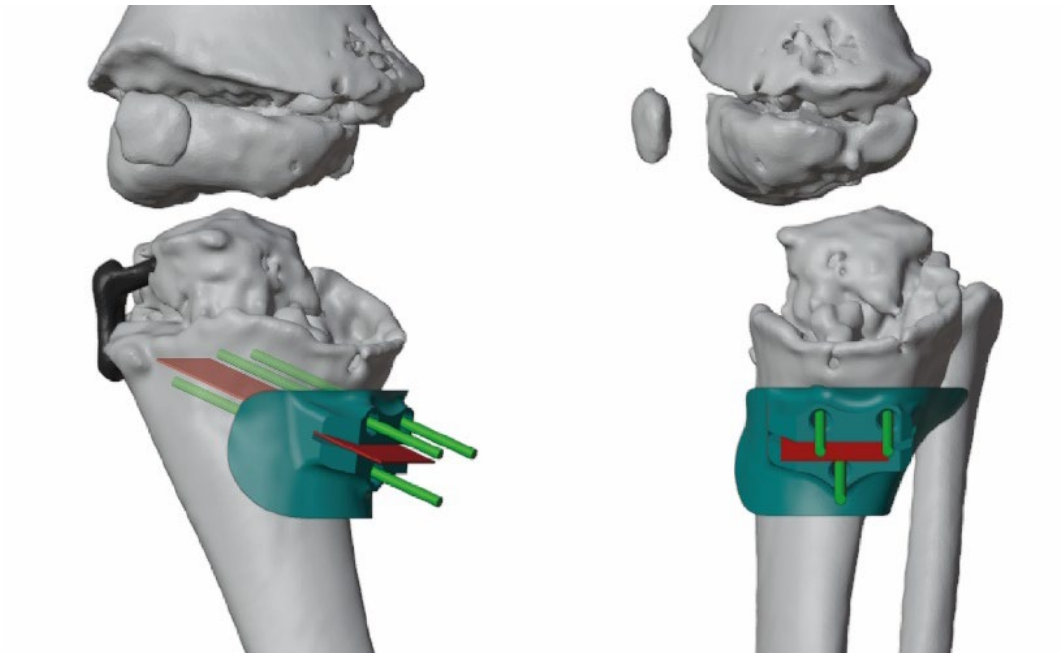

Figure 37. Place the first cutting guide and perform the osteotomy.

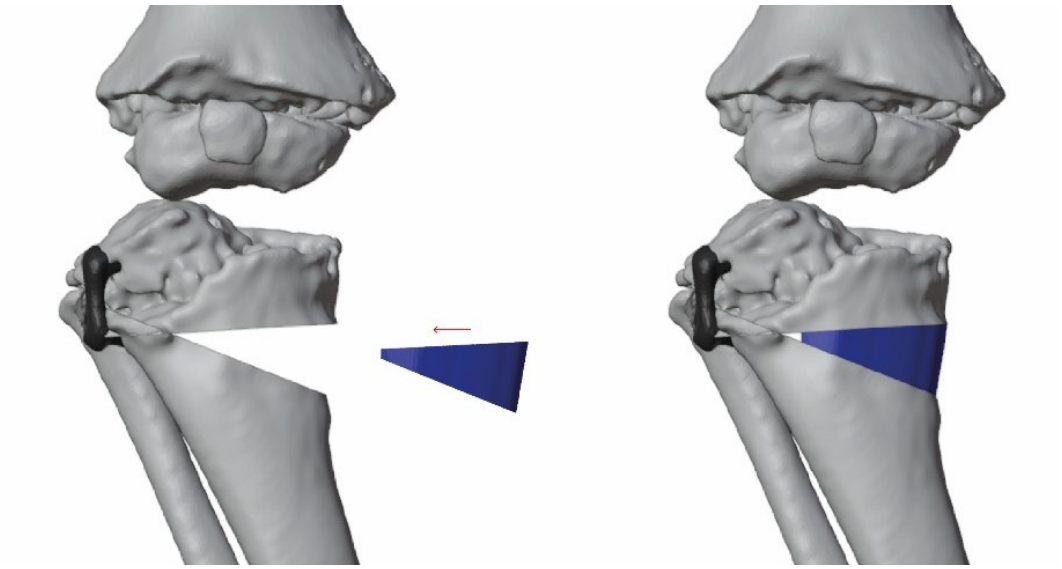

Figure 38. Allograft insertion.

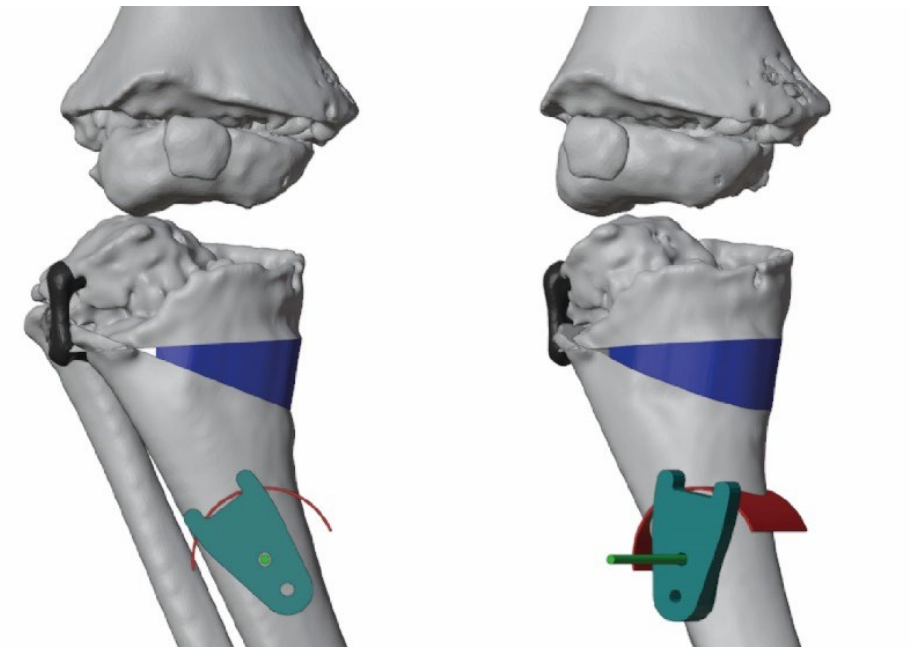

Figure 39. Placement of the second cutting guide and execution of the dome osteotomy.

Post-operative considerations

Despite a slight deformation of the PLA cutting guides for the proximal osteotomy, causing narrowing of the holes and blade slot, the first PSI was used with a thinner blade and smaller diameter Kirschner wires (Figure 40).

Intraoperative fluoroscopy was used to verify the direction of the wires and the cut, emphasizing the need to verify the cut before final execution. However, the cutting guide provided accurate direction for the proximal osteotomy (Figure 41).

The allograft wedge was implanted without intraoperative complications, and the osteotomies were stabilized with two 2.0 mm crossed Kirschner wires. Intraoperative fluoroscopy confirmed a final radiographic result very similar to the preoperative plan, showing a slight hypocorrection due to the surgical strategy and not the VSP (Figure 42).

Figure 40. 3D-printed cutting guide on the surgical table.

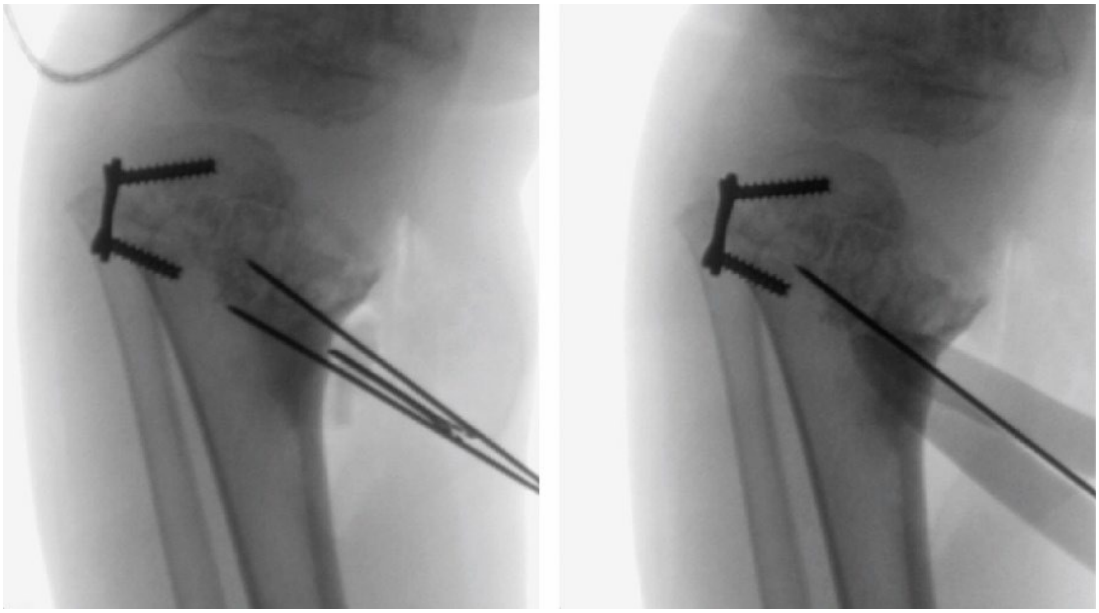

Figure 41. Intraoperative fluoroscopies to verify the direction of the guide wire.

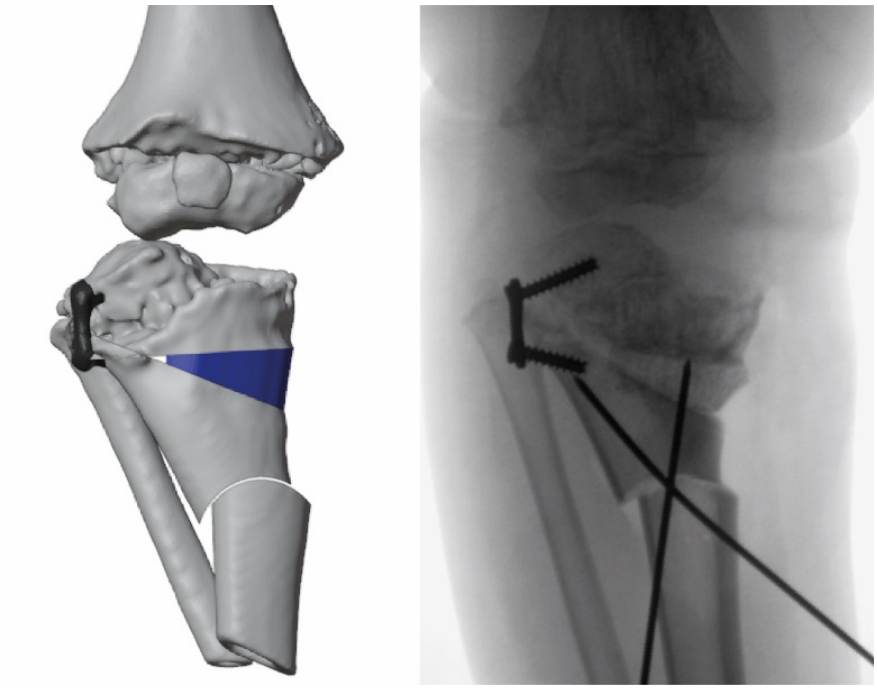

Figure 42. Comparison between surgical planning and the outcome.

4.2. Closing-wedge femoral osteotomy

Clinical case description

A 3-year-old, 2-month-old patient was treated for a unicameral bone cyst located in the left femoral neck. The presence of the cyst resulted in multiple fractures from the onset of ambulation that caused progressive varus deformation of the femoral neck. Under normal conditions, the frontal angle between the femoral neck and the diaphysis of the femur varies between 125° and 135°. A varus deformity reduces this angle below 125°; in this case, the angle was 110°. In addition to treating the cyst by filling it with bone substitutes, correction of the deformity by valgus osteotomy of the proximal femur was planned.

VSP

The surgical procedure involves performing osteotomy with the removal of a bony wedge at the level of the small trochanter. Two cuts were simulated with the VSP: one perpendicular to the bony surface, located at the level of the small trochanter, and a second one inclined 20°, at about 8 mm from the first one. After removal of the wedge, the proximal femur was rotated 20° to allow proper placement of the stabilization plate (Figure 43 and Figure 44).

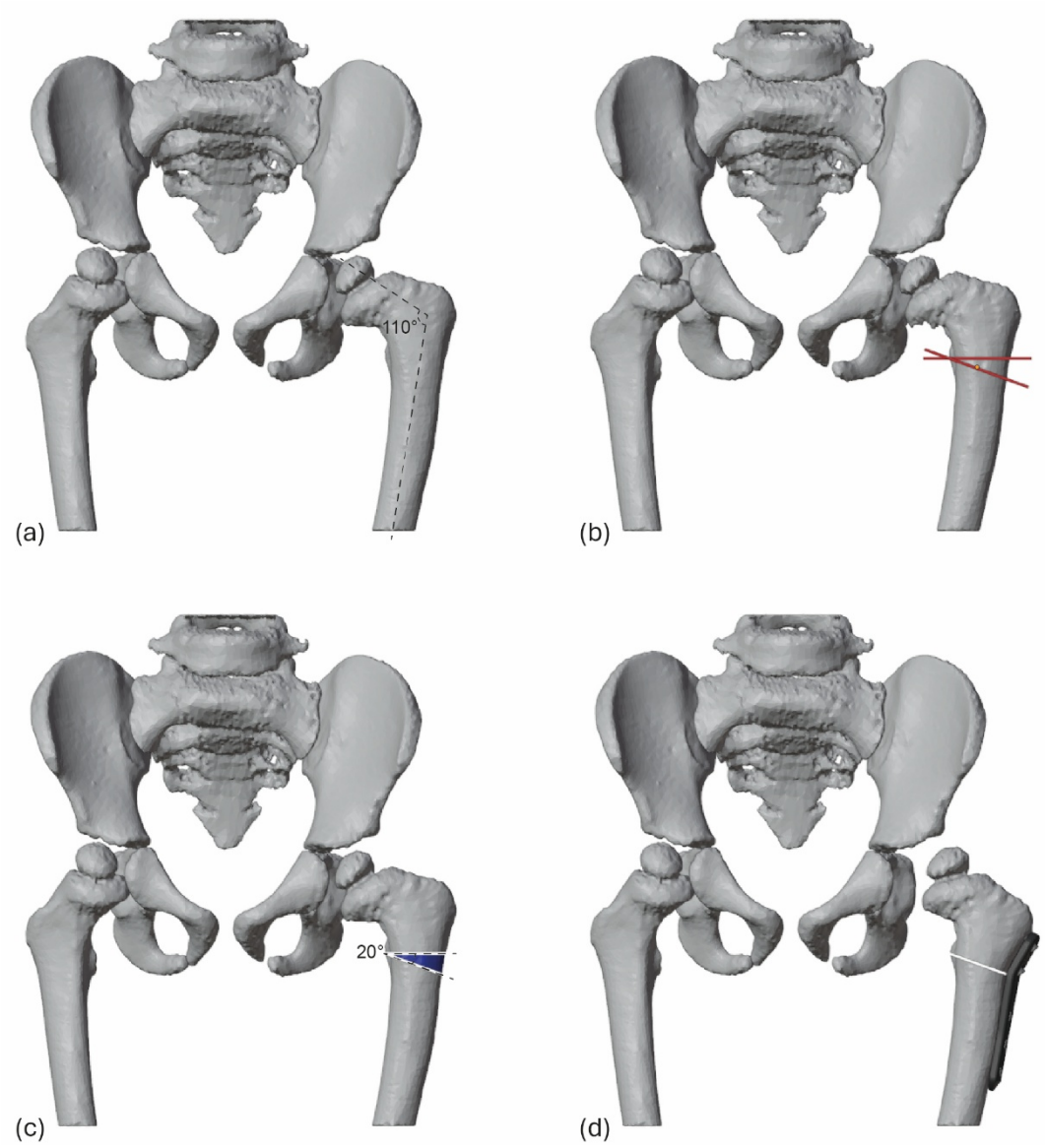

Figure 43. VSP: (a) calculation of femoral angles; (b) set of cutting planes; (c) definition of the closed-wedge; (d) simulation of the final correction.

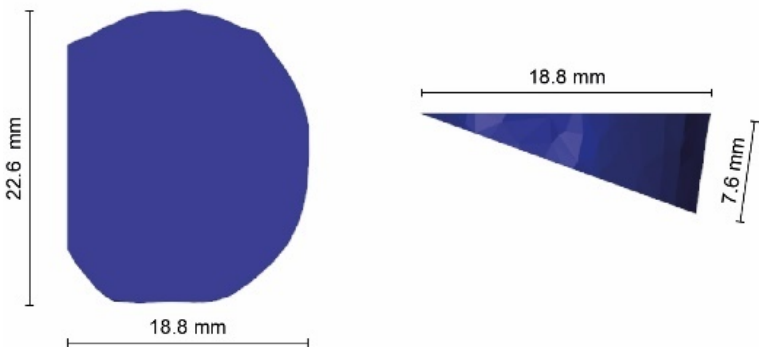

Figure 44. Closed-wedge defined by VSP.

Given the early age of the patient, and consequently the small size of the bone, good precision in the placement of both cuts and screws was essential. This virtual procedure allowed the medical staff to immediately visualize the effect of the various steps of the operation and to estimate with good accuracy both the extent of the correction achieved and the effectiveness of the chosen plate.

In this case, the plate used was the Locking Proximal Femur (LPF) Infant having an inclination of 130°, zero offset, and 3 holes, which is then modeled on PTC Creo Parametric starting from the known and detectable measurements, exported in STL format and placed on the 3D model of the case to evaluate the sizing of the screws to be used (Figure 45). Crucial is the precision of the placement of the holes and their orientation to ensure the accuracy of the directions of the initial guide wires that will be inserted. The modeling of the plate also allowed an easily 3D printable model to assess the various planning steps on printed models.

Figure 45. Placement of the plate and screws.

Design of PSIs

Considering the early age of the patient, one of the main critical issues was the extremely close placement of the screws and cuts, which have incident directions. The design of PSIs for osteotomy presented some critical issues due to both the small size and the mutual directions

of wires and cuts. The proximity between proximal cut and guide wires, as well as the interference between their directions, has undermined the design of a single cutting guide or with a closed slot for blade insertion. The proximity between the guide wire holes and a hypothetical slot for the cutting guide would prevent the practical use of the guide and impair its resistance to thermal deformation.

To optimize the procedure, the position of the endplate with its screw placements was exploited to derive the references for the fixation wires of the cutting guides, to take advantage of the same screw holes for the fixation wires and thus avoid drilling the patient's bone in multiple places, weakening it.

A total of three PSI was designed. The first PSI was shaped to include references for the insertion of three guide wires: two wires for correct plate placement and one coincident with the proximal screw of the plate. The use of three guide wires allows for good stability of the PSI once it rests on the bone, preventing unwanted displacement. Proper placement of the wires in the epiphysis of the femur is critical to the procedure. The first PSI of application of the guide wires was designed so that it had sufficient size to encompass a substantial portion of the surface of the bone, facilitating precise placement (Figure 46).

Figure 46. The plate and the first designed cutting guide show the references of the three guide wires holes.

The other two PSI for each cut fit into the three guide wires inserted with the previous PSI. These cutting guides are equipped with a handle for ease of use by the surgeon. The handle is molded with a thickness of 4.5 mm and a length of 150 mm.

The choice was also dictated by the familiarity of the shape compared to similar existing instruments. The size of the PSI was limited by both the small size of the bone and the fundamental need to maintain support at an appropriate distance from the growth line. The size of the PSI must still be small and proportionate to the geometry of the bone. Excessive size and thickness would limit the practicality and immediacy of the instrument.

The PSIs also show where to place the saw blade to make the two cuts. The first cutting guide is designed to guide the proximal cut, while the second is designed to guide the distal cut (Figure 47). All PSIs were fabricated with 3-mm diameter holes, sufficient to ensure the passage of 2-mm Kirschner wires, and were appropriately rounded and fitted with support feet to rest on the patient's anatomy.

Figure 47. Cutting guides designed for proximal and distal osteotomies.

3D printing of PSIs

The anatomical model of the femur and the PSIs were printed by FDM 3D printing for speed with 20% infill to physically evaluate the planned procedure (Figure 48). The anatomical model, including the cuts to be made, was printed as an assembly. This prototyping phase also allows the identification of design flaws that are not always easily visible in the CAD environment, as well as a realistic view of the thicknesses and overall dimensions. This allowed the medical staff to evaluate the model at the various stages of the operation in all its phases and to suggest any changes necessary to improve the instruments designed. The final models of the PSIs were

then printed in PLA Crystal and heat-treated before being sterilized and delivered to the hospital pharmacy for surgical use (Figure 49).

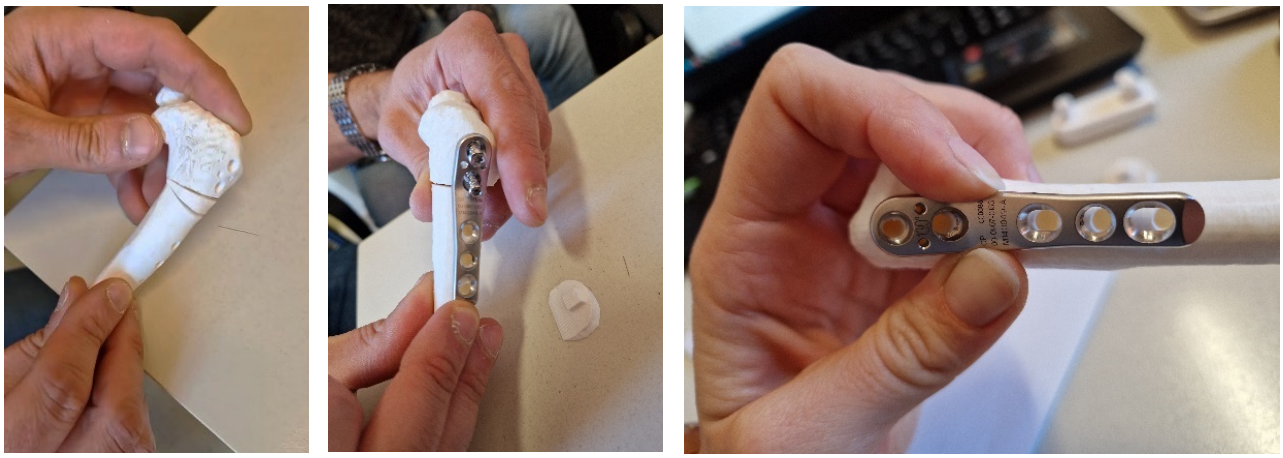

Figure 48. Testing of planning with 3D models and necessary instrumentation.

Figure 49. 3D-printed PSIs made of PLA Crystal, sterilized and prepared on the operating table.

Slight deformation of the handles was observed after sterilization. However, this did not affect the functional effectiveness of the instruments, suggesting that future versions should have thicker handles and shorter lengths to avoid deformation due to heat treatment. Analysis and

testing during prototyping revealed the need to keep the functional components of the instruments compact and solid.

How to use

Before surgery, the indications for the use of PSIs, how to place them, and the main steps of the surgery that they entail have been established. Once the femur is skeletonized, the first PSI is placed and the three Kirschner wires are inserted. Information on wire placement is provided, as well as information on PSI placement, both for the superior end of the femur (greater trochanter) (Figure 50).

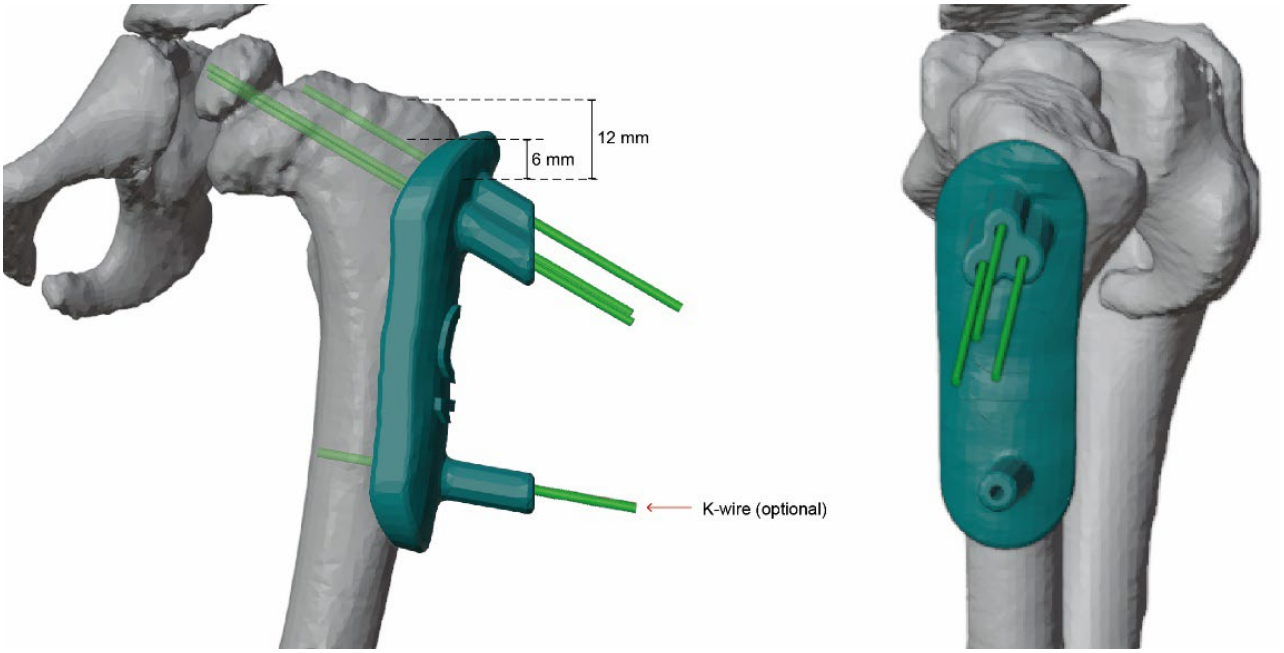

Figure 50. Positioning of the first PSI and guide wires.

After the wires are inserted in the same direction, the first PSI is removed and the other two cutting guides are inserted distally and proximally, respectively, by simply inserting them into the previously inserted guide wires. The positioning of these cutting guides is uniquely determined by the previously inserted guide wires (Figure 51 and Figure 52).

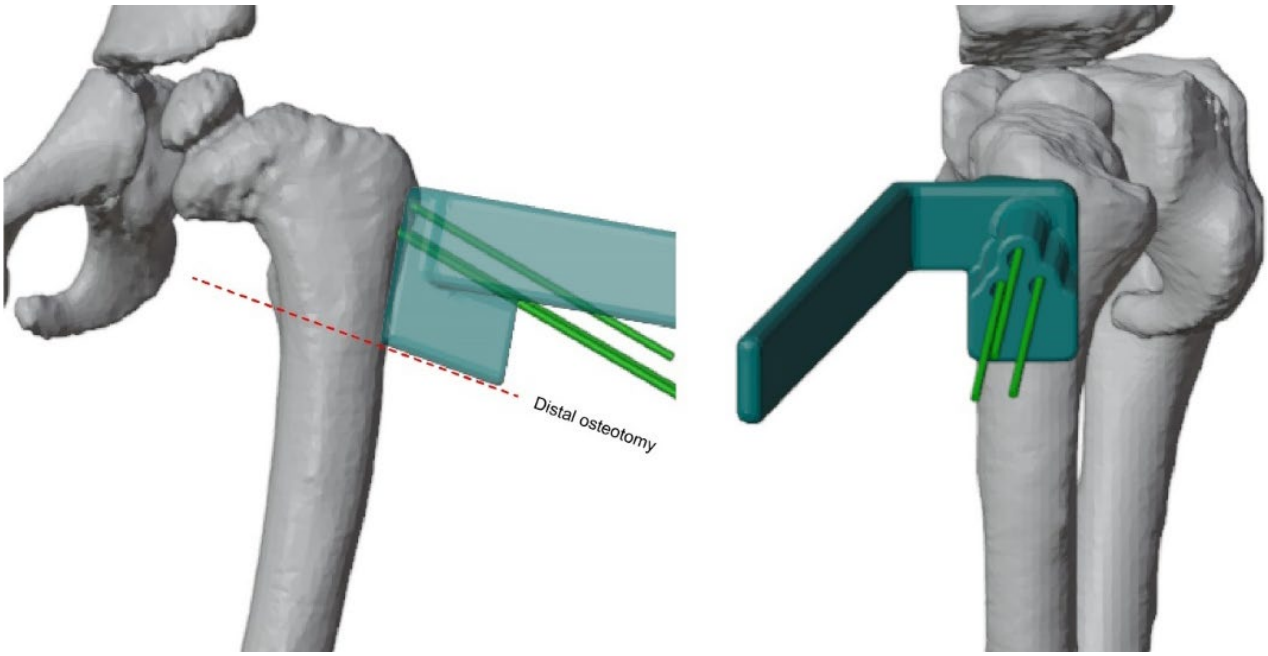

Figure 51. PSI for distal osteotomy.

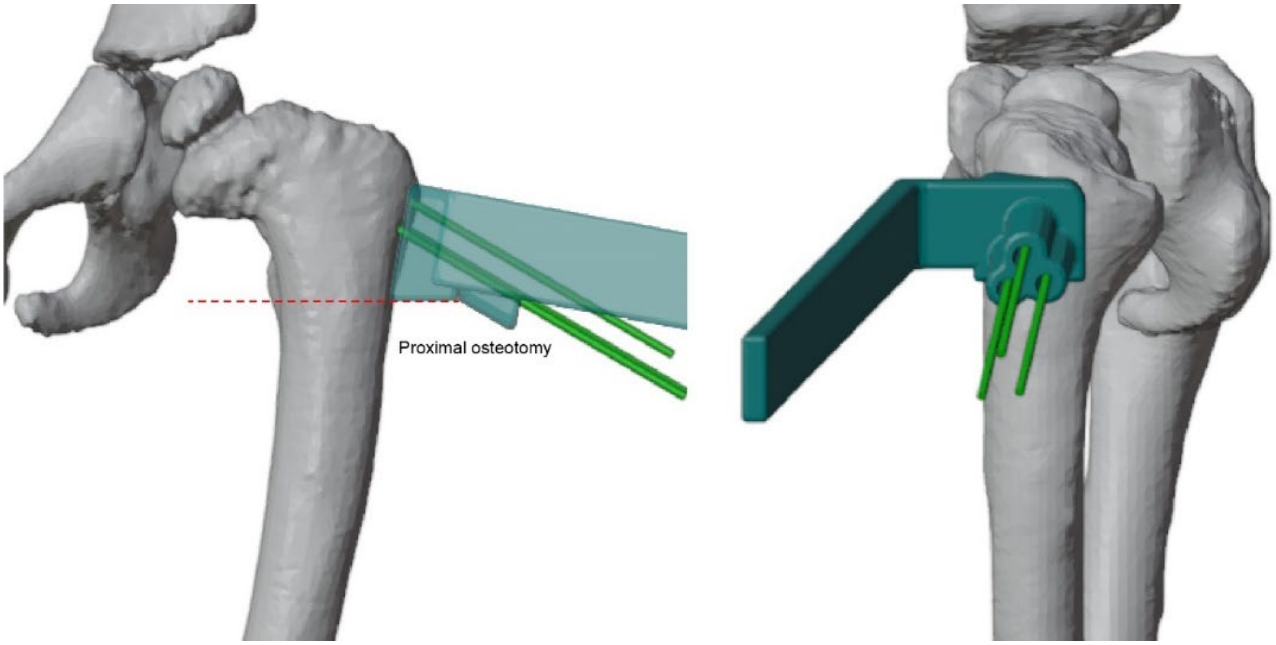

Figure 52. PSI for proximal osteotomy.

Post-operative considerations

The CT images used for preoperative planning and cutting guide design were taken approximately two months before surgery. This time discrepancy was a critical issue during the surgical procedure. Comparing the preoperative radiographs with the previously acquired CT

images and considering the patient's age, 3 years, there was a significant progression of the pathology resulting in a change in the anatomical defect. Consequently, it was necessary to promptly re-evaluate the applicability of the preoperative plan. During surgery, the 110° deformity measured two months earlier had increased to 120°. This change in rotation required repositioning the cutting guides, lowering them 3 mm from their original position, and increasing the planned wedge height to 9 mm. This reevaluation allowed the cutting guides to be used for proper guide wire positioning.

This case highlights the need to reduce the time between imaging and surgery, as well as the planning and preparation time, especially in pediatric patients. The usefulness and efficacy of "patient-specific" tools are closely related to the accuracy and timeliness of planning. For this to be effective, it must be based on recent data that does not show major anatomical changes. Intraoperative fluoroscopy was used to evaluate the effectiveness of the planning and the correct execution of the surgery (Figure 53 and Figure 54). Using the designed cutting guides, the necessary guide wires could be inserted, ensuring correct orientation and centering in the femur. To verify the accuracy of the cuts, control wires were inserted before proceeding with the actual cut. The final plate position also closely matched the planned simulation.

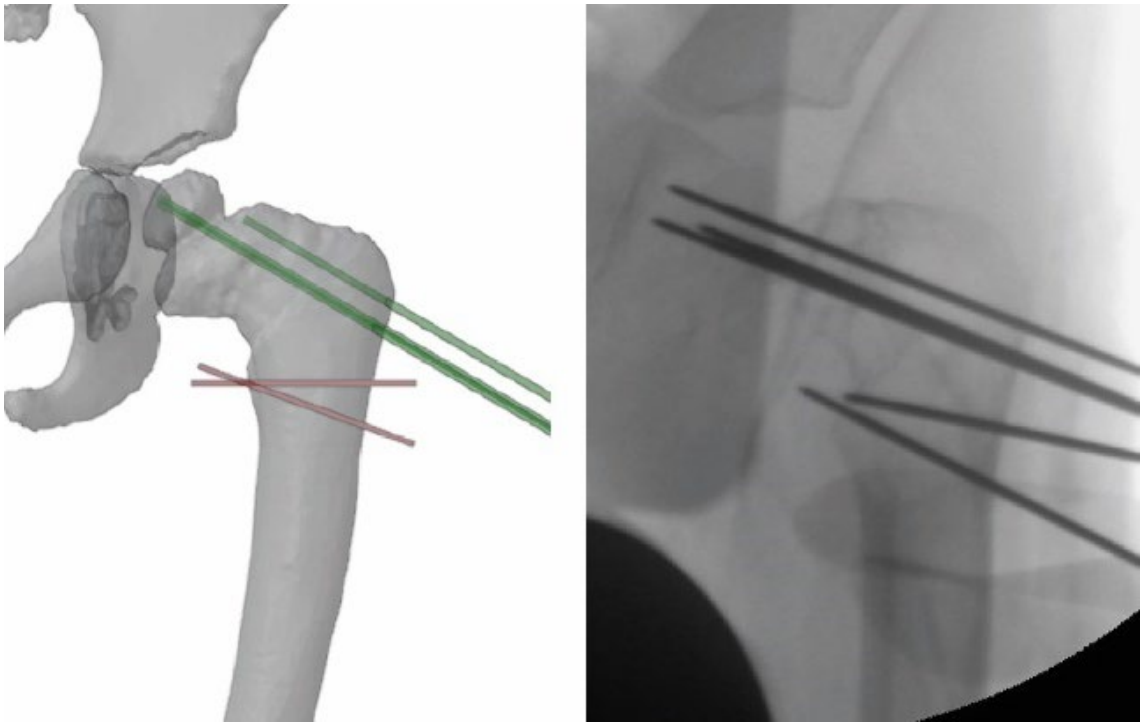

Figure 53. Comparison between surgical planning and intraoperative fluoroscopy, showing the alignment of guide wires and cut directions.

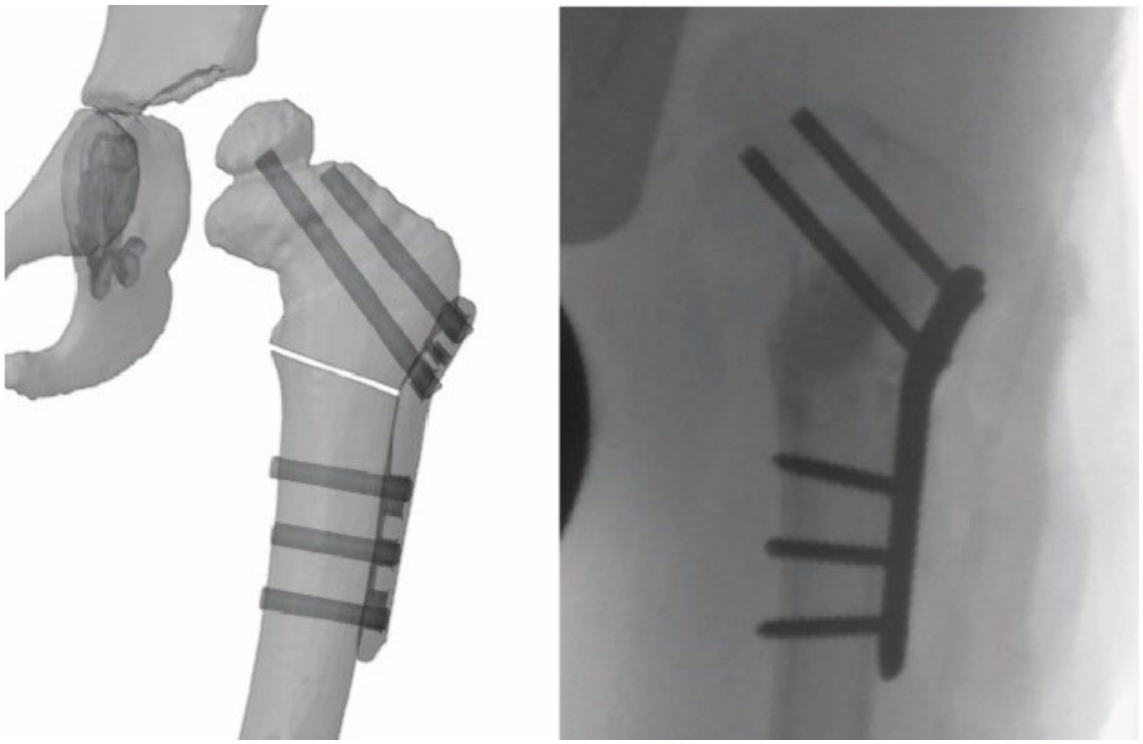

Figure 54. Comparisons between planning and intraoperative fluoroscopy, showing the final correction.

The results obtained in terms of planning can be considered satisfactory, despite the rapid evolution of pediatric pathology. The designed instruments were used effectively, despite the anatomical variations observed and the consequent need to re-evaluate the planning. The operation was completed with a total of 21 intraoperative fluoroscopies.

4.3. Femoral varus derotational osteotomy

Clinical case description

A 3-year-old, 7-month-old patient with Perthes' disease of the right hip. The disease involves necrosis of the femoral head resulting in deformity of the hip joint. In these cases, a centration osteotomy is planned in which the femoral epiphysis is placed completely below the acetabulum. The osteotomy is usually performed with a linear incision just below the femoral neck. The proximal fragment of the femur is variated (at an angle of less than 125°) and the anteversion of the femoral neck is reduced by 10°.

VSP

Because of the patient's early age and having already found the need to reduce the time between the receipt of CT images and the planning and design of surgery to ensure accuracy, image segmentation and virtual surgical planning (VSP) were conducted promptly.

The previously modeled 3D model of the blade plate is also imported into the simulation environment to verify its effectiveness and placement in the affected bone. By directly inserting the plate into the model, it was possible to evaluate the exact dimensions and placements of the screws and guide wires directly on the bone model. This made it easy to identify all the reference points necessary for subsequent modeling of the PSIs.

A cutting plane was placed under the small trochanter to simulate osteotomy, allowing rotation of the proximal femur fragment to align with the inner surface of the plate, without any wedge removal.

The chosen plate, a Locking Cannulated Blade (LCB) Child, has a length of 40 mm, a 90-degree angle, and a 6-mm offset. After positioning the blade plate, screws were inserted to determine the correct length and direction.

To obtain all the necessary references for modeling the PSIs, a reverse process was performed, from blade plate placement to model rotation while maintaining the parent link between the model and collocated plate (Figure 55).

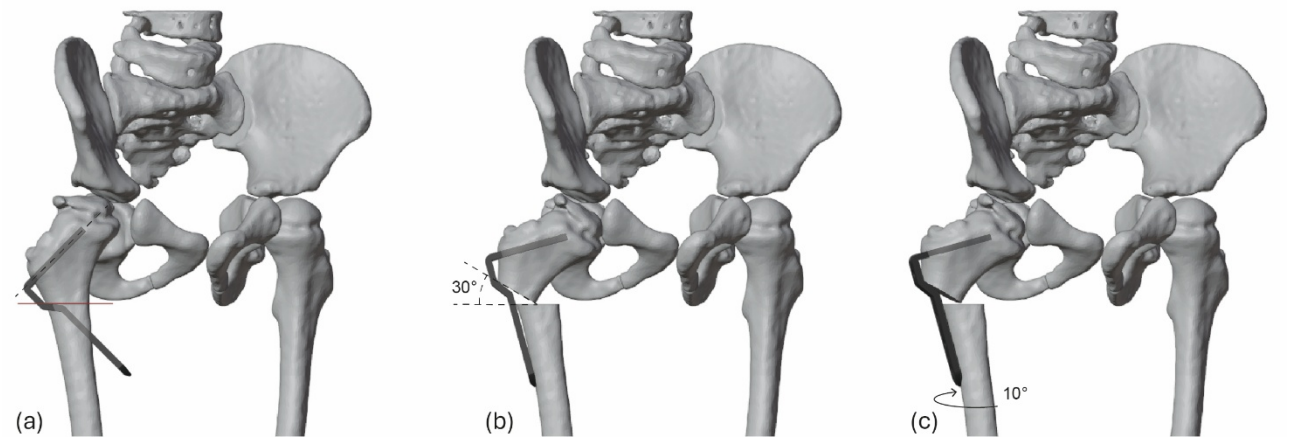

Figure 55. VSP to obtain plate blade placement and corrections. (a) Initial position of the blade plate, obtained through the reverse process of VSP; (b) execution of the varus osteotomy; (c) application of the derotational correction.

Design of PSIs

For the design of the PSIs, references were taken from the original anatomical model after VSP. One of the objectives was to limit the number of unnecessary holes in the bone by taking advantage of the references already provided for blade plate placement in the design of the cutting guides as well. To this end, the two guide wires for the cutting guides corresponding to the two control holes on the blade plate were selected (Figure 56).

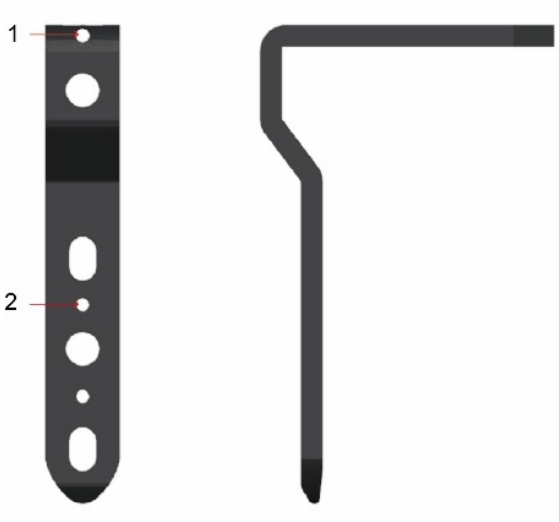

Figure 56. Holes for guide wires as reference for cutting guides.

The study of traditional surgical techniques has identified critical points that can be improved using customized cutting guides. The main problem encountered concerns the correct positioning of the initial guide wire, on which the blade plate is placed. Another critical issue is the determination of adequate references to ensure proper rotation of the femur. For this purpose, the second distal guidewire was exploited. In the preoperative phase, the two guide wires are not parallel, but their subsequent realignment ensures a planned rotation of the femur of 10° (Figure 57). The designed cutting guides are aimed at directing both the initial guide wire for the blade plate and the correct rotation of the femur after osteotomy. Multiple cutting guides were designed because of the different angles between the guidewires, which reduces unwanted movement of the guides during their removal and execution of the osteotomy. To model the second guide, we imported the reference of the chisel whose direction coincides with that of the initial guide wire (Figure 58).

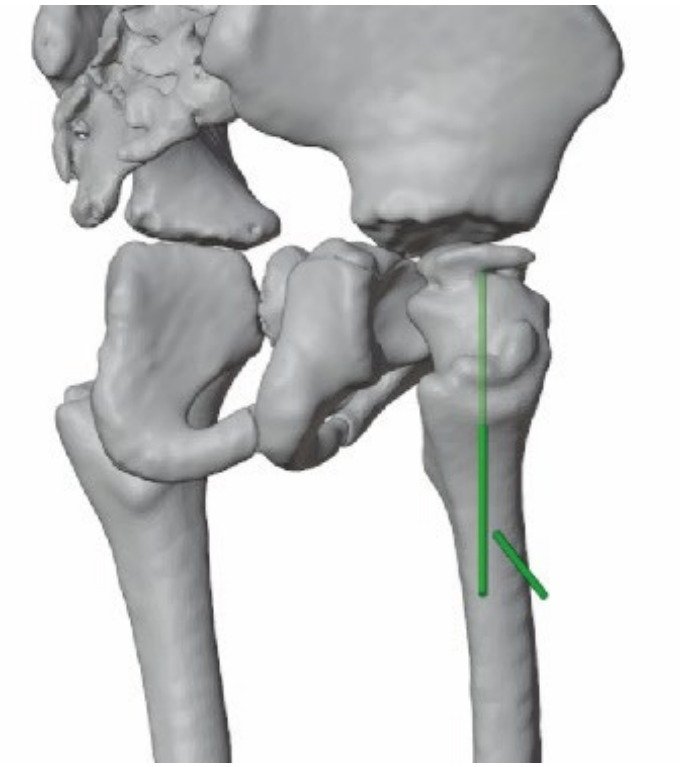

Figure 57. Different directions of the two guide wires.

Figure 58. Chisel reference for plate insertion.

The first cutting guide presents the insertion invitations for the two guide wires and the osteotomy blade. This guide allows for a proper incision for the blade and an additional open incision for the placement of the second guide wire. The holes have a diameter of 3 mm, which allows the insertion of 2 mm diameter Kirschner wires. The cutting invitation was shaped with a thickness of 1.6 mm to facilitate the insertion of a 0.38 mm blade. Aware of the criticality caused by the converging directions of the two wires, partial support was chosen at the distal hole to allow easy removal of the guide without interfering with the guide wires after use. The second guide fits over the second guide wire and allows the chisel to be inserted in the same planned direction as the plate, inserted into the initial guide wire. The direction of the blade is then guaranteed by the direction of the guide wire already inserted, but the relative rotation movement remains possible. The second guide is designed to solve this problem and assist in the correct insertion of the blade into the bone for proper plate application (Figure 59).

Figure 59. Designed cutting guides. On the left, PSI features two guide wire insertion points - one for plate positioning and one for rotational correction - along with a cutting slot; on the right, the chisel guide is aligned with the plate direction.

3D printing of PSIs

A 1:1 scale FDM 3D print of the PLA anatomical model was made to perform the steps of the surgery and to evaluate the alignment of the holes and the blade plate to be inserted (Figure 60). Cutting guides were printed in PLA Crystal, then heat-treated and delivered to the hospital's in-house pharmacy (Figure 61).

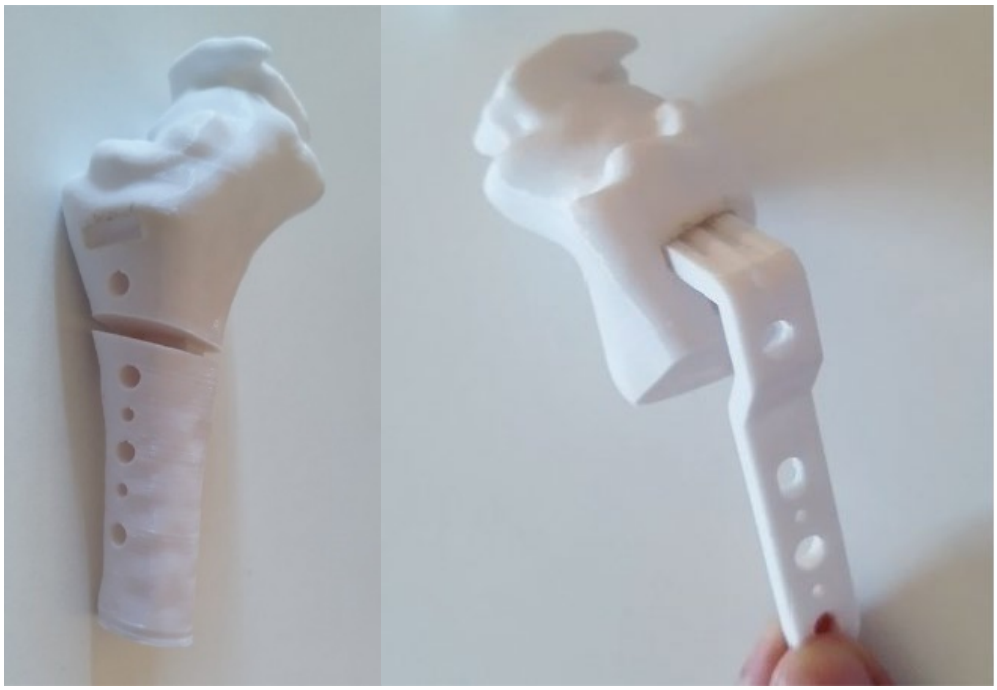

Figure 60. 3D-printed anatomical model.

Figure 61. 3D-printed PSIs made of PLA Crystal and heat-treated.

How to use

Once the femur has been skeletonized, the first cutting guide and associated 2 mm diameter Kirschner wires are applied (Figure 62). This guide also serves as a reference for the osteotomy position.

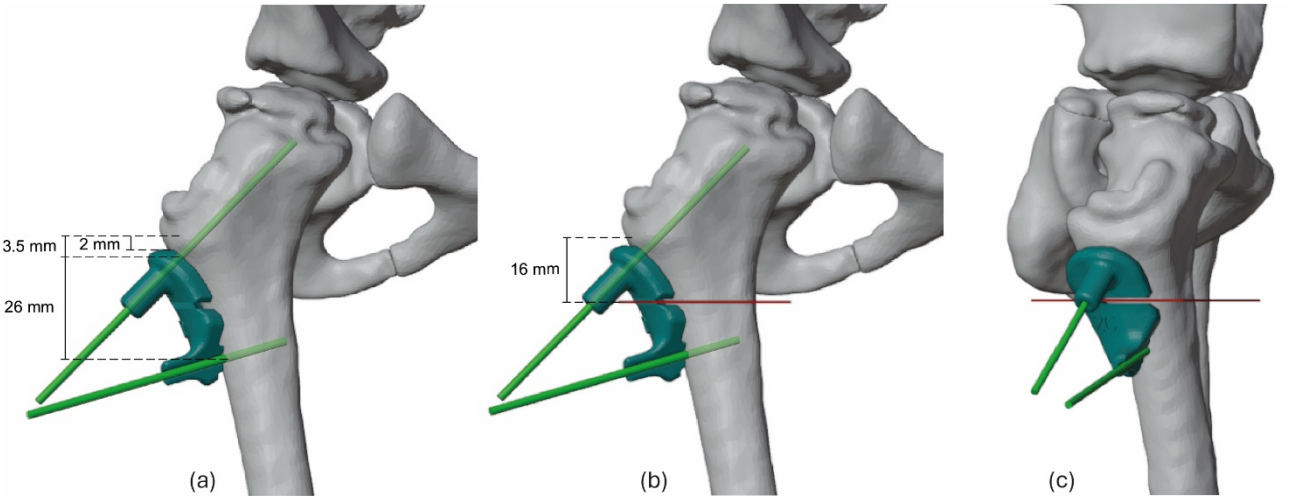

Figure 62. Positioning of the first cutting guide and its references: (a) and (b) frontal views, (c) lateral view.

After performing osteotomy, the first PSI is removed. Removal of the cutting guide is not too complicated, as one of the two thread invitations is open, allowing the cutting guide to be removed by sliding it off the other thread. The second PSI fits over the previously inserted distal wire and allows the insertion of the chisel, which will make the slot for the blade plate to be inserted later (Figure 63).

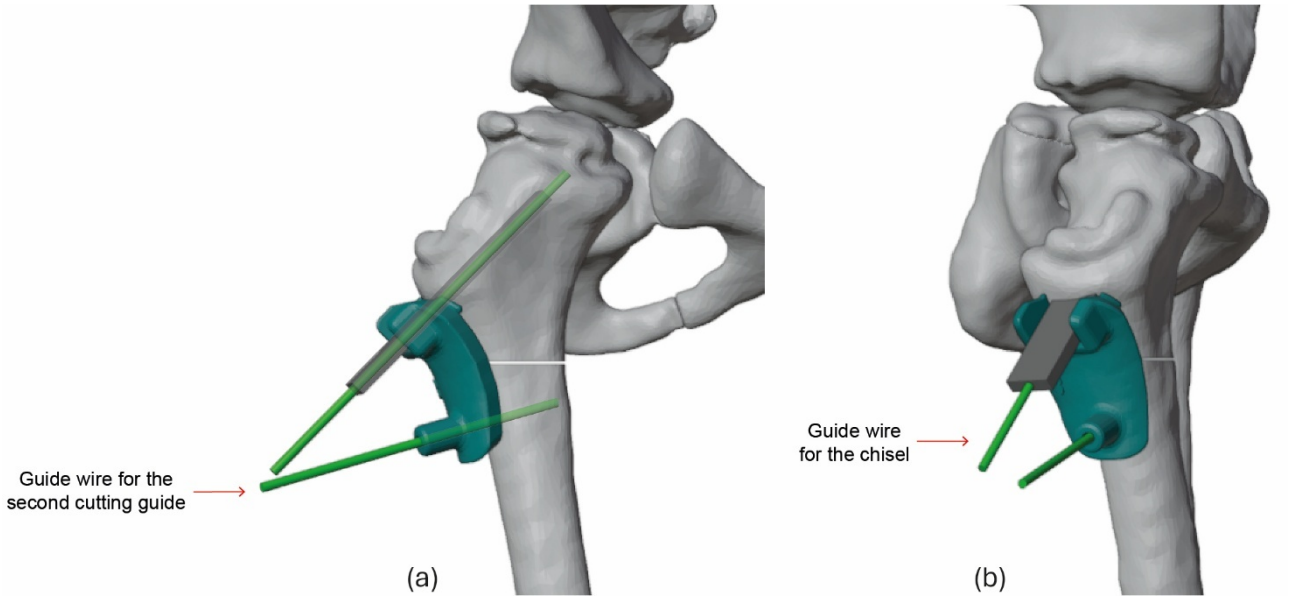

Figure 63. Placement of the second PSI: (a) on the distal guide wire and (b) insertion of the chisel on the proximal guide wire.

When the chisel has reached the proper depth, remove chisel and PSI. Finish the osteotomy and insert the blade plate into the “hole" previously created by the chisel. The geometry of the plate will guide the correction to be made, tilting the proximal femur and attaching it to the distal femur (Figure 64).

Figure 64. Final correction with the blade-plate fixation.

Post-operative considerations

Planning and subsequent design of the supporting instruments were performed immediately upon receipt of the CT scan and less than ten days after surgery. Due to the reduced time between the CT scan and surgery, no significant anatomical changes due to the progression of the pathology were detected. This allowed for greater confidence in the planning and measurements made on the 3D models.

The designed PSIs correctly guided the placement of the guide wires and blade plate, ensuring accurate execution of the cut and subsequent rotation of the osteotomy. The PSI design allowed for smooth removal without compromising the stability of the guide wires or the implant. The modeling and use of the PSIs proved critical to the accuracy of the surgery and the reduction of error margins, demonstrating the effectiveness of preoperative planning supported by advanced modeling and 3D printing technologies.

A comparison of intraoperative fluoroscopy with the planning showed that the directions of the guide wires and chisels were consistent with the planned directions (Figure 65). The final position of the blade plate was also compared to the planned position (Figure 66). The number of intraoperative fluoroscopies was 10.

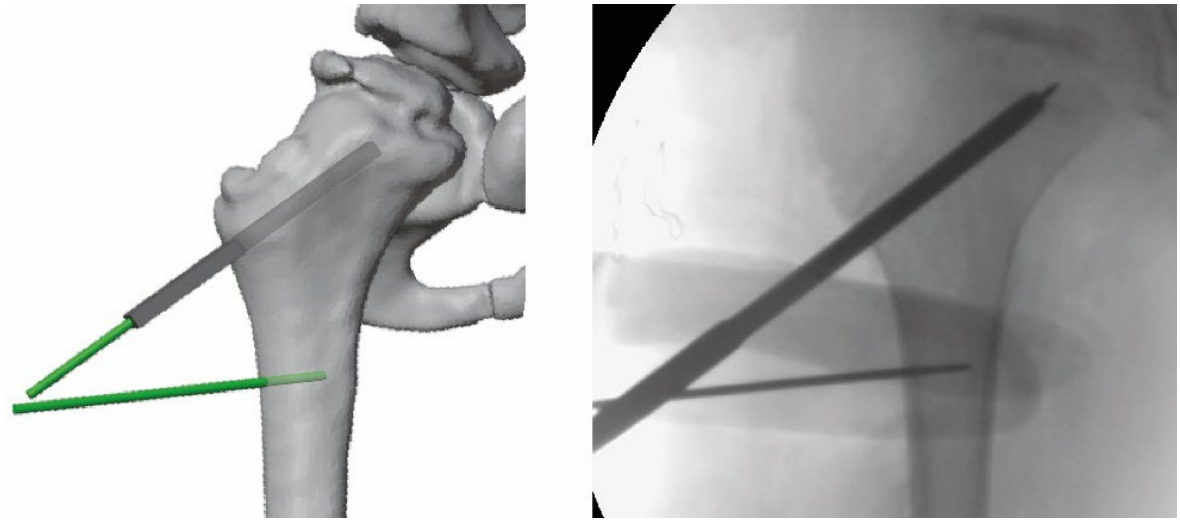

Figure 65. Comparison of surgical planning with intraoperative fluoroscopy of the directions and positions of guide wires and chisel.

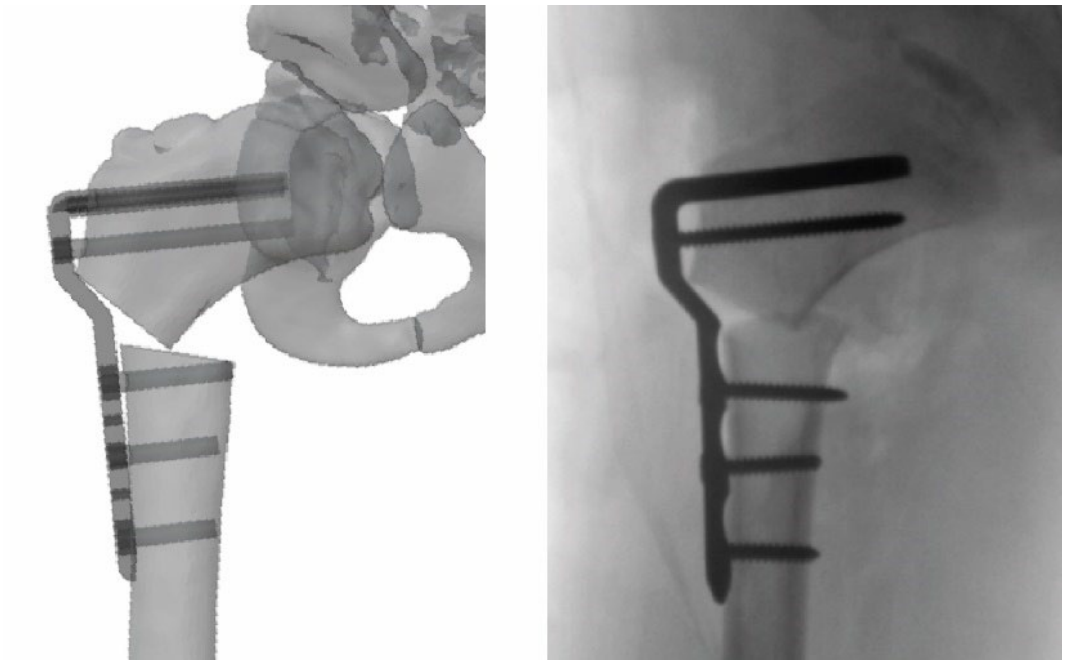

Figure 66. Comparison of surgical planning with intraoperative fluoroscopy of the final plate position.

4.4. Bifocal femoral osteotomy

Clinical case description

A 15-year-old patient presented a severe femoral deformity due to metabolic syndrome (deficient rickets). The presentation included a fatigue fracture of the left femoral neck resulting in a varus deformity associated with a severe valgus knee presentation. In this case, it was hypothesized that a bifocal osteotomy of the femur could be performed with valgus correction of the femoral neck and varus correction of the distal femur. Both osteotomies were performed with wedge subtraction and stabilized with plates.

VSP

The planning included two osteotomies of the left femur with the removal of two wedges, one distal and one proximal.

For the proximal osteotomy, we proceeded by locating the two cutting planes just below the small trochanter: a first plane perpendicular to the femoral axis at 64 mm from the superior end of the large trochanter, and a second plane inclined 20° to the previous one. A 4.5 mm Locking Proximal Femur (LPF) plate with an angle of 130°, zero offset, and 3 holes was selected as the screw plate. For the distal osteotomy, two planes inclined at 15° were identified, the first at 27 mm from the medial epicondyle. The plate for the distal osteotomy is a 4.5 mm Distal Femoral Osteotomy System (DFOS) plate with an 18° angle, 8 mm offset, and 4 holes (Figure 67 and Figure 68). For both osteotomies, the required screws have been measured to provide further practical guidance on the instrumentation to be used for the procedure (Figure 69).

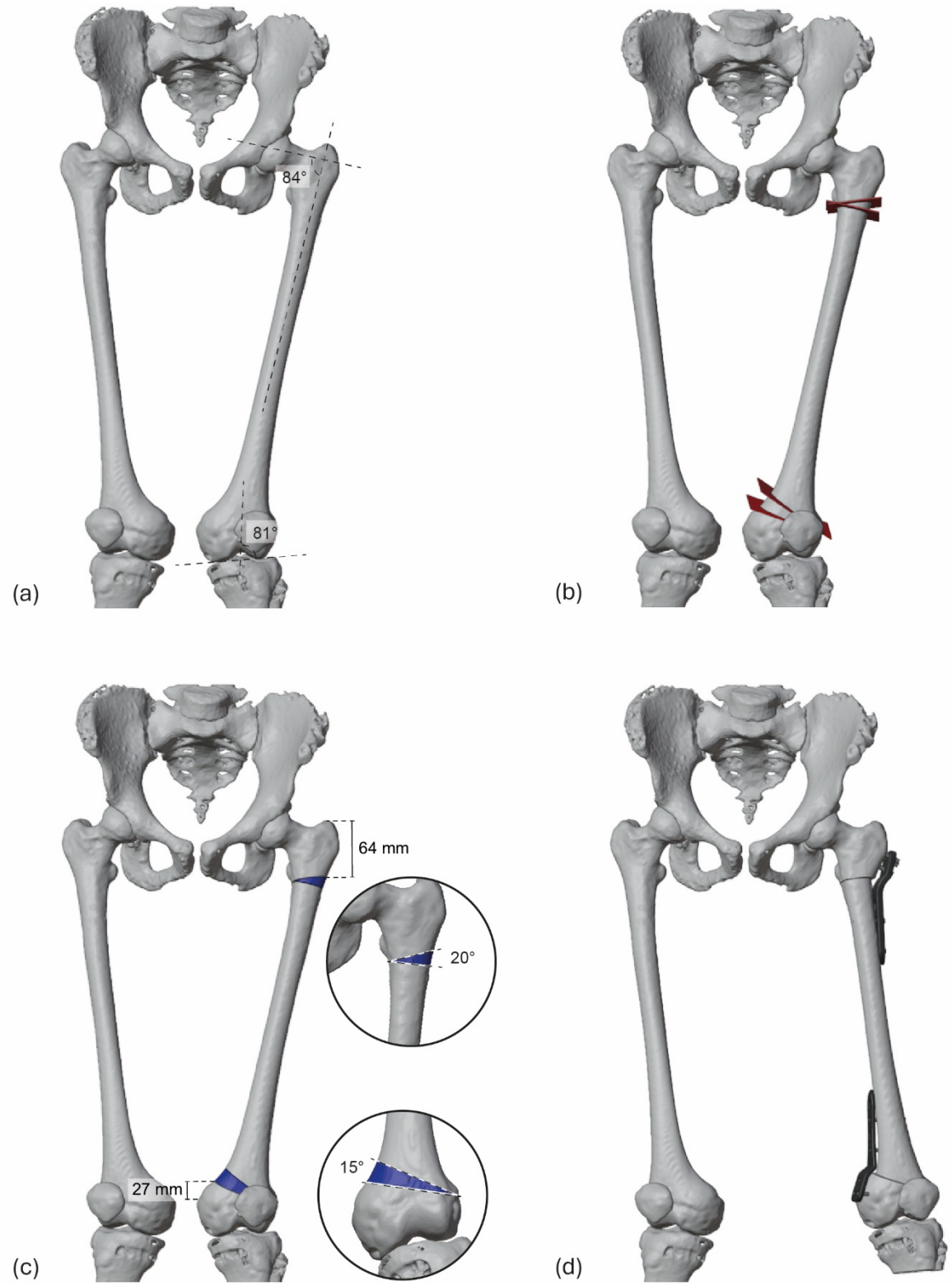

Figure 67. VSP process: (a) calculation of angles and axis alignment; (b) definition of cutting planes; (c) determination of closed-wedges; (d) simulation of the final correction.

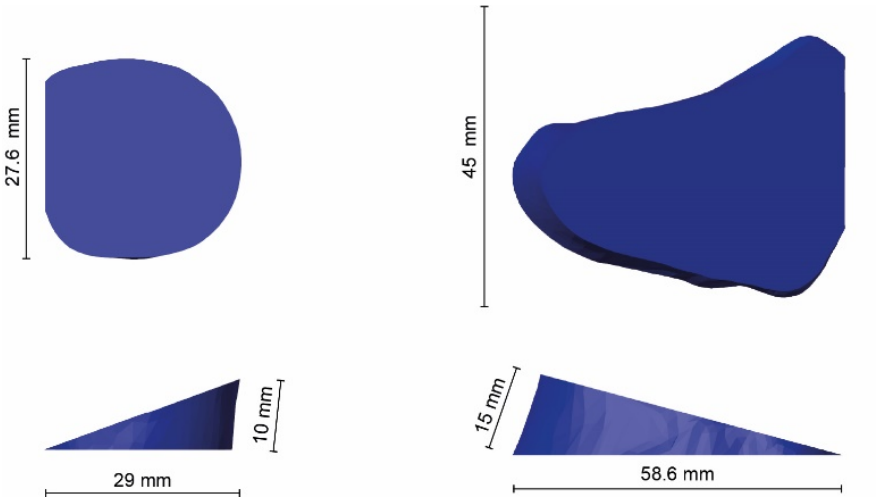

Figure 68. Sizing the closed wedges: on the left the proximal one, on the right the distal one.

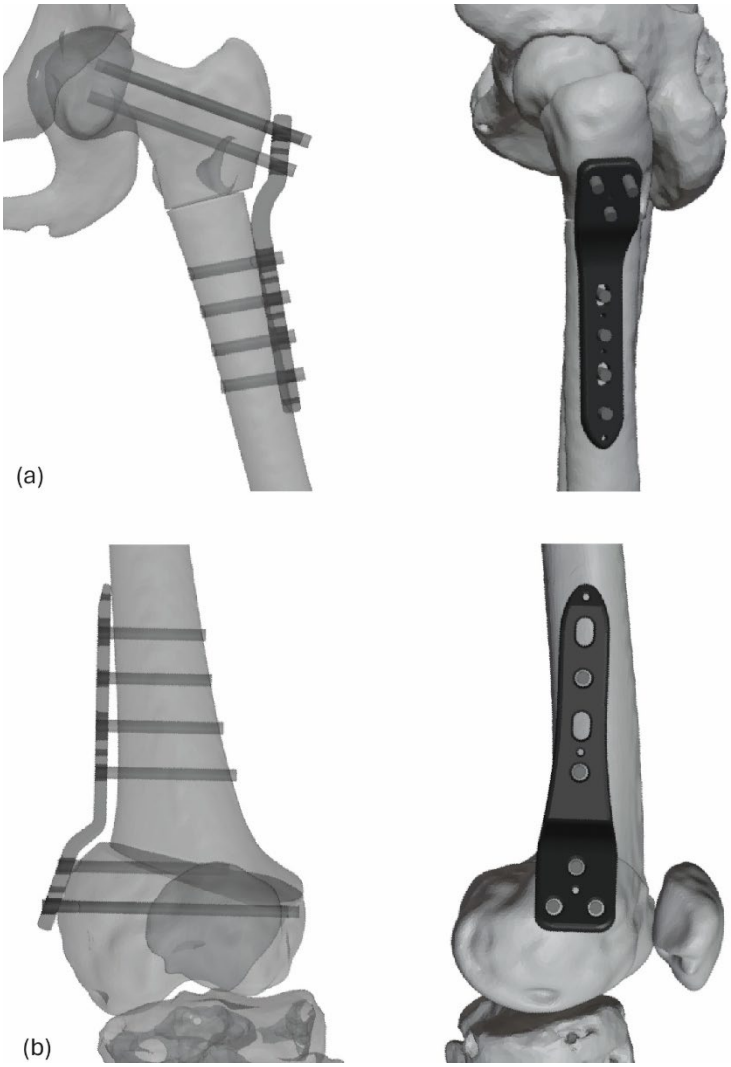

Figure 69. Placement of plates and screws: (a) proximal femur, frontal and lateral views; (b) distal femur, frontal and lateral views.

Design of PSIs

One then obtains the necessary references for the design of the PSIs, i.e., the cutting planes and guide wires of the plates in their final positions brought back to the starting position, through a backward planning procedure. The guide wires are inserted through the holes in the plates at their final positions, the objects are constrained to the bone, and a backward correction to the starting condition is made to obtain the position of the guide wires and use them as attachment wires for the cutting guides. This approach allows as much drilling into the bone, as necessary. These references are exported in STL format and imported into CAD modeling software such as PTC Creo Parametric.

Two cutting guides were designed for the proximal osteotomy, one for the distal cut and the other for the proximal cut (Figure 70). The references chosen were the proximal guide wire and the two proximal screws. Given the limited size of the femoral neck, it was essential to accurately assist in directing the guide wires to the correct position. It was decided to design a type of guide that would hug the bone and fit over it like an interlock, ideally reducing the margin of placement error. The choice was made to simply take advantage of the lower edge of the guide to guide the direction of the cut.

The operation of the guide is impaired by the need for thermal deformations, both during treatment and after sterilization, suffered by the guide to be minimal and tolerable for its use. The choice of an interlocking geometry based on the surface of the bone therefore necessitates precision in both the segmentation of the model whose surface is being traced and the fabrication of the guide itself. The choice of fabrication thickness is of utmost importance to maintain the geometry of the cutting guides during treatments without impairing their functionality due to excessive dimensions.

The modeling of the cutting guides followed the methodology of bone surface tracing, 1.5 mm offset, and 4.5 mm thickness. On the obtained volume, extrusions were made for the insertion of the 2 mm Kirschner wires and the corresponding 10 mm reinforcements. For the directions of the cuts, an extrusion was made, in the case of the first guide, at the lower end following the direction of the cutting plane for the proximal osteotomy; in the case of the second guide, the direction of the cutting plane for the distal osteotomy is followed. Modeling of the second cutting guide was done by making simple repositioning changes of the references for the

extrusion of the cut on the model of the first guide. This is followed by rounding of all edges and modeling of the supports.

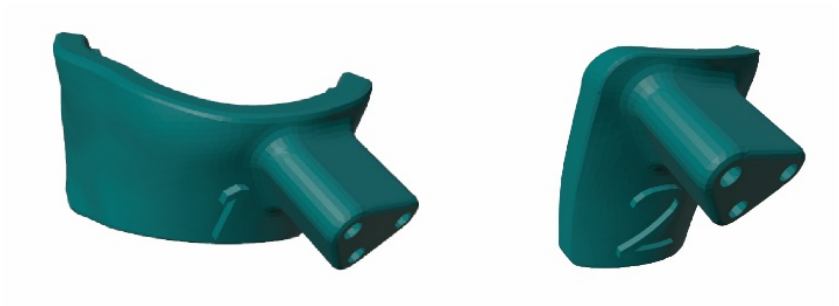

Figure 70. Design of PSIs for proximal osteotomy.

For the distal osteotomy, a single cutting guide was designed with the invitations for both cuts. The references chosen are the second guide wire and the hole of the locking screw more distal to the proximal holes of the plate. The different directions of the cuts in this case made it possible to design a single PSI (Figure 71). The modeling of this cutting guide also follows the methodology already applied with the offset and shimming of the surface and the realization of extrusions and removals to make the holes and invitations of the cuts and reinforcements.

Figure 71. Design of PSI for distal osteotomy.

3D printing of PSIs

To evaluate the effectiveness and use of the first proximal cutting guide, a 1:1 scale model of the affected portion of the femur was printed. The model of the proximal osteotomy cutting guides was then also printed to test the fit This allowed the medical staff to directly test both the guide and the alignment between the desired guide wire hole and the guide hole on the model (Figure 72). Again using these anatomical models, cutting guides made of PLA Crystal could also be tested (Figure 73 and Figure 74). Following the sterilization process, no visible deformations were detected, and the guides were made available for use in the operating room (Figure 75).

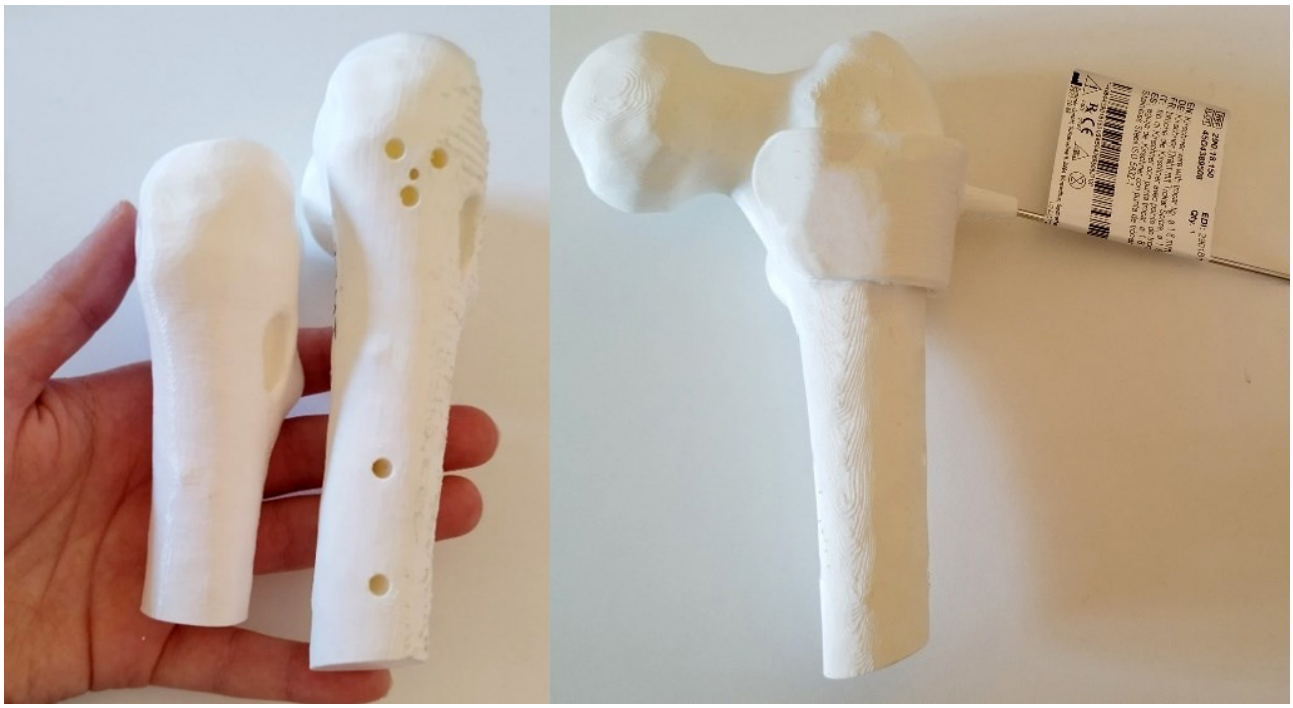

Figure 72. Testing of the proximal PSI on the 3D-printed anatomical model.

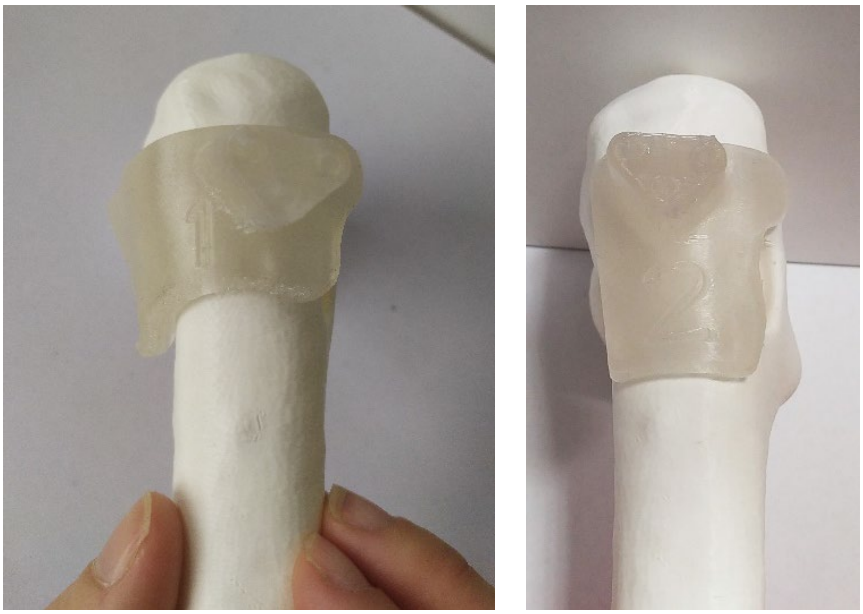

Figure 73. Testing of PLA Crystal proximal PSIs on the 3D anatomical model.

Figure 74. 3D-printed and heat-treated PSIs made of PLA Crystal.

Figure 75. 3D-printed PSIs made of PLA Crystal sterilized in the operating room.

How to use

With the proximal femur skeletonized, the first PSI is placed after the proximal cutting incision. The guide wires are inserted, and the osteotomy is made (Figure 76). After the first cut, the cutting guide along the wires is removed and the second cutting guide is inserted to make the distal cut (Figure 77). Once the two cuts are made, the wedge is removed, and the plate is applied.

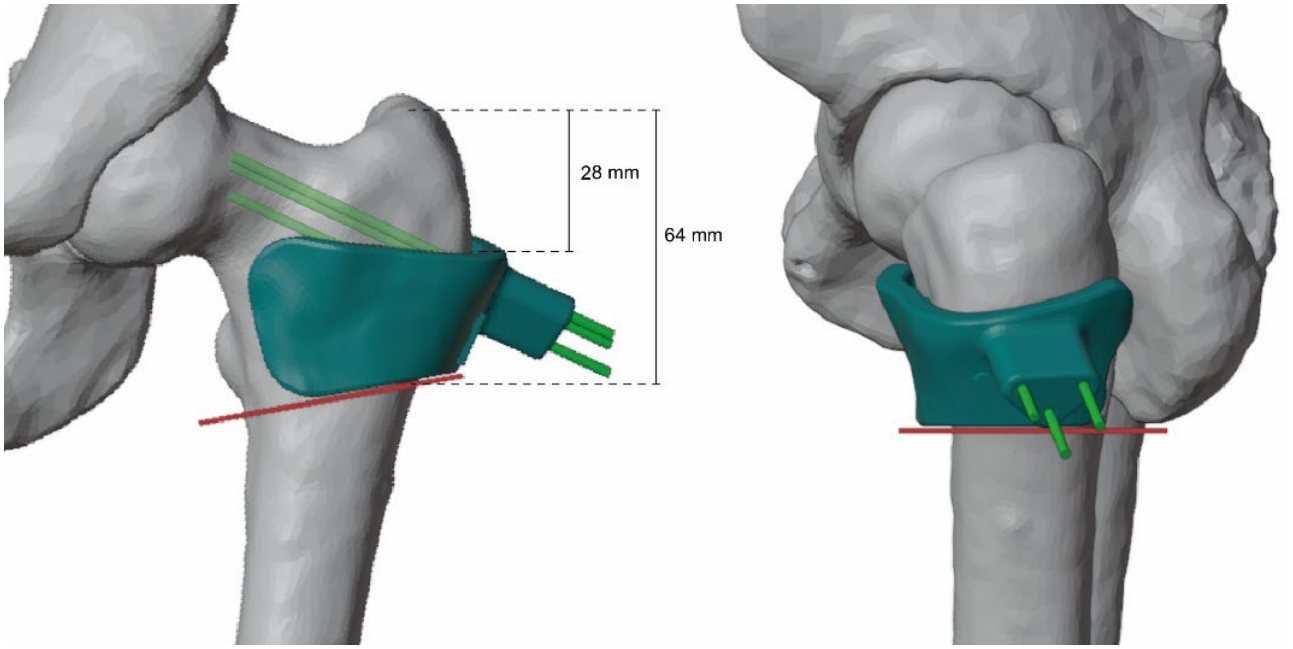

Figure 76. Positioning of the first cutting guide for proximal osteotomy, frontal and later views.

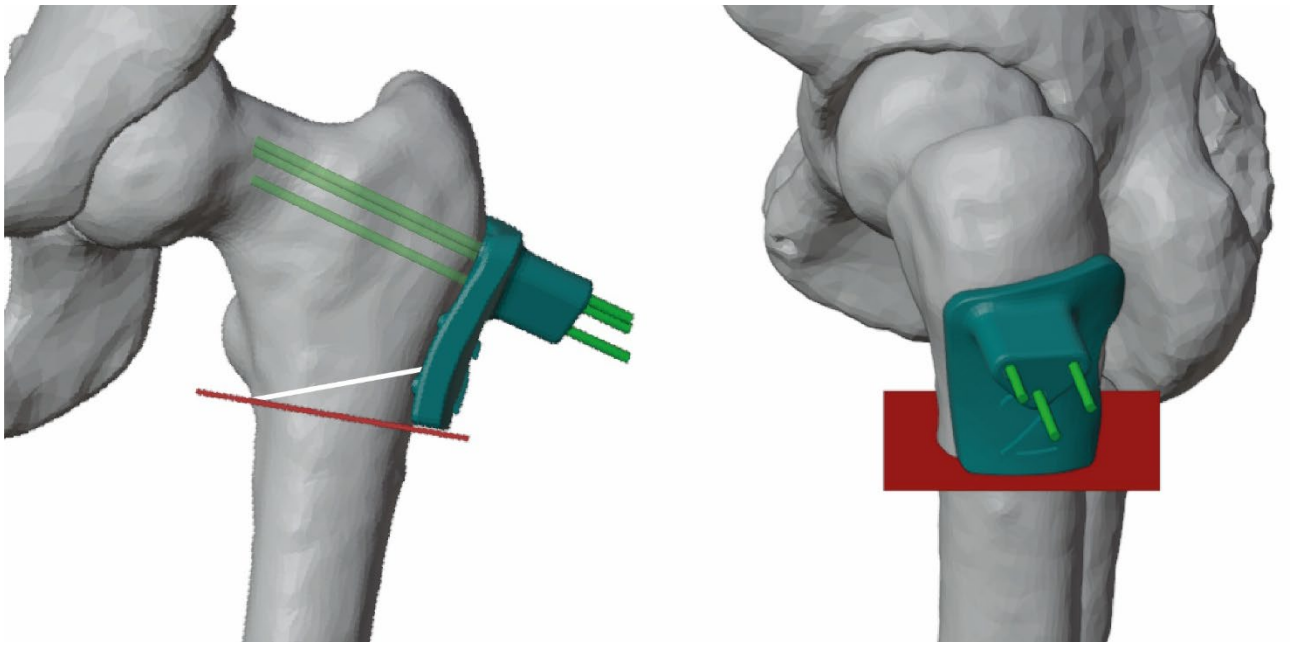

Figure 77. Positioning of the second cutting guide for proximal osteotomy, frontal and later views.

For the distal osteotomy, the area is always skeletonized, and the cutting guide is placed. The osteotomy is first made with the wires and cutting guides placed and then is completed following the directions of cutting planes on the PSI. Position of PSI is given from the medial epicondyle (Figure 78). Once the cuts are made, the wedge is removed, the segments are realigned, and the plate is fixed.

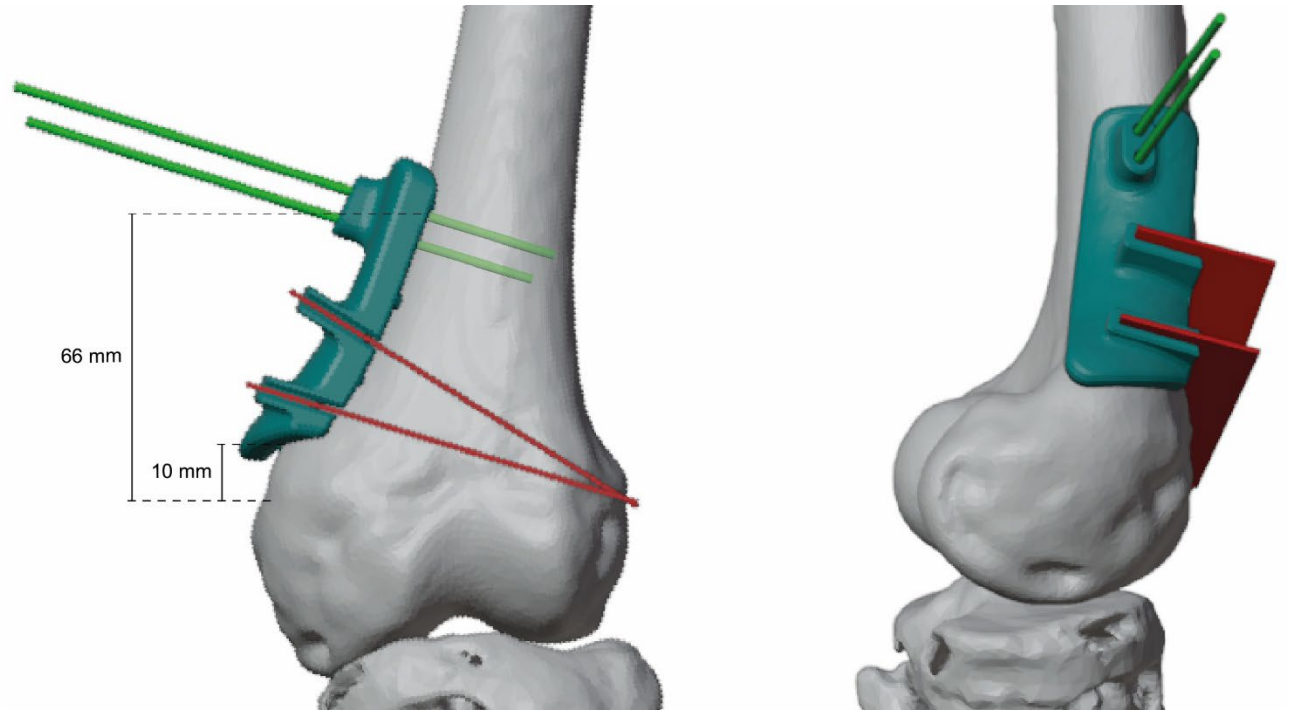

Figure 78. Positioning of the cutting guide for distal osteotomy, frontal and later views.

Post-operative considerations

The surgery was performed 50 days after the CT scan used for planning and design. No anatomical variations were found that could affect the effectiveness of the planning and cutting guides used. Thus, one could rely on planning with a good degree of confidence and use the designed instruments without altering the planning.

In this case, the age of the patient, 15 years old, and the different pathology, the time factor did not have the same relevance as in the infant cases from 0 to 6 years old.

From the distal osteotomy, it was found that the references chosen for the cutting guide fixation wires were not optimal for plate application. The references chosen (Figure 71) are not consistent with the surgical technique used to apply the plate itself, which involves inserting the distal screws first and then the proximal screws. As a result, the choice to use different placement guide wires may result in a lack of proper relative positioning of the two bone segments.

From the fluoroscopy, the proximal osteotomy and plate placement tracks are planned (Figure 79). The placement of the plate in the distal osteotomy also appears to follow the plan (Figure 80). The final radiograph shows the result after surgery (Figure 81).

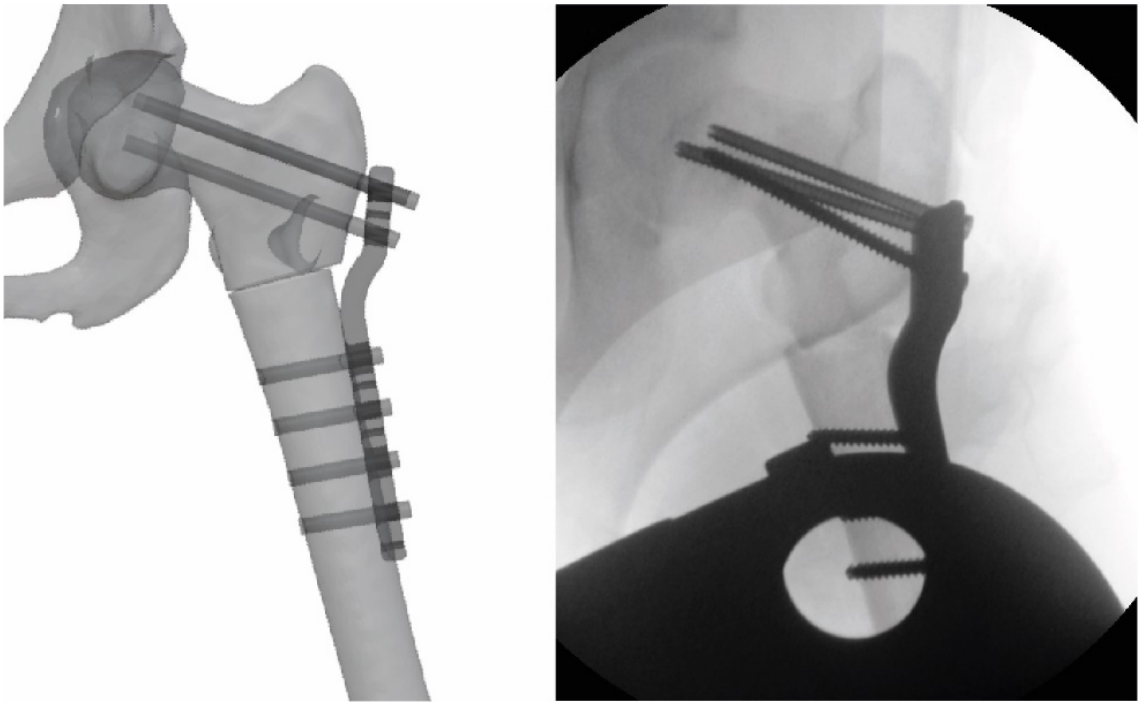

Figure 79. Comparison of VSP with intraoperative fluoroscopy of proximal osteotomy.

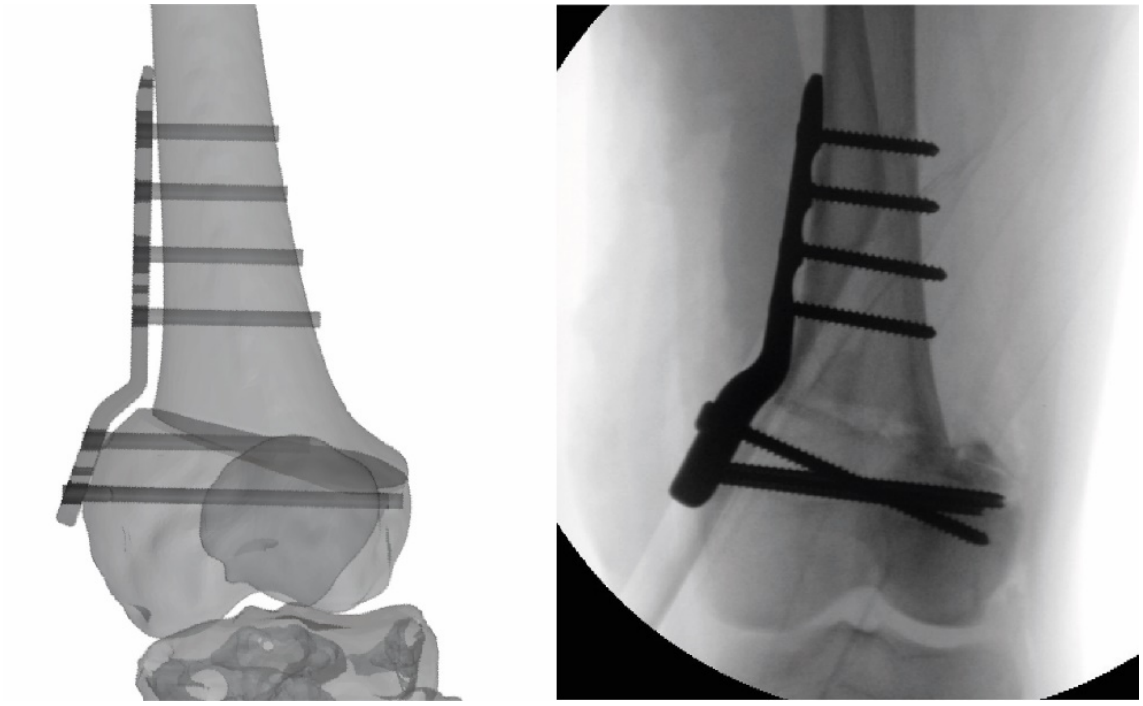

Figure 80. Comparison of VSP with intraoperative fluoroscopy of distal osteotomy.

Figure 81. Result of the surgical operation.

4.5. Results of clinical applications

The clinical case studies analyzed in this research revealed relevant interest and significant challenges, particularly in the design of customized anatomical models and patient-specific surgical instruments, such as cutting guides and implants. The diversity and complexity of the procedures underscored the impact of this approach on clinical workflows, which have progressively integrated and expanded the applications of this methodology, especially in fields such as oncology. In these cases, several types of PSIs were experimented with, with the constant goal of optimizing both the process and the methodology, while still creating unique, case-specific solutions. This flexibility demonstrated that these advanced techniques can be effectively integrated into standard clinical workflows, albeit with some logistical and coordination considerations.

The timing of each case depends on the specific surgical requirements, such as the need for anatomical templates, cutting guides, or bone grafts, which require coordination with the musculoskeletal tissue bank. In pediatric cases, especially in infants, the rapid progression of growth and pathology dictates a minimum interval between CT scan and surgery, as even a two-month delay can significantly affect the results. In older pediatric patients, the interval may extend to several months but ideally remains less than a year, with less critical time effects than in infant cases. To reduce the time between CT acquisition and surgery, some workflow steps can be optimized, such as reducing the time between imaging, planning, design, and modeling. Limiting factors include printing, post-processing, and sterilization times, which are non-compressible technical timelines. At least one business day must be allowed for printing and processing, while the hospital pharmacy requires a three-day lead time to prepare surgical instruments. Optimal coordination between hospital staff and planners is therefore essential, especially for pediatric cases with strict time constraints.

Another important aspect is the design and modeling of the PSIs, where experience has enabled more efficient production of the supporting tools. Specific requirements, such as the size of the cutting guides or the diameter of the holes for inserting the Kirschner wires, have been defined considering the thermal shrinkage of the materials and the characteristics of the wires used. This progressive refinement reduced the need for multiple prototype variations to ensure the usability of the final tools.

Effective communication between medical staff and designers was a key factor in the success of this customized approach. The integration of engineering design methodologies enabled the development of a reliable framework for the manufacture of custom surgical instruments. In addition, the software and tools used proved to be accessible and user-friendly for the designers. Initial difficulties included accurate understanding and translating clinical requirements into practical designs, a process that remains iterative. As the designers gained a better understanding of surgical techniques, they were able to speed up planning and more effectively tailor cutting guides to the specific requirements of each operation. Direct observation of surgical procedures proved extremely useful, allowing designers to identify needed improvements and gain first-hand knowledge of the operating environment, optimizing

instrument design for real-world application. This also facilitated direct interaction with surgical teams to resolve any concerns about the instrument designed. The creation of anatomical models through additive manufacturing proved especially useful for surgeons, allowing them to simulate the procedure and visualize the surgical sequence for optimal use of supporting instruments. Clear communication and the creation of easy-to-understand visual representations of the planning process have proven critical to successful outcomes.

Future developments in process optimization will address each stage of the workflow, from segmentation through planning, design, and 3D printing. Segmentation could benefit from the use of automated artificial intelligence-based tools to accelerate the identification of regions of interest (ROIs) to be examined and treated, not only of bone segments but also of specific pathological areas. Surgical planning could be improved by integrating tools for automatic angle correction and predictive models of surgical outcomes. Although planning still relies heavily on the experience of the designer, automation of reference settings derived from planning data and the use of predefined parameters could simplify the process. Additive manufacturing could be further advanced by expanding the range of materials and technologies for specific surgical instruments, exploring high-performance polymers and advanced resins, and balancing quality and cost. Improved predictability of the behavior of printed objects under thermal conditions, such as sterilization and post-processing, should be further explored through dimensional analysis and comparative scanning to ensure greater reliability for clinical use.

In conclusion, the implementation of VSP and 3D-printed PSIs has been shown to bring significant benefits in pediatric orthopedic surgery and for the correction of bone deformities. Between 2018 and 2024, VSP was applied in 111 surgeries, 88 of which employed PSIs, confirming the validity of the technology in terms of both surgical efficiency and patient safety. In the cases analyzed, the use of the PSIs resulted in an average reduction in surgical time of 52 minutes and an average decrease in intraoperative fluoroscopy exposures of 12 images, showing a significant improvement in working conditions in the operating room and a potential reduction in radiological exposure risks ($p=0.008$ and $p=0.001$, respectively).

From a safety point of view, crystalline PLA experienced no significant complications or increased risk of infection, confirming their suitability for reliable clinical use. This technology has emerged as an economical and practical alternative, especially because of the possibility of FDM printing and subsequent thermostabilization. However, some cases have shown limitations that need to be considered: 3D-printed PSIs encountered problems with positioning and structural strength in four surgeries. In one case, the guide was found to be deformed due to patient growth or double sterilization; in others, guide fractures occurred, due to delamination or environmental humidity, aspects that suggest a need to improve PSI manufacturing and handling protocols.

Another relevant element that emerged concerns the variability in PSI size depending on the site and complexity of the surgery. Printing long bone guides, which are typically more challenging in volume and time, highlighted the need for flexible structuring of production resources. Ranging in size from 3.8 cm^3 to 58.8 cm^3, the PSIs covered a wide range of bone segments and anatomical variability, successfully supporting complex procedures such as angular and multiplanar osteotomies.

The observed results are consistent with reports in the literature, which associate the use of PSIs with improved surgical times and reduced intraoperative fluoroscopic imaging. Sterilization of PLA guides with steam at 134°C has proven effective, but there remains a need for continued exploration and standardization of manufacturing processes to ensure consistency of results and to optimize operating costs, particularly when considering hospital-scale implementations such as 3D printing Point of Care.

In summary, VSP and 3D-printed PSI represent a promising advance in orthopedic surgery, with results justifying their integration as a routine tool, especially in pediatric orthopedic surgery centers. Continuing studies in this direction are crucial to consolidate efficacy, optimize costs, and improve operative protocols, laying the foundation for increasingly personalized and efficient medicine [95–100].

5. Experimental investigations

Several lines of research have been pursued during my Ph.D. studies, each of which addresses the central issue of surgical planning and patient-specific design. This section presents the experimental research that has been conducted, the results of which have attracted the interest of the scientific community and provides a starting point for further development and investigation in the future.

The experimental research focused primarily on the use of additive manufacturing technologies applied to materials of particular interest, including flexible, engineering, and metallic materials. Experiments on these materials were conducted in the laboratories of the Department of Industrial Engineering at the University of Bologna and the Department of Materials Science and Engineering at the University of Uppsala during my six months abroad.

Another line of research, however, explored the use of virtual reality (VR) in surgical planning. The goal was to create an interactive simulation environment for testing different surgical hypotheses, as realized by Blender, allowing the surgeon to take an active role in managing and planning the corrections to be made.

5.1. Evidence of 3D printing materials for reproducing cardiac models

This line of research focused on the use of flexible materials in 3D printing to create anatomical heart models affected by specific pathologies, such as aortic dissection. This study required the collaboration of a team of cardiac surgeons from the Sant'Orsola-Malpighi Polyclinic to support the validation of the results obtained. Aortic dissection is a serious cardiovascular condition characterized by a tear in the aorta, the largest blood vessel in the body, causing blood to leak between the layers of the aortic wall. This phenomenon creates a false lumen, a new channel within the arterial wall, separating the layers and causing abnormal blood flow. If not treated promptly, dissection can lead to serious complications such as heart failure, blockage of blood flow to vital organs, or even rupture of the aorta, which is fatal in most cases. The main objective was to obtain a realistic reproduction of cardiac structures that would be functional for both medical training and preoperative surgical planning. The selected

materials, including TPU and resin, proved to be crucial, as their flexibility and transparency allowed for accurate reproduction of the softness and viscoelastic properties of cardiac tissues, providing both tactile and visual feedback during the analysis of complex clinical cases. The objective was to develop 3D-printed anatomical models, focusing on sections of the aortic arch involved in aortic dissection, to produce high-quality and accurate models using different 3D printing technologies and materials. The models were generated from medical images obtained by angiographic computed tomography (CTA) and validated by a team of cardiac surgeons at the Sant'Orsola-Malpighi Polyclinic. Clinical validation demonstrated high accuracy in anatomical reproduction, highlighting the potential of these models for more informed and precise surgical planning.

The tests were conducted using 3D printers with FDM and SLA technology, using materials with specific properties. PLA was chosen for its ease of processing, TPU for its malleability, and resin for its transparency, which facilitated internal visualization of anatomical structures during clinical evaluation. The choice of materials was strategic, depending on the specific purpose of the model: white PLA provided a simple aesthetic representation, while transparent TPU and resin were ideal for detailed visualization and simulation of endovascular devices. During the printing process, PLA proved particularly suitable for creating formal models of anatomy due to its ease of use and stability. In contrast, TPU required careful printer setup and filament moisture control but provided a more realistic tactile experience. The transparent resin offered superior surface quality, making it ideal for detailed simulations.

The research approach used advanced CAD technologies and 3D printing to reproduce the aortic arch as an analytical tool for complex cardiac pathologies, such as aortic dissection. The process consists of several steps, already described in the methodology chapter, starting from the collection of medical images to the physical production of the 3D model. The goal is to support preoperative surgical planning and to improve the accuracy of the surgery. The process consists of several steps, already described in the methodology chapter, from the collection of medical images to the physical production of the 3D model. The workflow starts with the collection of medical images, such as CTAs, related to clinical cases of aneurysms or aortic dissections. Three-dimensional reconstruction of these images is performed using

segmentation software such as 3D Slicer, followed by digital manipulation and 3D printing of the model. This approach allows the patient-specific problem to be explored in three dimensions, providing a detailed visual representation of the anatomical structures involved. Using modeling software such as Blender, different surgical solutions can be hypothesized, and different surgical scenarios can be evaluated. In addition, the creation of a 3D-printed physical model provides tactile feedback that cannot be replicated in the virtual representation, allowing direct assessment of the physical dimensions of the anatomical area and deformity to be treated.

The segmentation phase is critical for identifying regions of interest in medical images, such as blood flow in arteries. In the case of aortic dissection, this step allows the distinction of the true lumen from the false lumen and the identification of the junctions between the two, which are critical for the choice of surgical access and operative strategy. Once the region of interest (ROI) has been identified through segmentation, the circumscribed areas are exported in STL format. In Blender, specific modifiers are applied to define the vessel wall thickness based on the reference cardiac tissue, simulating the inclusion of the anatomical structure and adapting the model thickness to the 3D printing parameters (Figure 82).

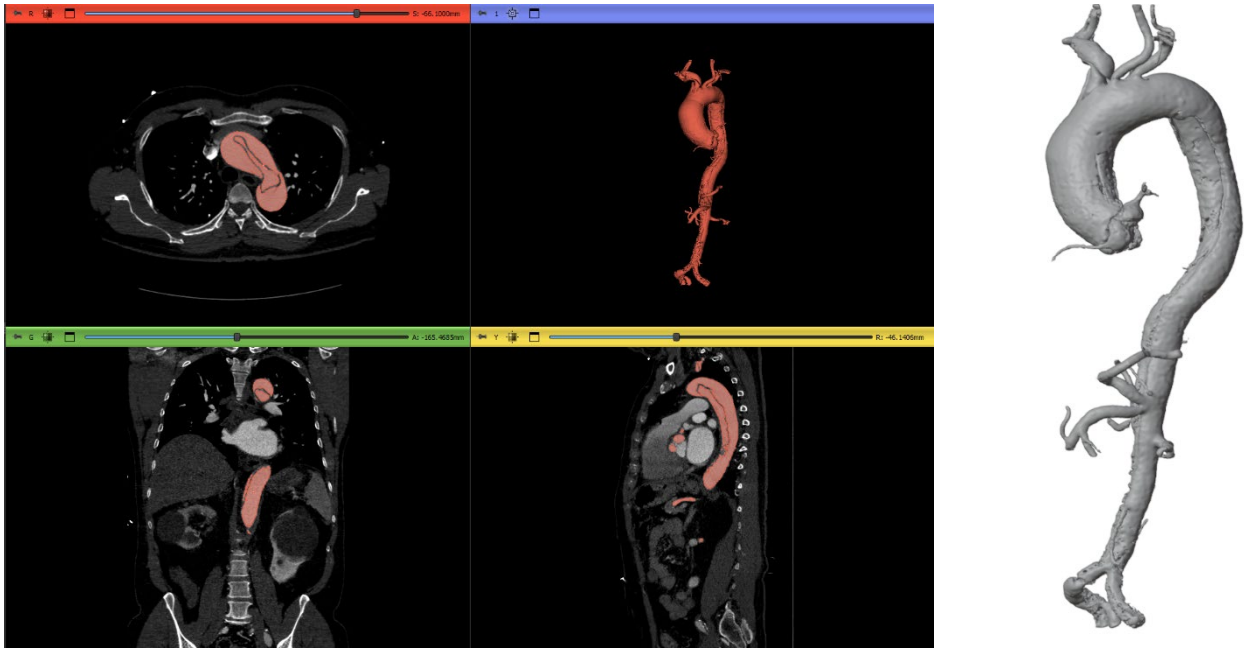

Figure 82. CTA segmentation of an aortic dissection case on 3D Slicer (on the left) and the 3D digital models (on the right).

The printed models were divided into sections to simplify the complexity of aortic dissection, allowing detailed analysis of anatomical features and providing an accurate physical preview of the surgical field. Several aortic dissection models have been created by converting the 3D model to STL format for compatibility with 3D printers. The choice of printing material varies according to the purpose of the model: polylactic acid (PLA) or flexible thermoplastic polyurethane (TPU) can be used for visualization and study of anatomy, while transparent TPU or clear resin are ideal for detailed simulations and representation of endovascular devices. The materials selected were white FiloAlfa® PLA, bone-colored TreeD© Pure FT, transparent Recreus© Filaflex 82A, and transparent Anycubic© Water-Wash resin. The white PLA provides a simple aesthetic representation, while the transparent TPU offers flexibility and transparency for studying interior walls; the transparent resin is well suited for specific technologies and desired results. The 3D models were printed layer by layer using Ultimaker Cura software for the Anycubic Predator FDM 3D printer and Lychee Slicer for the Anycubic Photon M3 Max SLA 3D printer, whose printing parameters are determined by referring to the filament suppliers' data sheets, considering recommended temperature settings and printing speeds. Adjustments to the optimal parameters were made through careful review and experimentation, particularly for uncommon materials (Table 3 and

Table 4).

Table 3. FDM 3D printing parameters.

3D printing parameters	**FiloAlfa® PLA**	**TreeD® Pure FT**	**Recreus® Filaflex 82A**
Printing Temperature	200 °C	235 °C	250 °C
Heated Bed Temperature	60 °C	80 °C	50 °C
Nozzle Diameter	0.4 mm	0.4 mm	0.4 mm
Layer Height	0.2 mm	0.2 mm	0.2 mm
Printing Speed	60 mm/s	50 mm/s	60 mm/s
Retraction Distance	4 mm	2 mm	2 mm
Retraction Speed	35 mm/s	25 mm/s	25 mm/s
Fan	100%	0%	100%
Color	White	Bone	Clear

Table 4. SLA 3D printing parameters.

3D printing parameters		Anycubic® Water-Wash Resin+
Bottom layers	Number of Layers	3
	Exposure Time	25 s
	Lift Distance	4 – 7 mm
	Lift Speed	60 – 180 mm/m
	Retract Speed	180 – 40 mm/m
Normal Layers	Layer Thickness	50 µm
	Light-off Delay	2 s
	Exposure Time	3 s
	Lift Distance	4 – 7 mm
	Lift Speed	60 – 180 mm/m
	Retract Speed	180 – 40 mm/m
Color		Clear

One of the main challenges encountered during the printing process involved the need to accurately balance temperature and printing speed, especially in the case of materials such as TPU and resin. TPU, due to its flexible nature, requires an accurate and consistent extrusion temperature, as even a slight variation can affect the quality of the print, leading to problems with poor adhesion between layers. A high printing speed can cause irregularities in the model surface or a lack of sufficient material deposition. Resin, on the other hand, is sensitive to the duration of exposure to UV light, which controls the curing of the material. Excessive exposure time can cure the resin too quickly, reducing the quality of surface details and risking the curing of the resin in the underlying layers as well, while insufficient exposure compromises the soundness of the model. The first layer needs special consideration to enable good adhesion of the first layer to the printing plate.

An additional challenge was to try to make the models without internal filling, limited to the outer walls of the blood vessel, to ensure clear visualization of internal sections and cardiac malformations. So that the segmented model represents the blood flow, the vascular wall is added during digital modeling. From the medical images, it is possible to determine the

average thickness of the intimal flap, which separates the true lumen from the false lumen, in this case about 1.8 mm, and set this value as the wall thickness for the entire aortic blood bladder. Cura's "Vase Mode" printing mode also enabled the printing of three-dimensional objects with minimal thickness, optimizing the printing path, and reducing the time and material used. Supporting structures, on the other hand, are removed after printing in post-processing to ensure a defect-free result.

The 3D-printed models, using the FiloAlfa® PLA material, provided an accurate physical preview of the surgical field, representing the dimensions of anatomical structures (Figure 83). Similarly, the TreeD Pure FT TPU printed model showed interesting tactile characteristics, being sufficiently compact and representative (Figure 84).

Figure 83. FDM 3D-printed cardiac models in FiloAlfa PLA.

Figure 84. FDM 3D-printed cardiac model in TPU TreeD Pure FT.

Models made of transparent materials, such as Recreus® Filaflex 82A and Anycubic® Water-Wash Resin, proved invaluable in predicting the optimal access points for endoprosthesis insertion. In particular, the transparent TPU model provided tactile feedback, enhancing the

flexibility of the aortic tract and increasing realism (Figure 85). On the other hand, the transparent resin model facilitated a more detailed exploration of the anatomy, but the model was found to be much more fragile (Figure 86).

Figure 85. FDM 3D-printed cardiac models in Recreus Filaflex 82A.

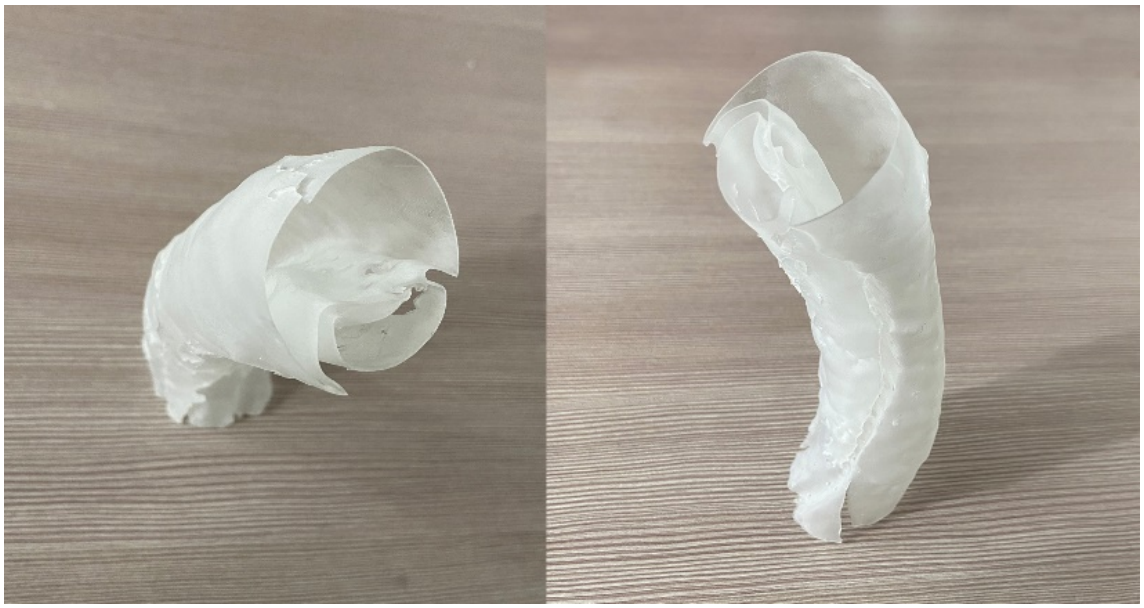

Figure 86. SLA 3D-printed cardiac model in Anycubic Water-Wash Resin.

Clinical validation of the anatomical models was achieved through feedback sessions with the cardiac surgeons involved, who were able to manipulate the models and evaluate their accuracy against the original medical images. This method proved to be particularly effective in reconstructing thin, soft tissue, a critical aspect of cardiac surgery. In addition, using varied

materials and careful control of printing parameters, the models provided valuable insight into the analysis of aortic dissection and offered an accurate physical representation of the surgical field, like real structures. The combination of PLA, TPU, and resin ensured an extremely accurate reproduction of the cardiac anatomy, allowing a thorough understanding of anatomical features and pathologies.

These models have played a key role in creating physical prototypes that faithfully reproduce anatomical structures, improving understanding and increasing tangibility for clinicians. The high accuracy in reproducing both anatomy and pathology, coupled with low cost, further demonstrated the effectiveness of these tools for surgical planning. The results confirm the potential of these models as innovative tools for surgical training and care and open new perspectives for the implementation of 3D printing in complex clinical settings. This research represents a first step toward increasingly accurate reproduction of patient-specific anatomical models, even in the presence of complex pathology. The use of more innovative and high-performance materials may allow the reproduction of even more sophisticated structures, such as customized heart valves and aortic stents, or even the mechanical simulation of the cardiovascular system, contributing to the study and application of cardiovascular endoprostheses and implants [101,102].

5.2. Design and 3D printing of lattice structures for scaffolds

Driven by the need to develop biocompatible and customized materials for bone replacement, the second line of research focuses on the use of 3D printing to produce customized and personalized bone scaffolds made of PEEK, a high-performance thermoplastic polymer widely used in medical applications due to its mechanical strength and biocompatibility properties.
Customized scaffolds serve as scaffolds that support bone tissue growth, facilitating functional recovery in patients undergoing bone repair or replacement surgery. However, while scientific literature has extensively explored the kinetic and mechanical aspects of scaffold materials, the custom geometric design of the structures remains underdeveloped. This aspect is essential to meet the specific anatomical needs of each patient. This study aims to develop a methodology for the design and fabrication of scaffolds using additive printing

technologies with lattice structures made of PEEK. The main objective is to create variable density scaffolds that can mimic different zones of bone tissue, from the densest cortical to the least dense medullary. This structural variability is critical to ensure that the scaffolds integrate effectively into the body, promoting not only mechanical support but also regeneration of the surrounding bone tissue. In contrast to studies using standard geometry such as cubes or cylinders, this research takes a patient-specific approach by designing scaffolds based on individual anatomical geometry. In the context of personalized medicine, standardization of geometric design and manufacturing parameters is complex because the properties of 3D-printed objects vary significantly based on geometry. For this reason, a custom design methodology was investigated that, while more time and resource-consuming, provides greater accuracy in meeting specific patient needs.

The approach used involves using CAD software to model variable-density lattice structures inspired by the composition of human bone. The lattice structures modulate the mechanical properties of the implants and reduce the phenomenon of stress shielding. TPMS, like the Gyroid, are particularly effective in tissue engineering because of their similarity to trabecular bones. Designing variable density scaffolds with these TPMS structures can mimic the mechanical properties of natural bone tissue, with higher densities in cortical areas and lower densities in trabecular and medullary areas. The geometric customization of the filling of these structures based on the patient's CT images allows for a high degree of accuracy, ensuring an optimal fit between the device and the bone anatomy.

The design process begins with the segmentation of DICOM images obtained from CT scans to generate a 3D anatomical model in STL format. In this study, we focused on a section of the femur where different bone types were distinguished: cortical, trabecular, and medullary. Based on the Hounsfield scale, specific density ranges were defined for each area, with cortical bone varying between 484 and 1814 HU, trabecular bone between 333 and 484 HU, and medullary bone between 230 and 333 HU (Figure 87).

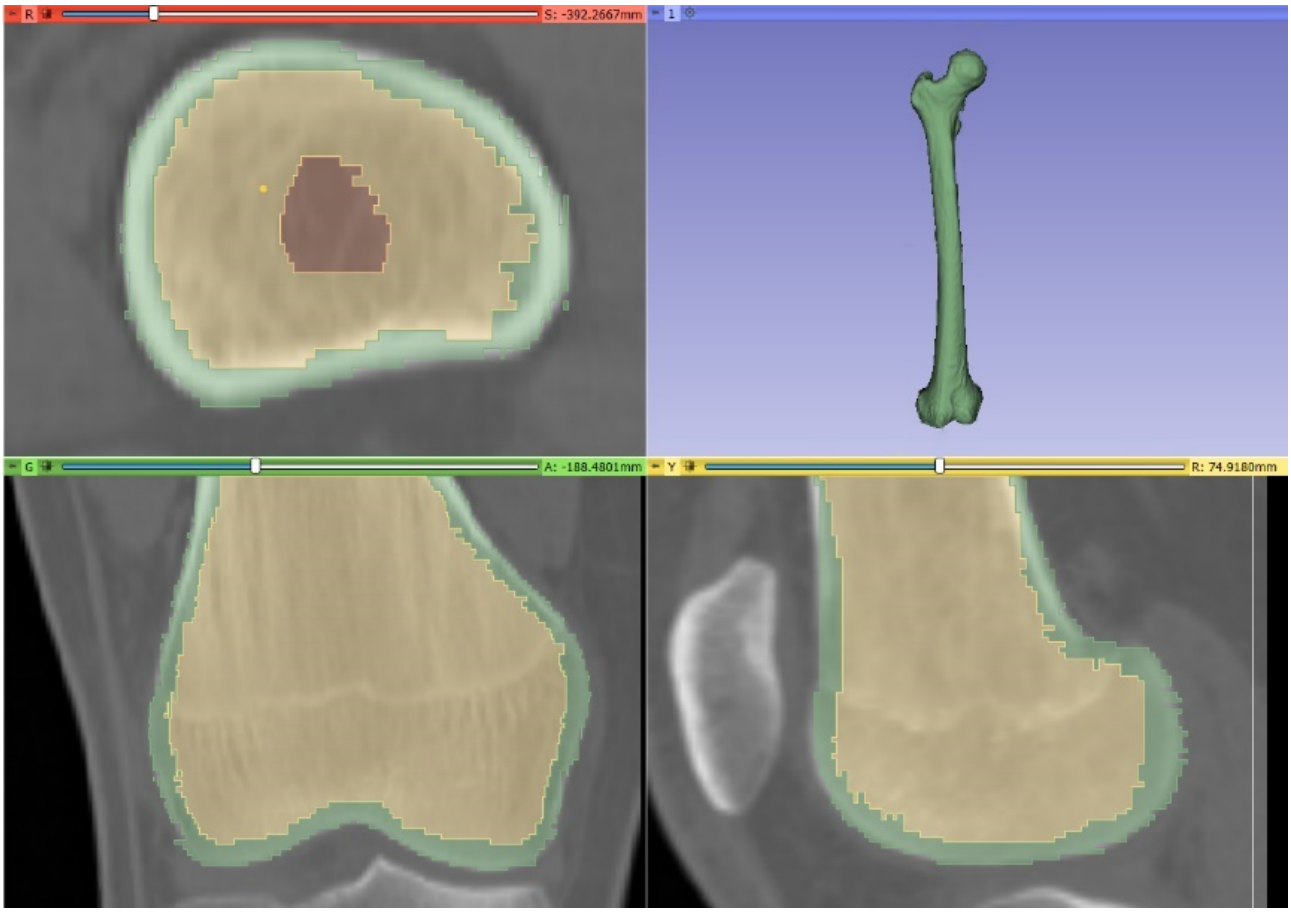

Figure 87. Differentiated segmentation of TC images: cortical bone (green), trabecular bone (yellow), and medullary bone (red).

After segmentation, three separate meshes corresponding to each bone type are exported. To simplify the modeling process and reduce the weight of the digital model, a section was identified where all three bone types coexisted. It is also critical to maintain the consistency of the relevant reference systems during the import and export processes between the different software used.

Scaffold modeling is performed in 3D CAD environments such as nTopology, where meshes are converted to implicit bodies and a TPMS gyroid structure, selected for its similarity to trabecular bone, is applied. Specifically, three cell sizes were set for illustrative purposes: 4x4x4 mm for cortical bone, which is denser, 8x8x8 mm for trabecular bone, and 16x16x16 mm for medullary bone (Figure 88). For this study, a correlation between gyroid cell size and bone density was not calculated, but a correlation will be used in the future to create a scaffold that has mechanical properties like those of real bone.

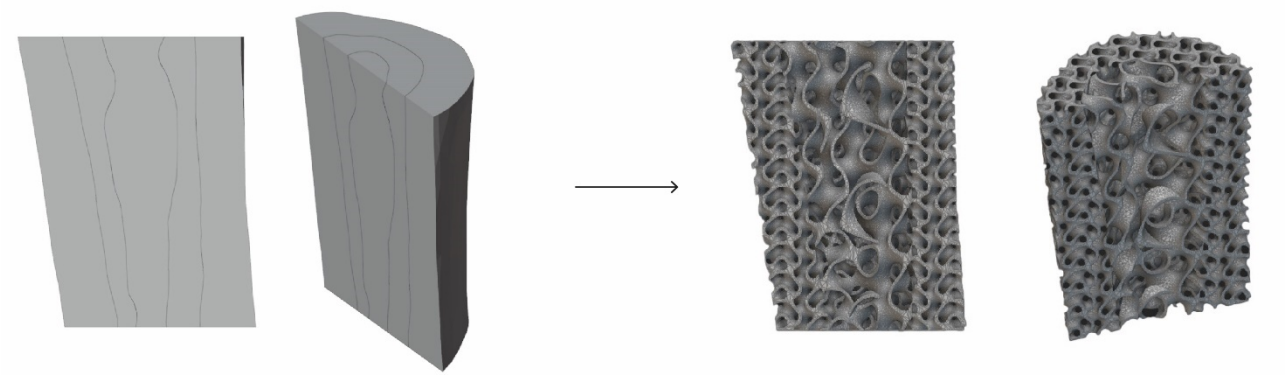

Figure 88. 3D model of a femoral section: on the left the three different meshes, on the right the different applied infill gyroids.

Fabrication is by 3D printing, using FDM technology and TreeD Filaments© PEEK Nat as the material. In the context of this study, the printability of PEEK using advanced FDM additive manufacturing techniques was investigated. 3D printing of PEEK presents significant challenges, as this polymer requires extremely high printing temperatures, both for extruding the material and for maintaining optimal thermal conditions throughout the fabrication process. The CreatBot PEEK-300 industrial printer, equipped with an advanced temperature control system, available in the laboratory of the Department of Industrial Engineering at the University of Bologna, was used for this research. The printing parameters used are shown in Table 5. After about 1 hour of printing, the object was obtained (Figure 89).

Table 5. 3D printing parameters for TreeD Filaments© PEEK Nat.

3D printing parameters	**Value**
Layer height	0.2 mm
Extrusion width	0.4 mm
Extruder temperature	440 °C
Plate temperature	140 °C
Chamber temperature	100 °C
Fan	0%
Print speed	30 mm/s

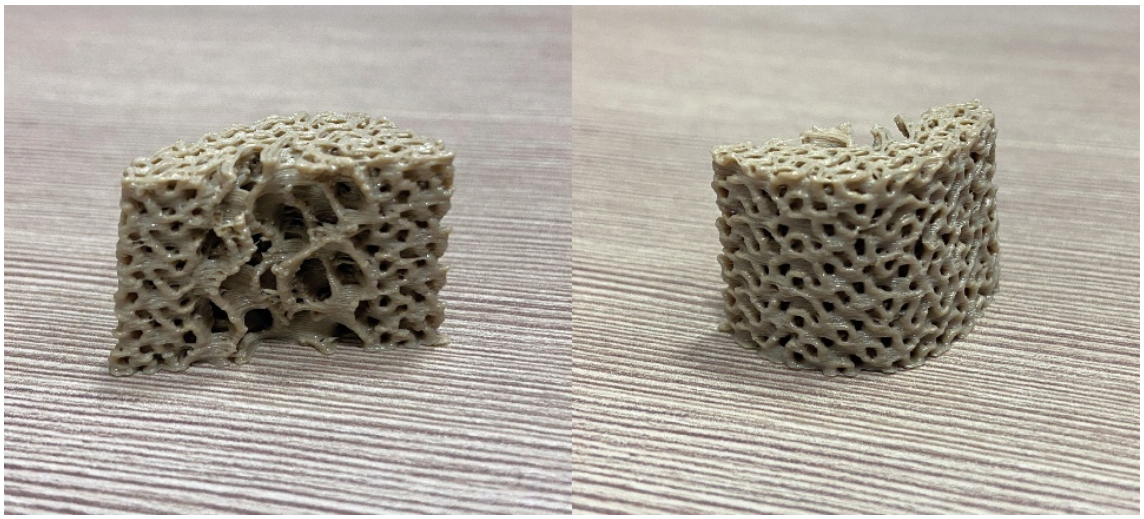

Figure 89. FDM 3D-printed model of lattice-based structure in PEEK.

PEEK's mechanical properties make it ideal for the fabrication of bone scaffolds that must withstand high biological loads, such as those found in the lower extremity, ensuring mechanical integrity over time and making it suitable for custom implantable devices such as bone grafts, especially in situations where natural bone tissue is unavailable or incompatible with the patient's anatomy.

Although PEEK is an inert material with a limited ability to biologically promote osseointegration, the possibility of combining it with bioactive materials represents a promising direction for future bioprinting-oriented development.

Preliminary results demonstrate the feasibility of 3D printing PEEK into lattice structures that can be used for both the fabrication of custom scaffolds and specific bone grafts for open wedge osteotomies or the replacement of damaged or missing bone segments.

However, given the complexity of PEEK during the FDM process and its high sensitivity to geometric and thermal variables, further studies are needed to optimize printing parameters and validate the overall process.

This research lays the foundation for an innovative approach to the design and fabrication of bone scaffolds that starts with patient-specific geometry and thus real clinical needs, rather than simple material characterization.

5.3. Design and 3D printing of lattice structures in Ti alloy for implants

3D printing also enables the creation of highly customized, patient-specific medical devices. In particular, the use of lattice structures and the ability to optimize the materials used represent an important advance for maxillofacial reconstruction cases where biomechanical and bone regeneration requirements are particularly high. During my research period at the Department of Materials Science and Engineering, Uppsala University, the research activity focused on the design of titanium lattice structures for use in mandibular plates for maxillofacial surgery. Indeed, mandibular reconstruction is often required in patients with damage due to trauma, congenital anomalies, or oncological resections, but is complicated by specific clinical problems such as loosening of the plates and poor vascularization of the surrounding tissues. In response to these challenges, this project aimed to develop customized and structurally optimized mandibular plates to reduce stress shielding and improve osseointegration.

The design of the mandibular plates was based on a lattice design, created using CAD software, and manufactured using the Laser Powder Bed Fusion (L-PBF) technique. This additive manufacturing technology allows the creation of structures with controlled porosity and complex geometries that mimic trabecular bone, which promotes not only the lightness of the implant but also an even distribution of stresses. This technique minimizes the risk of fracture associated with traditional solid implants and significantly improves the mechanical and biological performance of implants. One of the main design goals is to counteract the phenomenon of stress shielding. This phenomenon, caused by the difference in stiffness between the implant and the bone, can lead to progressive bone resorption and compromise the long-term stability of the implant. To address this issue, the project included the creation of triply periodic minimal surface (TPMS) lattice geometries, which distribute forces evenly, promote bone regeneration, and are particularly suited to providing a more durable and stable solution. Titanium and its alloys, particularly Ti-6Al-4V, were chosen for their high biocompatibility, corrosion resistance, and ability to integrate the properties required for maxillofacial applications. In addition, the properties of the lattice structures were further optimized by post-processing treatments such as sandblasting and chemical etching to increase surface roughness, promote cell adhesion, and improve bone integration.

Design of lattice-based structures

The design of the lattice structures was performed using nTopology 3D modeling software. The unit cells that make up the specimen filling were mathematically generated based on TPMS, such as the gyroid, which was selected for its optimal mechanical, structural, and biological properties for mandibular implant applications. The samples were generated by a Boolean operation combining an internal solid part (10x5x8 mm) with a lattice section (8x3x8 mm) (Figure 90). The unit cell sizes investigated for the gyroid lattice are 2x2x2 mm, 3x3x3 mm, and 4x4x4 mm, with a wall thickness of 0.25 mm and no offset from the median surface. The TPMS structures smoothly integrate with the surrounding solid walls (Figure 91). The designed models were then exported to STL format in preparation for 3D printing.

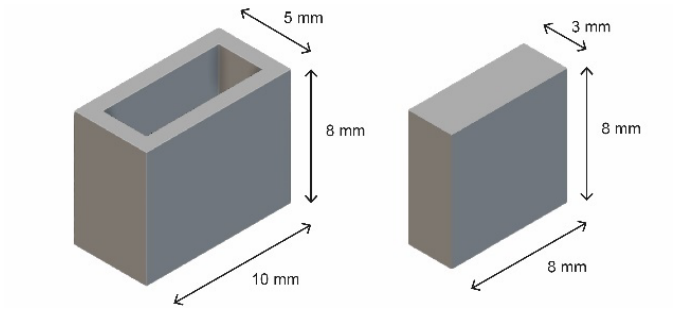

Figure 90. Dimensions of the samples: on the left, the external structure without filling; on the right, the internal structure to which filling will be applied.

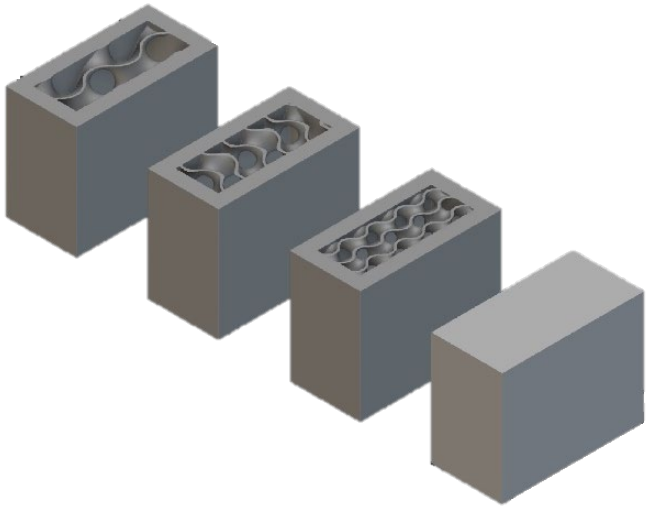

Figure 91. 3D CAD models of the sample.

Fabrication of specimens using Laser-Powder Bed Fusion

The lattice structures were fabricated using Laser Powder Bed Fusion (L-PBF) technology with an EOS M100 printer (EOS GmbH, Krailling, Germany) located at the Department of Materials Science and Engineering at Uppsala University. This technology enables the creation of complex geometries by melting metal powder layer by layer using a high-energy laser. The printer was chosen for its ability to reproduce minute details that are difficult to achieve with traditional methods. The powder used, Osprey® Ti6Al4V (supplied by Sandvik Additive Manufacturing AB, Sandviken, Sweden), has a particle size distribution with values of d10 = 29.0 µm, d50 = 42.7 µm and d90 = 62.4 µm. This alloy was selected for its biocompatibility, light weight, excellent surface finish, and established use in implant applications.

The exported STL models were prepared for printing using Autodesk NetFabb software, with the layer thickness set to 0.02 mm. The files were then converted to SLI format for processing by the EOSPrint M100-S12809 printing software. The exposure parameters for printing were configured as shown in Table 6. The samples were printed directly onto a pure titanium build plate without the use of media. Twenty specimens were 3D-printed, the types of which are shown in Figure 92.

Table 6. Exposure parameters for L-PBF printing.

Exposure parameter	**Value**
Distance	0.06 mm
Speed	1300 mm/s
Power	100 W
Beam offset	0.02 mm
Stripe width	5 mm
Stripes overlap	0 mm
Skywriting	ON
Hatching	X and Y Alternating Rotated

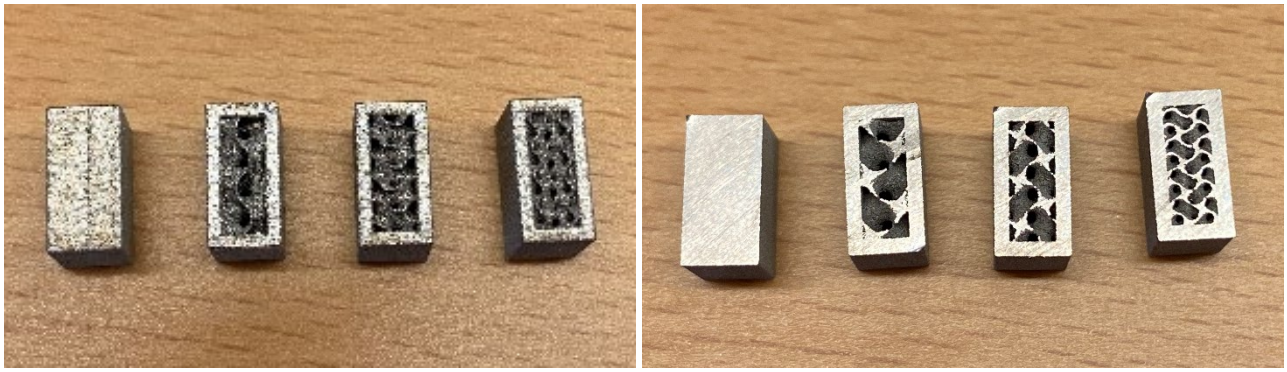

Figure 92. 3D-printed lattice-base structures, top and bottom views.

Post-Processing Surface Treatments

At the end of the printing process, post-treatments were required to improve surface quality and reduce roughness, which are critical aspects to ensure the comfort and biocompatibility of mandibular plates. Evaluation of the surface after treatment is critical to determine which technology achieves optimal roughness while maintaining structural integrity and promoting cell adhesion on 3D-printed models. Samples were sandblasted with glass beads (Guyson Sandblasting) and then treated with chemical etching to remove impurities and oxides. Two etching solutions were used: Keller's etch and Kroll's reagent, with a variable immersion time of 15 seconds, followed by rinsing with ethanol and drying with compressed air.

Evaluating the structural integrity, strength, and durability of lattice structures through mechanical testing is of paramount importance. This study focuses on the structural characterization of lattice structures by analyzing aspects such as microstructure and macrostructure, grain size, and the presence of defects or impurities. The characterization is performed using light optical microscopy (LOM) and scanning electron microscopy (SEM) techniques. Light optical microscopy allows the examination of the material structure at low magnification, allowing observation of grain size, phase distribution, and macroscopic defects. In contrast, scanning electron microscopy provides high-resolution images of the material surface, allowing detailed analysis of the surface topography.

Figure 93 and Figure 94 show the microscope images of the samples, solid and with 2x2x2 mm gyroid units, respectively. Both figures illustrate the four main treatments applied: L-PBF 3D printing, sandblasting, Keller’s etching, and etching with Kroll's reagent. The two samples show

similar characteristics for each type of treatment, but significant differences can be seen for each type. After 3D printing with L-PBF technology, the surface of the samples appears linear and wavy, typical of the traces left by the laser melting process. In particular, the visible lines are due to the laser path, highlighting a microstructure with elongated or directional grains. The sandblasted specimens, on the other hand, show no surface irregularities and have a more uniform texture. However, the surface appears rough and dull with a reduction in the number of laser marks. This treatment significantly altered the surface morphology of the samples. The etchings with Keller's and Kroll's solutions are used to reveal the internal microstructure of the material. In both cases, the solutions highlighted differences in the microstructure by outlining grain boundaries. Kroll's solution is more aggressive than Keller's, revealing a more defined microstructure and greater contrast between different areas of the sample.

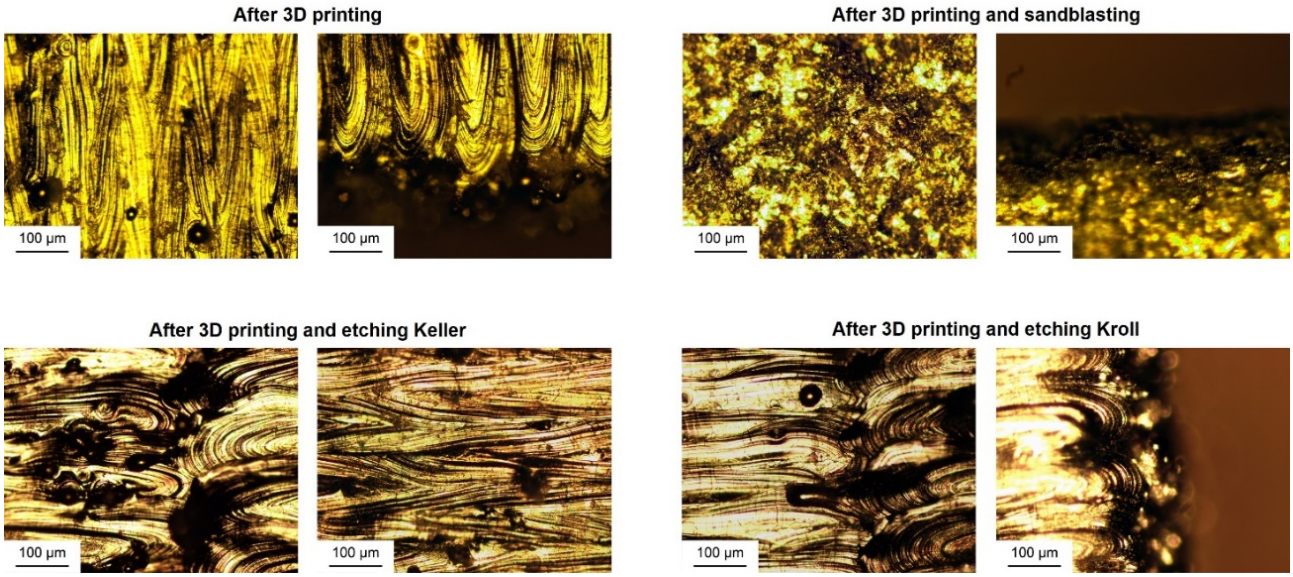

Figure 93. Micrographs of the solid sample: after 3D printing via L-PBF (top left), after sandblasting (top right), after Keller etching (bottom left), and after Kroll etching (bottom right).

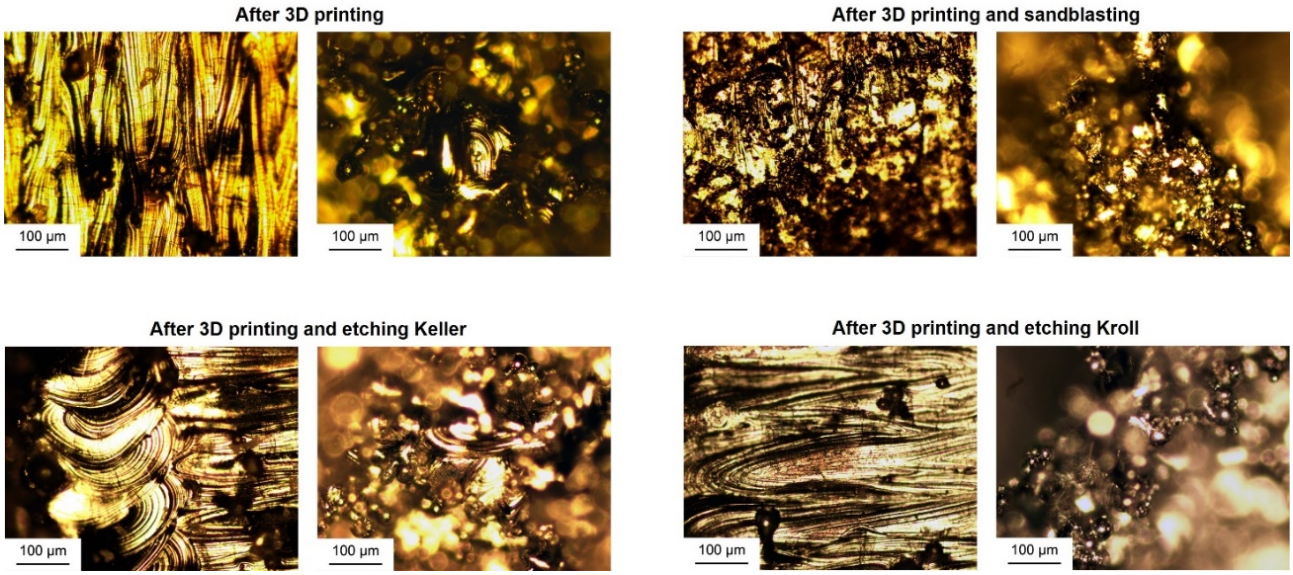

Figure 94. Micrographs of the sample with 2x2x2 mm gyroid units: after 3D printing via L-PBF (top left), after sandblasting (top right), after Keller etching (bottom left), and after Kroll etching (bottom right).

In-vitro study

A methodological protocol was developed for the analysis of cell adhesion on printed and processed samples. Two types of samples were studied: one solid and one with a lattice structure of 2x2x2 mm gyroid units. For each sample, the effect of 3D printing, Keller and Kroll etchings, and sandblasting combined with Keller etching was evaluated.

The samples, previously sterilized by soaking in 70% ethanol for 30 min, were placed in a 24-well plate. They were then immersed in 1.5 mL of culture medium (αMEM with 10% FBS) and incubated for 24 hours. The reagents required for cell seeding (PBS, αMEM, TrypLE) were heated to 37°C. Cell counts were performed using a hemocytometer and concentrations were adjusted to obtain three different densities: 50,000 cells in 500 µL for the solid sample and 812,000 cells in 500 µL for the gridded sample. The cells were then seeded onto the corresponding samples and incubated for one hour, followed by replenishment of the medium to a final volume of 1.4 mL and an additional 72-hour incubation. Finally, live/dead staining was performed by adding the reagents (calcein and ethidium homodimer) to the culture medium and incubating for one hour at 37°C in an atmosphere of 5% CO2. After removing the medium containing the reagents, the samples were prepared for observation under a confocal microscope.

The evaluation of cell adhesion on 3D-printed Ti6Al4V powder samples was performed using a confocal microscope (Leica Stellaris 5). This technology allowed the acquisition of high-resolution images of cell interactions with the surfaces of the samples, revealing details of cell distribution. Figure 95 and Figure 96 show the images obtained with the confocal microscope for the solid sample and the sample with 2x2x2 mm gyroid units, always highlighting the four treatments applied: 3D printing with L-PBF, sandblasting, Keller's etching, and Kroll's reagent etchings.

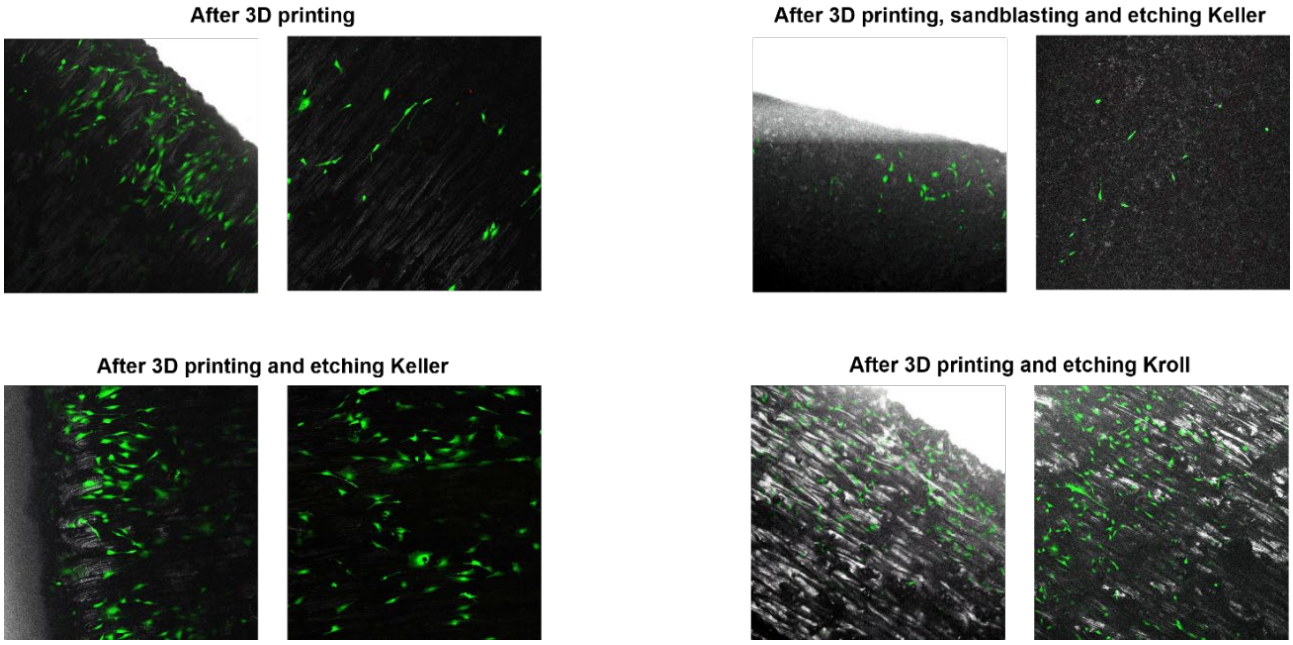

Figure 95. Confocal micrographs of the solid sample: after 3D printing via L-PBF (top left), after sandblasting (top right), after Keller etching (bottom left), and after Kroll etching (bottom right).

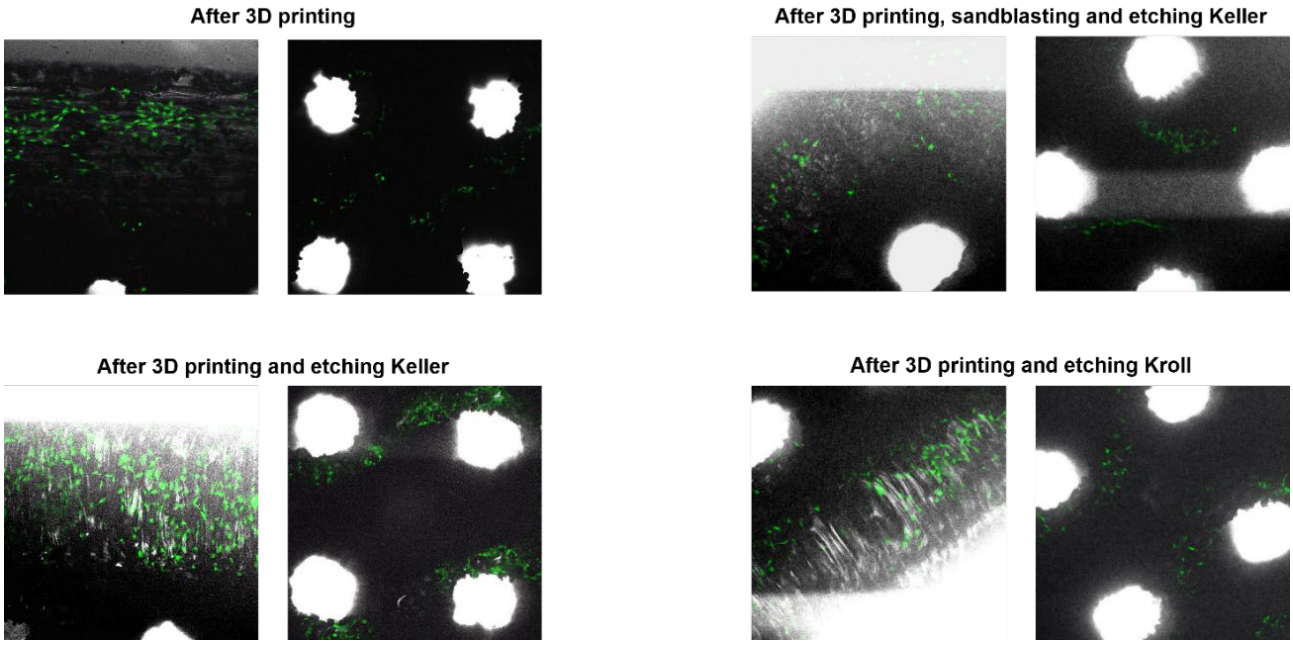

Figure 96. Confocal micrographs of the sample with 2x2x2 mm gyroid units: after 3D printing via L-PBF (top left), after sandblasting (top right), after Keller etching (bottom left), and after Kroll etching (bottom right).

In freshly printed solid samples, the cells appear evenly distributed over the surface, with a particular concentration at the edges. The cells appear elongated and tend to orient along the lines left by the printing. However, cell density is low in the interior areas and on the lattice structures. Keller's and Kroll's etchings improve cell distribution in both types of samples, with more cells distributed more evenly over the entire surface, including the inner areas and lattice structures. The exposure of the microstructure and etch lines may have helped to increase the biocompatibility of the surface. The combination of sandblasting and Keller's etching has a significant effect on the distribution of cells, which are much more dispersed than in the other samples, with a visibly reduced density. This suggests that sandblasting may have reduced the ability of the cells to adhere or alter the surface to make it less suitable for adhesion. The surface may appear too rough or irregular, reducing favorable sites for cell adhesion, or it may have removed microstructures critical for adhesion. In samples with lattice structures, cells are visible on the inside, which may indicate that the blasting had a greater effect on the outer surface than on the inner surface. In general, Keller's and Kroll's etchings improve cell adhesion by exposing favorable microstructures, whereas the combination of sandblasting and Keller's etching significantly reduces adhesion. The untreated printed sample shows a less dense cell distribution, suggesting that surface modifications may play a critical role in cell

adhesion. In the gridded sample, cells are also distributed around the gyroid units, with a higher concentration in the curved or angular areas. This suggests that the complex topography of the sample may favor greater adhesion in areas with pronounced irregularities or curvatures. The gyroid structure provides a three-dimensional surface that could enhance cell interaction, creating more adhesion points and stimulating a different cellular response than a solid sample. Cells appear to prefer areas characterized by curvature or voids, suggesting that complex geometry may enhance adhesion.

This study highlights the significant potential of 3D printing to improve the efficacy and precision of custom surgical implants, focusing on the use of innovative materials, such as titanium alloys, for the fabrication of mandibular plates. The integration of lattice structures into these plates represents a significant step toward optimizing components designed for additive manufacturing. Gyroid cells, inspired by the morphology of trabecular bone, have been designed and optimized to improve biomechanical performance. These structures allow a reduction in the material used without compromising the mechanical and functional performance of the implants. The sample with the gyroid cell structure showed a more concentrated cell distribution in the lattice areas than the solid sample. This interaction with the three-dimensional structure suggests that gyroid design may be particularly effective in promoting cell adhesion, especially in areas characterized by complex topography. These observations can be further investigated through quantitative analyses, such as counting adherent cells per unit area, to gain a more detailed understanding of adhesion dynamics.

Although the research project at Uppsala University is still at an experimental stage, the results obtained indicate that lattice structures adapted to mandibular plates have the potential to overcome the limitations of conventional implants. Preliminary cell response tests have shown significant cell adhesion in lattice structures, suggesting that such designs may stimulate bone regeneration and promote implant osseointegration. This research opens new perspectives in maxillofacial implant design by proposing a mandibular plate model that not only improves mechanical performance but also promotes bone regeneration. However, it is important to note that there was no direct collaboration with surgeons for the implementation of these implants, as there are no standardized protocols for the clinical application of mandibular

plates. Unlike cutting guides, which are designed for temporary use, implants remain in the body and require strict safety and quality control of the printing process. This situation represents an additional limitation to the practical application of research in real clinical settings.

5.4. Exploring Virtual Reality Surgical Planning applications

Another strand of experimental research has explored the use of VR in preoperative surgical planning, particularly in the case of musculoskeletal disorders such as tibia vara. This condition, characterized by a varus deformity of the knee, requires precise surgical interventions, such as a corrective osteotomy of the tibial plateau, to correct the axis of the tibia and ensure optimal growth.

In the context of VSP, the conventional process begins with segmentation of CT images to obtain a detailed 3D model of the tibia, which is then refined using 3D modeling software such as Blender to define the osteotomy plans and design the bone graft to be used, concluding with the preparation of files for 3D printing of the custom surgical instruments. Adapting the planning phase in a VR context has enabled the development of an immersive platform on Unity3D that allows surgeons to perform VSP independently, without the constant assistance of specialized technicians. In this environment, surgeons can interact with the anatomical model, control its visualization, and apply rotations and cutting angles in real-time. Using controllers or manual manipulation, the surgeon can set the cutting plane, apply transformations, and observe the effects of changes in real-time. The prototype was designed to be intuitive and modular, making it accessible to those with limited familiarity with advanced 3D modeling tools. The choice to use the OpenXR standard ensured the platform's compatibility with various VR devices, making the application flexible and easily extensible.

The user interface of the VR platform is designed for ease of use (Figure 97 and Figure 98). The first step is to authenticate and import the patient's anatomical model using a virtual keyboard that allows the user to select the OBJ file to be loaded into the 3D environment. On the main screen, the user has access to a "home" for visualization settings, including aspects such as application language, pass-through, and the ability to select other clinical cases. Once the

tibia model is imported, it can be freely interacted with using VR controllers or manual manipulation, allowing in-depth analysis of the anatomical structure. To start the osteotomy simulation, the virtual cutting tool, represented by a surgical saw with a cutting plane and a cylindrical fulcrum at the end, is activated. By placing the saw in the ideal position and pressing a dedicated button, the system performs a simulation of the cut on the bone model, which is displayed in two parts. Following the cut, a control panel is displayed for setting the correction angle of the tibial segment. The user can adjust the angle of the superior segment relative to the section plane using the up and down buttons, with the degrees of rotation displayed in real-time on a side panel. Once the desired correction angle is reached, the user can acquire two images of the bone model from a lateral and frontal perspective. These images are displayed on panels positioned behind the virtual operating table, allowing the surgeon to examine changes in the cutting plane and the applied angle of rotation.

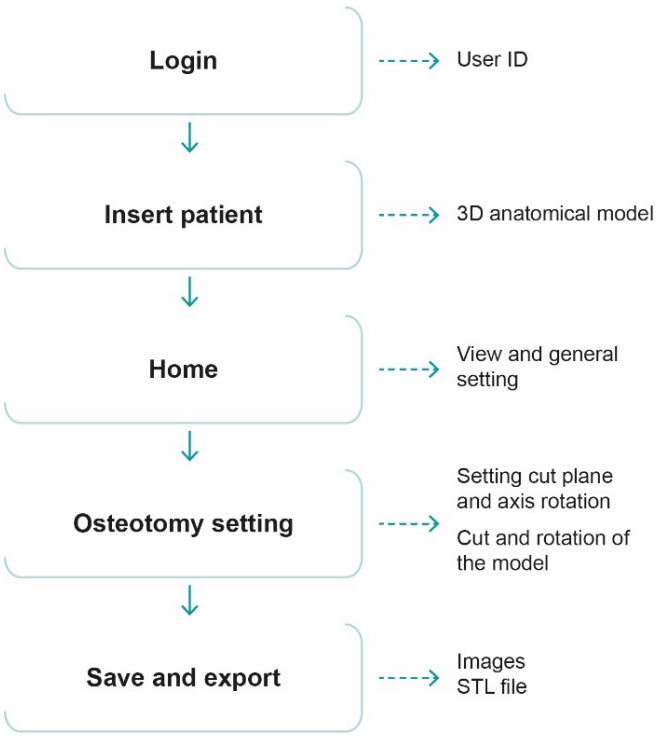

Figure 97. VR application logic.

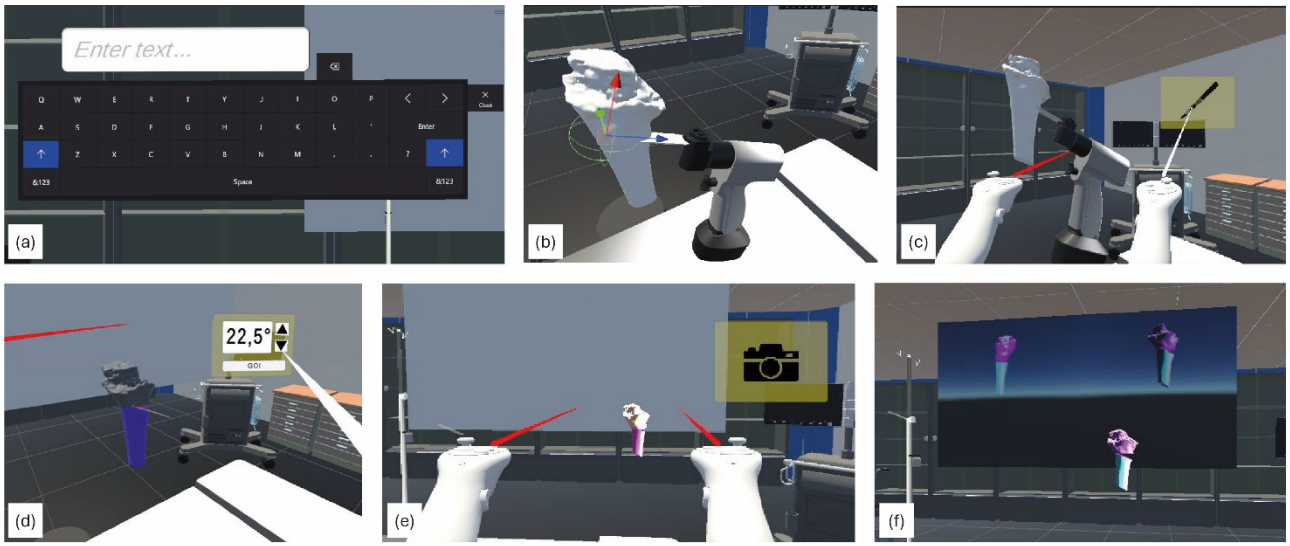

Figure 98. User interface on Unity during VSP: (a) login; (b) position of the cutting plane; (c) cut the model; (d) set the correction angle; (e) finalize and save; (f) export images and STL files.

The study conducted, although in a preliminary stage, highlights the potential of VR technology in orthopedic surgery, especially for the preoperative planning of complex surgeries such as tibial osteotomy. The VR application developed allows the surgeon to perform the VSP independently, transforming what was at the time a technical process into a more accessible and intuitive experience in which the surgeon becomes the primary user. This approach promotes a model in which surgical strategy and decisions do not depend on technical support from the engineer, making the process more effective and direct.

Despite promising results, the transition from VSP in a digital environment such as Blender to a VR environment is still incomplete. To completely replace the role of the designer in the planning phase, further improvements are needed to give the surgeon full operational independence. A major limitation of the current simulation is the partial representation of the anatomy, limited to a single bone segment, without including soft tissues, muscles, and ligaments, a limitation also shared by VSP performed in software such as Blender. Greater realism and a more complete VR experience could be achieved by integrating elements such as patient positioning, a body model for better spatial orientation, and virtual tools to simulate the surgical procedure more accurately, including the start of the incision.

A potential technological advance is the direct integration of bone wedge design and cutting guides within the VR environment, eliminating steps in external software and making the procedure smoother. Additional features such as automatic alignment of cutting planes with

anatomical references, e.g., parallelism of the correction plane with the tibial plateau, could further improve spatial awareness and surgical accuracy. Linking a database of medical images (CT, MRI) directly to the VR viewer would provide immediate access to diagnostic data, reducing the need for external devices and improving planning efficiency. In addition to clinical use, this application has significant educational value, providing young surgeons with an immersive platform to develop and refine their skills in a realistic and safe simulated environment.

Desirable future developments include improvements to the graphical user interface and ease of use, which, with regular updates, could make the application even more intuitive and versatile, and enhance the collaborative experience through the active participation of other users. Finally, adapting the application for mobile devices such as smartphones and tablets would provide convenient access to the visualization of 3D models while maintaining the difference with the immersive experience of virtual reality. These developments could make the application more versatile and accurate, expanding its use and improving its efficiency in both clinical and medical research settings [103].

5.5. Results of experimental investigations

The integration of advanced digital technologies such as 3D modeling, 3D printing, and virtual surgical simulation has significantly improved the representation of patients' cardiac and skeletal anatomy, allowing for much more detailed analysis than traditional two-dimensional visualization of diagnostic images (CT, MRI, ultrasound).

In the field of cardiac surgery, the use of 3D printing to represent complex pathologies such as aortic dissection has proven to be a valuable tool for surgeons, allowing them to study patient-specific cardiac anatomy by manipulating a physical model that is otherwise difficult to interpret with digital images alone.

From an engineering point of view, the application of different additive manufacturing materials and technologies in this field has allowed experimentation with specific printing parameters for materials with different properties, from the most rigid, such as PLA, to the most flexible, such as TPU and resin. Research has progressively moved towards an increasingly realistic

representation of anatomical models, aiming not only to reproduce aesthetics but also the physical-mechanical properties that determine their functional behavior.
The possibility of using different technologies, such as FDM and ALS, to reproduce the same heart section has allowed us to gain a thorough understanding of their technological characteristics, with their advantages and disadvantages. For example, for the representation of blood vessels, which often require thin walls, the use of FDM technology can be complex because of the post-processing required to apply to the media. However, by separating and printing individual parts of the object, FDM is the fastest and most cost-effective solution for this type of model. While SLA technology provides a high-quality representation of surface detail, it is extremely sensitive to printing parameters, requiring numerous trials for each specific object. As a result, the use of SLA for custom anatomy may not be ideal, as it is difficult to standardize and less adaptable to unique or variable geometries, as printing parameters do not always lend themselves to a variety of configurations.

The additive design and fabrication of patient-specific scaffolds represent an innovative approach to meeting the geometric requirements of bone grafts. This line of research offers significant opportunities for the development of integrated solutions that combine inert materials, such as PEEK, with biologically active materials that can stimulate bone regeneration. The integration of biologically active materials, such as hydrogels or collagen-based biomaterials, could further enhance the regenerative properties and promote a healing environment. It is critical to expand the research team to include biotechnologists to further investigate the interfaces between varied materials and the potential synergies from their combination. Such collaboration could facilitate the characterization of cell-material interactions, which is essential for evaluating the efficacy of scaffolds in promoting bone growth and vascularization. One aspect to consider regarding PEEK is its excessive cost, which limits its applications compared to materials used to produce anatomical models or cutting guides, tools designed for temporary use. PEEK is therefore more suitable for more permanent applications, such as grafts or implants, where its biocompatibility and excellent mechanical properties can be fully exploited. In this context, it is essential to conduct economic studies to assess the feasibility of clinical applications and cost optimization so that research can be translated into established and affordable clinical practices. From an engineering perspective,

the scaffold design study has paved the way for alternative solutions that can correlate the modeled object with the patient's specific bone structure from non-standard, customized geometries. This approach allows for greater precision in graft design to best meet individual anatomical needs. In addition, PEEK is a complex material whose unique properties require careful analysis of printing parameters. A thorough understanding of process variables such as extrusion temperature, printing speed, and substrate geometries is a critical foundation for optimizing the additive manufacturing of PEEK scaffolds and expanding their applications. Therefore, further investigation into the mechanical characterization and biological properties of PEEK could promote the adoption of this material in clinical settings and increase its potential for use in the fabrication of bone grafts and durable implants.

In this sense, the research conducted during the period of study abroad is particularly interesting, in which titanium powder produced and sintered using L-PBF technology was experimented with for the fabrication of mandibular implants, again in a specific design context. In both implants and prostheses, there is a significant bone resorption that can lead to implant failure due to poor osseointegration. Therefore, the development of an innovative design that allows the redesign of a standardized solid object has made the research particularly fascinating, especially considering the results obtained, which show that lattice structures, due to their porosity, promote greater cellular infiltration within molded objects. Ideally, this could lead to improved bone regeneration and osseointegration of implants. This is a crucial step in the development of more effective and biocompatible maxillofacial implants. In addition, it has been interesting to observe how academic research in an environment without direct university-hospital collaboration encounters difficulties in practical application. Although there have been contacts and meetings with the medical team, the need to certify the quality of the printed objects has limited the actual application of these innovations, since they are implants that remain inside the body. To translate research results into practical applications, it is essential to create synergies between the academic and clinical sectors, as well as to develop norms and standards that can guarantee the safety and efficacy of the implants produced.

The integration of advanced virtual reality into surgical planning has the potential to radically transform this traditional technical and engineering phase into an interactive and intuitive moment in which the surgeon simulates preoperative decisions firsthand. This approach not only makes planning more accessible, but also highly customizable for the user. Current immersive reality applications are simulation-oriented for training and follow standardized paths, with predefined and unchanging steps set by the software. In contrast, the proposed innovation aims to reverse this dynamic, giving the surgeon the freedom to create operative steps independently, following a procedure tailored to the specific case and not constrained by rigid patterns. More than a simple simulation, this approach takes the form of a true planning platform, leaving room for the surgeon's assumptions and decisions during the preoperative phase. Future developments in this direction could therefore have a significant impact on surgery, making preoperative planning not just a technical moment, but a dynamic, accessible, and user-centered experience.

6. Future Paradigms

Prospects in virtual surgical planning and the fabrication of patient-specific instruments look particularly promising due to the increasing integration of engineering and clinical expertise. The close collaboration between design and surgical teams during this research project confirmed the importance of a multidisciplinary approach in translating theoretical research into concrete applications, enabling the development of solutions that address real clinical needs and enhance personalized medicine.

A key development in this area is the creation of in-hospital 3D printing laboratories, known as Point-of-Care. These centers have the potential to revolutionize surgical care by reducing lead times for implant production and fostering greater control over the entire process, from planning to clinical implementation. Promoted by initiatives such as the European 3D Printing in Hospitals Special Interest Group, these laboratories define a new care paradigm by consolidating engineering and medical expertise in a single facility. The management of in-hospital units by hybrid teams - engineers with medical expertise and surgeons with advanced technical knowledge - provides an optimal setup for producing complex devices swiftly and responding to specific patient needs.

A significant challenge for these laboratories is developing specific certifications and regulations to ensure the safety and quality of the instruments produced. This necessitates adapting existing certifications to the hospital environment, where on-demand manufacturing must meet high standards in the context of limited time and resources.

From a technological perspective, future innovations will focus on advanced printing methods and biocompatible materials to improve the mechanical properties and durability of cutting guides and implants. The development of artificial intelligence algorithms to optimize surgical planning and automatically generate patient-specific guide models is another crucial step forward. Such technologies could be integrated into PoCs to help surgeons assess deformities and enhance decision-making.

The integration of intra-hospital 3D laboratories and the adoption of hybrid engineers with clinical expertise represents a new frontier for personalized medicine, poised to make customized surgery a standard service that improves patient care.

7. Conclusion

The purpose of this dissertation was to investigate and illustrate the potential of emerging engineering technologies in surgical planning, with a focus on CAD modeling, 3D printing, and XR technologies for patient-specific design of anatomical models, surgical instruments, bone grafts, and implants. This study evaluated the integration of these technologies into surgical planning, analyzing their potential in terms of accuracy, customization, and effectiveness. The study also aimed to examine the technological, regulatory, and economic challenges that still limit the widespread adoption of these tools in clinical settings.

The findings indicate that the utilization of 3D printing technology in the fabrication of anatomical models and patient-specific surgical devices represents a significant advancement in surgical planning and practice. The capacity to physically manipulate an anatomical model before surgery enables surgeons to enhance their comprehension of anatomical complexity and anticipate potential critical issues, thereby leading to improved surgical accuracy. Concurrently, the utilization of virtual reality has been demonstrated to be an effective tool for preoperative simulation, enabling surgeons to engage with an interactive three-dimensional environment to assess and evaluate surgical strategies in a more intuitive manner than conventional approaches.

A significant aspect that has emerged relates to the impact of these technologies on reducing surgical timelines and optimizing decision-making processes. The ability to virtually assess a surgery before its execution reduces the margin of error and improves patient safety. At the same time, the utilization of customized surgical cutting guides and implants fabricated via 3D printing allows procedures to be performed with greater precision, reducing the necessity for intraoperative adjustments and enhancing post-surgical prognosis.

However, for these technologies to be systematically integrated into clinical practice, several obstacles must be overcome. On the technological side, limitations persist related to model resolution, material fidelity, and compatibility between design, simulation, and 3D printing software. Future research should focus on improving interoperability between different platforms and optimizing digital workflows, making them more accessible and standardized for healthcare providers. From an economic perspective, the sustainability of implementing

these technologies relies on their potential to optimize resource utilization, streamline workflows, and enhance overall efficiency in clinical practice, contributing to a more effective and accessible healthcare system. Demonstrating cost-benefit benefits will be key to encouraging the adoption of these methodologies in health systems, incentivizing investment by hospital institutions and medical companies.

In addition, there is a need to standardize procedures and clinical validation of technologies on broader scenarios, as well as to initiate multicenter studies aimed at assessing the clinical and economic impact of the developed solutions, since their application is currently limited to one specific clinical-university setting. Although the validation of experimental studies, analyses, and processes requires considerable time and resources, the long-term benefits justify such investments. The processes and methodologies examined in this paper show high potential for improving clinical practice and identifying areas of innovation in healthcare.

Another critical factor is regulatory barriers. Currently, the lack of standardized regulations for the certification of 3D-printed models and devices is a barrier to their large-scale adoption. Further study and implementation of the EU Medical Device Regulation No. 2017/745 (MDR) and regulations ensuring a process and product quality system are essential to develop an operational procedure to ensure the safety, reliability, and reproducibility of these technologies within an in-hospital patient care service. The implementation of a clinical trial protocol, approved by the Ethics Committee of Area Vasta Emilia Centro (CE AVEC), allowed the implementation of a workflow that initially allowed the management of pediatric orthopedic cases, characterized by high complexity and uniqueness. In this context, the rapid evolution of pediatric pathologies represents a crucial challenge that requires the development of customized and rapid solutions by designers. The expertise gained in engineering and the impact of this research have extended beyond pediatric orthopedics to oncologic orthopedics, further demonstrating the value and versatility of this methodology within one of the world's leading orthopedic centers.

Future research prospects in this area will focus on the integration of 3D printing, virtual reality, artificial intelligence, and computational simulation to create unified digital platforms to support surgical planning and execution. The application of artificial intelligence algorithms for medical image analysis could automate and improve anatomical segmentation, enabling the generation of even more accurate and personalized 3D models. At the same time, the evolution

of 3D printing materials, with the development of biodegradable polymers, bio-absorbable composites, and innovative metal alloys, will open new possibilities in the field of regenerative surgery and the production of personalized implants. Printing biomimetic structures that mimic the mechanical and biological properties of natural tissues could be one of the most promising directions for the future of personalized medicine.

A crucial aspect that emerged from the study concerns the need for new professionals capable of managing and using these advanced technologies. The integration of digital tools into clinical pathways requires the training of professionals with multidisciplinary skills, capable of operating at the intersection of medicine and engineering, understanding and aligning clinical needs with the requirements of industrial engineering design. To meet this challenge, it is essential to train highly skilled professionals with flexibility, adaptability, and an open vision for innovation in an ever-changing field. The creation of dedicated programs and in-hospital laboratories specializing in 3D printing and virtual surgical planning and simulation is a key step in facilitating the transition to an advanced digital surgical model.

In the coming years, we can expect to see the growth of dedicated intra-hospital units that can provide highly personalized care and strengthen the integration of engineering and medicine. This innovative model will not only improve the efficiency and accuracy of surgical planning, but also contribute to a more collaborative, dynamic, and patient-oriented healthcare system.

In conclusion, this research has demonstrated the feasibility of integrating the advanced engineering technologies of CAD modeling, 3D printing, and virtual reality into surgical planning, which represents a significant breakthrough in the clinical practice of pediatric orthopedics. However, widespread adoption of these innovations will require a concerted effort by the scientific community, healthcare professionals, and regulatory agencies to overcome current technical, economic, and regulatory challenges. Investing in these technologies would mean improving the efficacy and safety of surgical procedures and redefining the paradigms of personalized medicine, paving the way for a future in which treatment is increasingly customized for each patient, with a tangible impact on quality of life.

Acknowledgments

These three years as a PhD student have been a path of intense growth for me, made up of discoveries and challenges. The opportunity to work in different environments and explore innovative techniques and technologies has deeply enriched my skills and fostered greater personal awareness. Over time, I have learned to smooth out my character traits that, although motivated by the desire to always do my best, sometimes limited a more open and collaborative approach. Along the way, my background in industrial design has been essential in understanding and translating the clinical needs of surgeons into patient-specific solutions, integrating a vision that is attentive to the practical needs of the surgical environment.

Looking back, I recognize in many of the events of my journey a sense of serendipity that led me to the right opportunities. Every decision and every step seemed to flow naturally, as if each opportunity was there on purpose, ready to be taken. I felt that I was in the right place at the right time, and that gave me confidence and motivation.

Every person I met along the way gave me something, and often those I expected less from guided me with fresh perspectives, encouraging me to keep going and questioning my way of seeing things.

I would like to thank Professor *Leonardo Frizziero*, supervisor of this project, who has believed in my abilities since my master's degree, and Professor *Alfredo Liverani*, esteemed co-supervisor, for his listening and inspiration; thanks also to Dr. *Giovanni Trisolino*, co-supervisor and mentor, who has guided and supported my development from the beginning, both professionally and personally.

I would also like to express my gratitude to my colleagues in the DIN and the Pediatric Orthopedics and Traumatology Unit of the IOR. *Gian Maria*, who introduced me to the research team and taught me every first step; *Grazia Chiara*, friend, colleague, roommate, and indispensable mate with whom I shared this swinging adventure; *Patrich*, the most innovative dreamer; *Andrea*, the practical and innovative person; *Curzio*, the most self-confident person; *Marco*, the most non-conformist person; *Edoardo*, persistent and convinced of his ideas; *Giulio*, fellow designer in a world of engineers; *Marella*, *Francesca*, *Irene*, *Alessandro*, *Simone*, *Adriano*, with whom I have shared fun social moments both in and out of work.

I would like to express my gratitude to the collaborators at the Musculoskeletal Tissue Bank, *Carmelo* and *Leonardo*, for their valuable support in this research, and to the doctors at the Sant-Orsola-Malpighi Polyclinic, Drs. *Antonio Loforte* and *Gianluca Folesani*, for allowing expanding the application of the research.

To my Uppsala team, especially *Cecilia* and *Francesco*, for giving me the opportunity and the great chance to spend six amazing months in Sweden, the country I have always admired and dreamed of. *Zaki* and *Estefanìa*, who accompanied me in the experiments and taught me fascinating things; *Edona* and *Salim*, with whom I spent a fantastic time in and out of the university and thanks to whom I felt more confident with my English, deserve a heartfelt thank you. The time I spent with all of you still makes me proud that I chose this experience.

Special thanks to my friends, *Veronica*, who was always ready to support and listen; *Diego*, who opened me up to the medical world without being unaware of what could happen; *Elena F.* and *Elena C.*, who, despite the distance, always have a way of being there, even unexpectedly.

Finally, to those who mean the most, my family. They have unconditionally placed great trust and support in me. To mom and dad, *Federica* and *Giuseppe*, my brother *Francesco*, my grandmother *Silviana* and *Matteo*, a warm hug.

To all of you, thank you.

References

[1] J.I. Efanov, A.A. Roy, K.N. Huang, D.E. Borsuk, Virtual surgical planning: The Pearls and pitfalls, Plast Reconstr Surg Glob Open 6 (2018) e1443. https://doi.org/10.1097/GOX.0000000000001443.

[2] G.D. Singh, M. Singh, Virtual surgical planning: Modeling from the present to the future, J Clin Med 10 (2021). https://doi.org/10.3390/jcm10235655.

[3] Z. Chen, S. Mo, X. Fan, Y. You, G. Ye, N. Zhou, A Meta-analysis and Systematic Review Comparing the Effectiveness of Traditional and Virtual Surgical Planning for Orthognathic Surgery: Based on Randomized Clinical Trials, Journal of Oral and Maxillofacial Surgery 79 (2021) 471.e1-471.e19. https://doi.org/10.1016/j.joms.2020.09.005.

[4] Y. Lou, L. Cai, C. Wang, Q. Tang, T. Pan, X. Guo, J. Wang, Comparison of traditional surgery and surgery assisted by three dimensional printing technology in the treatment of tibial plateau fractures, Int Orthop 41 (2017) 1875–1880. https://doi.org/10.1007/s00264-017-3445-y.

[5] G.N. Hounsfield, Computed Medical Imaging, J Comput Assist Tomogr 4 (1980) 665–674. https://doi.org/10.1097/00004728-198010000-00017.

[6] M.W. Vannier, J.L. Marsh, J.O. Warren, Three dimensional CT reconstruction images for reconstruction images for craniofacial surgical planning and evaluation, Radiology 150 (1984) 179–184. https://doi.org/10.1148/radiology.150.1.6689758.

[7] R. Marmulla, H. Niederdellmann, Surgical planning of computer-assisted repositioning osteotomies, Plast Reconstr Surg 104 (1999) 938–944. https://doi.org/10.1097/00006534-199909020-00007.

[8] D. Mattavelli, A. Fiorentino, F. Tengattini, A. Colpani, S. Agnelli, B. Buffoli, M. Ravanelli, M. Ferrari, A. Schreiber, V. Rampinelli, S. Taboni, V. Verzeletti, A. Deganello, L.F. Rodella, R. Maroldi, E. Ceretti, L. Sartore, C. Piazza, M.M. Fontanella, P. Nicolai, F. Doglietto, Additive Manufacturing for Personalized Skull Base Reconstruction in Endoscopic Transclival Surgery: A Proof-of-Concept Study, World Neurosurg 155 (2021) e439–e452. https://doi.org/10.1016/j.wneu.2021.08.080.

[9] A. Valls-Esteve, A. Tejo-Otero, N. Adell-Gómez, P. Lustig-Gainza, F. Fenollosa-Artés, I. Buj-Corral, J. Rubio-Palau, J. Munuera, L. Krauel, Advanced Strategies for the Fabrication of Multi-Material Anatomical Models of Complex Pediatric Oncologic Cases, Bioengineering 11 (2024) 31. https://doi.org/10.3390/bioengineering11010031.

[10] B. Zhang, T. Masuzawa, E. Tatsumi, Y. Taenaka, C. Uyama, H. Takano, M. Takamiya, Three-dimensional thoracic modeling for an anatomical compatibility study of the implantable total artificial heart, Artif Organs 23 (1999) 229–234. https://doi.org/10.1046/j.1525-1594.1999.06313.x.

[11] J.H. Shi, W. Lv, Y. Wang, B. Ma, W. Cui, Z.Z. Liu, K.C. Han, Three dimensional patient-specific printed cutting guides for closing-wedge distal femoral osteotomy, Int Orthop 43 (2019) 619–624. https://doi.org/10.1007/s00264-018-4043-3.

[12] J. Arnal-Burró, R. Pérez-Mañanes, E. Gallo-del-Valle, C. Igualada-Blazquez, M. Cuervas-Mons, J. Vaquero-Martín, Three dimensional-printed patient-specific cutting guides for femoral varization osteotomy: Do it yourself, Knee 24 (2017) 1359–1368. https://doi.org/10.1016/j.knee.2017.04.016.

[13] C. Pool, A. Moroco, J.G. Lighthall, Utilizing Virtual Surgical Planning and Patient-Specific Cutting Guides in Microtia Repair with Autologous Costal Cartilage Graft, Plast Reconstr Surg 154 (2024) 569e–572e. https://doi.org/10.1097/PRS.0000000000010897.

[14] B. Schlatterer, J.M. Linares, J. Cazal, P. Merloz, S. Plaweski, Posterior tibial slope accuracy with patient-specific cutting guides during total knee arthroplasty: A preliminary study of 50 cases, Orthopaedics and Traumatology: Surgery and Research 101 (2015) S233–S240. https://doi.org/10.1016/j.otsr.2015.06.005.

[15] S. Chaouche, C. Jacquet, M. Fabre-Aubrespy, A. Sharma, J.N. Argenson, S. Parratte, M. Ollivier, Patient-specific cutting guides for open-wedge high tibial osteotomy: safety and accuracy analysis of a hundred patients continuous cohort, Int Orthop 43 (2019) 2757–2765. https://doi.org/10.1007/s00264-019-04372-4.

[16] S. Fidvi, J. Holder, H. Li, G.J. Parnes, S.B. Shamir, N. Wake, Advanced 3D Visualization and 3D Printing in Radiology, Adv Exp Med Biol 1406 (2023) 103–138. https://doi.org/10.1007/978-3-031-26462-7_6.

[17] F. Altahawi, J. Pierce, M. Aslan, X. Li, C.S. Winalski, N. Subhas, 3D MRI of the Knee, Semin Musculoskelet Radiol 25 (2021) 455–467. https://doi.org/10.1055/s-0041-1730400.

[18] P.K. Chan, C. Fang, E. Fang, M. Leung, C.H. Yan, K.Y. Chiu, Three-dimensional printing and computer navigation for correction of multiple deformities in osteogenesis imperfecta, JBJS Case Connect 11 (2021). https://doi.org/10.2106/JBJS.CC.20.00501.

[19] E.J. Moore, D.L. Price, K.M. Van Abel, J.R. Janus, E.T. Moore, E. Martin, J.M. Morris, A.E. Alexander, Association of Virtual Surgical Planning with External Incisions in Complex Maxillectomy Reconstruction, JAMA Otolaryngol Head Neck Surg 147 (2021) 526–531. https://doi.org/10.1001/jamaoto.2021.0251.

[20] I. Valverde, G. Gomez-Ciriza, T. Hussain, C. Suarez-Mejias, M.N. Velasco-Forte, N. Byrne, A. Ordoñez, A. Gonzalez-Calle, D. Anderson, M.G. Hazekamp, A.A.W. Roest, J. Rivas-Gonzalez, S. Uribe, I. El-Rassi, J. Simpson, O. Miller, E. Ruiz, I. Zabala, A. Mendez, B. Manso, P. Gallego, F. Prada, M. Cantinotti, L. Ait-Ali, C. Merino, A. Parry, N. Poirier, G. Greil, R. Razavi, T. Gomez-Cia, A.R. Hosseinpour, Three-dimensional printed models for surgical planning of complex congenital heart defects: An international multicentre study, European Journal of Cardio-Thoracic Surgery 52 (2017) 1139–1148. https://doi.org/10.1093/EJCTS/EZX208.

[21] H. Younis, C. Lv, B. Xu, H. Zhou, L. Du, L. Liao, N. Zhao, W. Long, S.A. Elayah, X. Chang, L. He, Accuracy of dynamic navigation compared to static surgical guides and the freehand approach in implant placement: a prospective clinical study, Head Face Med 20 (2024) 30. https://doi.org/10.1186/s13005-024-00433-1.

[22] V.J. Sabesan, R.T. Rudraraju, B. Sheth, J. Grauer, M. Stankard, K. Chatha, D.J.L. Lima, Three-dimensional preoperative planning accurately guides surgeons for intraoperative implant selection in shoulder arthroplasty, Seminars in Arthroplasty JSES 30 (2020) 360–367. https://doi.org/10.1053/j.sart.2020.08.009.

[23] R.A. Borracci, L.M. Ferreira, J.M. Alvarez Gallesio, O.M. Tenorio Núñez, M. David, E.P. Eyheremendy, Three-dimensional virtual and printed models for planning adult cardiovascular surgery, Acta Cardiol 76 (2021) 534–543. https://doi.org/10.1080/00015385.2020.1852754.

[24] L. Klimek, H.M. Klein, W. Schneider, R. Mösges, B. Schmelzer, E.D. Voy, Stereolithographic modelling for reconstructive head surgery., Acta Otorhinolaryngol Belg 47 (1993) 329–334. http://www.ncbi.nlm.nih.gov/pubmed/8213143.

[25] D.H. Yang, S.H. Park, N. Kim, E.S. Choi, B.S. Kwon, C.S. Park, S.G. Cha, J.S. Baek, J.J. Yu, Y.H. Kim, T.J. Yun, Incremental Value of 3D Printing in the Preoperative Planning of Complex Congenital Heart Disease Surgery, JACC Cardiovasc Imaging 14 (2021) 1265–1270. https://doi.org/10.1016/j.jcmg.2020.06.024.

[26] J.R. Miller, G.K. Singh, P.K. Woodard, P. Eghtesady, S. Anwar, 3D printing for preoperative planning and surgical simulation of ventricular assist device implantation in a failing systemic right ventricle, J Cardiovasc Comput Tomogr 14 (2020) e172–e174. https://doi.org/10.1016/j.jcct.2020.04.008.

[27] J. Stana, M. Grab, R. Kargl, N. Tsilimparis, 3D printing in the planning and teaching of endovascular procedures, Radiologie 62 (2022) 28–33. https://doi.org/10.1007/s00117-022-01047-x.

[28] M. Rama, L. Schlegel, D. Wisner, R. Pugliese, S. Ramesh, R. Penne, A. Watson, Using three-dimensional printed models for trainee orbital fracture education, BMC Med Educ 23 (2023) 467. https://doi.org/10.1186/s12909-023-04436-5.

[29] C. Jacquet, A. Sharma, M. Fabre, M. Ehlinger, J.N. Argenson, S. Parratte, M. Ollivier, Patient-specific high-tibial osteotomy's 'cutting-guides' decrease operating time and the number of fluoroscopic images taken after a Brief Learning Curve, Knee Surgery, Sports Traumatology, Arthroscopy 28 (2020) 2854–2862. https://doi.org/10.1007/s00167-019-05637-6.

[30] H.R. Bin Abd Razak, C. Jacquet, A.J. Wilson, R.S. Khakha, K. Kley, S. Parratte, M. Ollivier, Minimally Invasive High Tibial Osteotomy Using a Patient-Specific Cutting Guide, Arthrosc Tech 10 (2021) e431–e435. https://doi.org/10.1016/j.eats.2020.10.029.

[31] C.B. Marti, E. Gautier, S.W. Wachtl, R.P. Jakob, Accuracy of Frontal and Sagittal Plane Correction in Open-Wedge High Tibial Osteotomy, Arthroscopy - Journal of Arthroscopic and Related Surgery 20 (2004) 366–372. https://doi.org/10.1016/j.arthro.2004.01.024.

[32] S.F. Fucentese, P. Meier, L. Jud, G.L. Köchli, A. Aichmair, L. Vlachopoulos, P. Fürnstahl, Accuracy of 3D-planned patient specific instrumentation in high tibial open wedge valgisation osteotomy, J Exp Orthop 7 (2020). https://doi.org/10.1186/s40634-020-00224-y.

[33] W. Van Genechten, A. Van Haver, S. Bartholomeeusen, T. Claes, N. Van Beek, J. Michielsen, S. Claes, P. Verdonk, Impacted bone allograft personalised by a novel 3D printed customization kit produces high surgical accuracy in medial opening wedge high tibial osteotomy: a pilot study, J Exp Orthop 10 (2023) 24. https://doi.org/10.1186/s40634-023-00593-0.

[34] R.J. Narayan, Advances in 3D bioprinting, 2023. https://doi.org/10.1201/9781351003780.

[35] J.C. Yuk, K.H. Nam, S.H. Park, Additive-manufactured synthetic bone model with biomimicking tunable mechanical properties for evaluation of medical implants, Int J Bioprint 10 (2024) 417–432. https://doi.org/10.36922/ijb.1067.

[36] K.S. Ahmed, H. Ibad, Z.A. Suchal, A.K. Gosain, Implementation of 3D Printing and Computer-Aided Design and Manufacturing (CAD/CAM) in Craniofacial Reconstruction, Journal of Craniofacial Surgery 33 (2022) 1714–1719. https://doi.org/10.1097/SCS.0000000000008561.

[37] Y.Z. Zhang, S. Lu, B. Chen, J.M. Zhao, R. Liu, G.X. Pei, Application of computer-aided design osteotomy template for treatment of cubitus varus deformity in teenagers: A pilot study, J Shoulder Elbow Surg 20 (2011) 51–56. https://doi.org/10.1016/j.jse.2010.08.029.

[38] J.P. Pöppe, M. Spendel, C.J. Griessenauer, A. Gaggl, W. Wurm, S. Enzinger, Point-of-Care 3-Dimensional–Printed Polyetheretherketone Customized Implants for Cranioplastic Surgery of Large Skull Defects, Operative Neurosurgery (2024). https://doi.org/10.1227/ons.0000000000001154.

[39] H. Aiba, B. Spazzoli, S. Tsukamoto, A.F. Mavrogenis, T. Hermann, H. Kimura, H. Murakami, D.M. Donati, C. Errani, Current Concepts in the Resection of Bone Tumors Using a Patient-Specific Three-Dimensional Printed Cutting Guide, Current Oncology 30 (2023) 3859–3870. https://doi.org/10.3390/curroncol30040292.

[40] A. Benady, S.J. Meyer, E. Golden, S. Dadia, G. Katarivas Levy, Patient-specific Ti-6Al-4V lattice implants for critical-sized load-bearing bone defects reconstruction, Mater Des 226 (2023) 111605. https://doi.org/10.1016/j.matdes.2023.111605.

[41] A. Tel, E. Kornfellner, F. Moscato, S. Vinayahalingam, T. Xi, L. Arboit, M. Robiony, Optimizing efficiency in the creation of patient-specific plates through field-driven generative design in maxillofacial surgery, Sci Rep 13 (2023) 12082. https://doi.org/10.1038/s41598-023-39327-8.

[42] V. Al Georgeanu, O. Gingu, I. V. Antoniac, H.O. Manolea, Current Options and Future Perspectives on Bone Graft and Biomaterials Substitutes for Bone Repair, from Clinical Needs to Advanced Biomaterials Research, Applied Sciences (Switzerland) 13 (2023) 8471. https://doi.org/10.3390/app13148471.

[43] V. Raeisdasteh Hokmabad, S. Davaran, A. Ramazani, R. Salehi, Design and fabrication of porous biodegradable scaffolds: a strategy for tissue engineering, J Biomater Sci Polym Ed 28 (2017) 1797–1825. https://doi.org/10.1080/09205063.2017.1354674.

[44] M. Filippi, G. Born, M. Chaaban, A. Scherberich, Natural Polymeric Scaffolds in Bone Regeneration, Front Bioeng Biotechnol 8 (2020). https://doi.org/10.3389/fbioe.2020.00474.

[45] S. Kanwar, S. Vijayavenkataraman, 3D printable bone-mimicking functionally gradient stochastic scaffolds for tissue engineering and bone implant applications, Mater Des 223 (2022) 111199. https://doi.org/10.1016/j.matdes.2022.111199.

[46] S. Simorgh, N. Alasvand, M. Khodadadi, F. Ghobadi, M. Malekzadeh Kebria, P. Brouki Milan, S. Kargozar, F. Baino, A. Mobasheri, M. Mozafari, Additive manufacturing of bioactive glass biomaterials, Methods 208 (2022) 75–91. https://doi.org/10.1016/j.ymeth.2022.10.010.

[47] C.N. Kelly, A.T. Miller, S.J. Hollister, R.E. Guldberg, K. Gall, Design and Structure–Function Characterization of 3D Printed Synthetic Porous Biomaterials for Tissue Engineering, Adv Healthc Mater 7 (2018) 1701095. https://doi.org/10.1002/adhm.201701095.

[48] X. Yue, J. Shang, M. Zhang, B. Hur, X. Ma, Additive manufacturing of high porosity magnesium scaffolds with lattice structure and random structure, Materials Science and Engineering: A 859 (2022) 144167. https://doi.org/10.1016/j.msea.2022.144167.

[49] X. Wang, F. Yu, L. Ye, Epigenetic control of mesenchymal stem cells orchestrates bone regeneration, Front Endocrinol (Lausanne) 14 (2023) 1126787. https://doi.org/10.3389/fendo.2023.1126787.

[50] M.P. Bernardo, B.C.R. da Silva, A.E.I. Hamouda, M.A.S. de Toledo, C. Schalla, S. Rütten, R. Goetzke, L.H.C. Mattoso, M. Zenke, A. Sechi, PLA/Hydroxyapatite scaffolds exhibit in vitro immunological inertness and promote robust osteogenic differentiation of human mesenchymal stem cells without osteogenic stimuli, Sci Rep 12 (2022) 2333. https://doi.org/10.1038/s41598-022-05207-w.

[51] Y. Li, L. Chen, Y. Stehle, M. Lin, C. Wang, R. Zhang, M. Huang, Y. Li, Q. Zou, Extrusion-based 3D-printed "rolled-up" composite scaffolds with hierarchical pore structure for bone growth and repair, J Mater Sci Technol 171 (2024) 222–234. https://doi.org/10.1016/j.jmst.2023.07.018.

[52] Q.L. Loh, C. Choong, Three-dimensional scaffolds for tissue engineering applications: Role of porosity and pore size, Tissue Eng Part B Rev 19 (2013) 485–502. https://doi.org/10.1089/ten.teb.2012.0437.

[53] X. Li, Y. Wang, B. Zhang, H. Yang, R.T. Mushtaq, M. Liu, C. Bao, Y. Shi, Z. Luo, W. Zhang, The design and evaluation of bionic porous bone scaffolds in fluid flow characteristics and mechanical properties, Comput Methods Programs Biomed 225 (2022) 107059. https://doi.org/10.1016/j.cmpb.2022.107059.

[54] E. Kornfellner, S. Reininger, S. Geier, M. Schwentenwein, E. Benca, S. Scheiner, F. Moscato, Mechanical properties of additively manufactured lattice structures composed of zirconia and hydroxyapatite ceramics, J Mech Behav Biomed Mater 158 (2024) 106644. https://doi.org/10.1016/j.jmbbm.2024.106644.

[55] H. Huang, L. Qiang, M. Fan, Y. Liu, A. Yang, D. Chang, J. Li, T. Sun, Y. Wang, R. Guo, H. Zhuang, X. Li, T. Guo, J. Wang, H. Tan, P. Zheng, J. Weng, 3D-printed tri-element-doped hydroxyapatite/ polycaprolactone composite scaffolds with antibacterial potential for osteosarcoma therapy and bone regeneration, Bioact Mater 31 (2024) 18–37. https://doi.org/10.1016/j.bioactmat.2023.07.004.

[56] D. Wu, A. Spanou, A. Diez-Escudero, C. Persson, 3D-printed PLA/HA composite structures as synthetic trabecular bone: A feasibility study using fused deposition modeling, J Mech Behav Biomed Mater 103 (2020) 103608. https://doi.org/10.1016/j.jmbbm.2019.103608.

[57] N. Sabahi, E. Farajzadeh, I. Roohani, C.H. Wang, X. Li, Material extrusion 3D printing of polyether-ether-ketone scaffolds based on triply periodic minimal surface designs: A numerical and experimental investigation, Appl Mater Today 39 (2024) 102262. https://doi.org/10.1016/j.apmt.2024.102262.

[58] Z. Zheng, P. Liu, X. Zhang, Jingguo xin, Yongjie wang, X. Zou, X. Mei, S. Zhang, S. Zhang, Strategies to improve bioactive and antibacterial properties of polyetheretherketone (PEEK) for use as orthopedic implants, Mater Today Bio 16 (2022) 100402. https://doi.org/10.1016/j.mtbio.2022.100402.

[59] E. Yang, M. Leary, B. Lozanovski, D. Downing, M. Mazur, A. Sarker, A.M. Khorasani, A. Jones, T. Maconachie, S. Bateman, M. Easton, M. Qian, P. Choong, M. Brandt, Effect of geometry on the mechanical properties of Ti-6Al-4V Gyroid structures fabricated via SLM: A numerical study, Mater Des 184 (2019) 108165. https://doi.org/10.1016/j.matdes.2019.108165.

[60] G.A. Longhitano, M. Chiarelli, D. Prada, C.A. de C. Zavaglia, R. Maciel Filho, Personalized lattice-structured prosthesis as a graftless solution for mandible reconstruction and prosthetic restoration: A finite element analysis, J Mech Behav Biomed Mater 152 (2024). https://doi.org/10.1016/j.jmbbm.2024.106460.

[61] A. Arjomandi Rad, R. Vardanyan, S.G. Thavarajasingam, A. Zubarevich, J. Van Den Eynde, M.P.B.O. Sá, K. Zhigalov, P. Sardiari Nia, A. Ruhparwar, A. Weymann, Extended, virtual and augmented reality in thoracic surgery: A systematic review, Interact Cardiovasc Thorac Surg 34 (2022) 201–211. https://doi.org/10.1093/icvts/ivab241.

[62] A. Tel, L. Raccampo, S. Vinayahalingam, S. Troise, V. Abbate, G.D. Orabona, S. Sembronio, M. Robiony, Complex Craniofacial Cases through Augmented Reality Guidance in Surgical Oncology: A Technical Report, Diagnostics 14 (2024) 1108. https://doi.org/10.3390/diagnostics14111108.

[63] F. Ceccariglia, L. Cercenelli, G. Badiali, E. Marcelli, A. Tarsitano, Application of Augmented Reality to Maxillary Resections: A Three-Dimensional Approach to Maxillofacial Oncologic Surgery, J Pers Med 12 (2022) 2047–2047. https://doi.org/10.3390/jpm12122047.

[64] C.A. Molina, N. Theodore, A. Karim Ahmed, E.M. Westbroek, Y. Mirovsky, R. Harel, E. Orru, M. Khan, T. Witham, D.M. Sciubba, Augmented reality-assisted pedicle screw insertion: A cadaveric proof-of-concept study, J Neurosurg Spine 31 (2019) 139–146. https://doi.org/10.3171/2018.12.SPINE181142.

[65] F.A. Casari, N. Navab, L.A. Hruby, P. Kriechling, R. Nakamura, R. Tori, F. de Lourdes dos Santos Nunes, M.C. Queiroz, P. Fürnstahl, M. Farshad, Augmented Reality in Orthopedic Surgery Is Emerging from Proof of Concept Towards Clinical Studies: a Literature Review Explaining the Technology and Current State of the Art, Curr Rev Musculoskelet Med 14 (2021) 192–203. https://doi.org/10.1007/s12178-021-09699-3.

[66] J. Hajek, M. Unberath, J. Fotouhi, B. Bier, S.C. Lee, G. Osgood, A. Maier, M. Armand, N. Navab, Closing the Calibration Loop: An Inside-Out-Tracking Paradigm for Augmented Reality in Orthopedic Surgery, Springer International Publishing, 2018. https://doi.org/10.1007/978-3-030-00937-3_35.

[67] S. Malhotra, O. Halabi, S.P. Dakua, J. Padhan, S. Paul, W. Palliyali, Augmented Reality in Surgical Navigation: A Review of Evaluation and Validation Metrics, Applied Sciences 13 (2023) 1629. https://doi.org/10.3390/app13031629.

[68] M.I. Muntahir, S. Sukaridhoto, D.K. Basuki, R.P.N. Budiarti, I.A. Al-Hafidz, E.D. Fajrianti, K. Hanifati, N.A. Satrio, A. Syahry, Implementation of Immersive Technology on Medical Education, IES 2022 - 2022 International Electronics Symposium: Energy Development for Climate Change Solution and Clean Energy Transition, Proceeding (2022) 651–657. https://doi.org/10.1109/IES55876.2022.9888379.

[69] J. Ruparelia, N. Manjunath, D.S. Nachiappan, A. Raheja, A. Suri, Virtual Reality in Preoperative Planning of Complex Cranial Surgery, World Neurosurg 180 (2023) e11–e18. https://doi.org/10.1016/j.wneu.2023.06.014.

[70] D. Abjigitova, A.H. Sadeghi, J.J. Peek, J.A. Bekkers, A.J.J.C. Bogers, E.A.F. Mahtab, Virtual Reality in the Preoperative Planning of Adult Aortic Surgery: A Feasibility Study, J Cardiovasc Dev Dis 9 (2022) 31. https://doi.org/10.3390/jcdd9020031.

[71] C. Piramide, L. Ulrich, P. Piazzolla, E. Vezzetti, Toward Supporting Maxillo-Facial Surgical Guides Positioning with Mixed Reality—A Preliminary Study, Applied Sciences (Switzerland) 12 (2022). https://doi.org/10.3390/app12168154.

[72] P. Caligiana, A. Liverani, A. Ceruti, G.M. Santi, G. Donnici, F. Osti, An Interactive Real-Time Cutting Technique for 3D Models in Mixed Reality, Technologies (Basel) 8 (2020) 23. https://doi.org/10.3390/technologies8020023.

[73] J.A. Sánchez-Margallo, C. Plaza de Miguel, R.A. Fernández Anzules, F.M. Sánchez-Margallo, Application of Mixed Reality in Medical Training and Surgical Planning Focused on Minimally Invasive Surgery, Front Virtual Real 2 (2021) 1–11. https://doi.org/10.3389/frvir.2021.692641.

[74] S. Su, P. Lei, C. Wang, F. Gao, D. Zhong, Y. Hu, Mixed Reality Technology in Total Knee Arthroplasty: An Updated Review With a Preliminary Case Report, Front Surg 9 (2022) 1–8. https://doi.org/10.3389/fsurg.2022.804029.

[75] E. Yildiz, C. Møller, A. Bilberg, Demonstration and evaluation of a digital twin-based virtual factory, International Journal of Advanced Manufacturing Technology 114 (2021) 185–203. https://doi.org/10.1007/s00170-021-06825-w.

[76] D. Yu, Z. He, Digital twin-driven intelligence disaster prevention and mitigation for infrastructure: advances, challenges, and opportunities, Natural Hazards 112 (2022) 1–36. https://doi.org/10.1007/s11069-021-05190-x.

[77] E.H. Glaessgen, D.S. Stargel, The digital twin paradigm for future NASA and U.S. Air force vehicles, Collection of Technical Papers - AIAA/ASME/ASCE/AHS/ASC Structures, Structural Dynamics and Materials Conference (2012). https://doi.org/10.2514/6.2012-1818.

[78] M. Klimo, M. Kvassay, N. Kvassayova, Digital Twin and Modelling a 3D Human Body in Healthcare, ICETA 2023 - 21st Year of International Conference on Emerging ELearning Technologies and Applications, Proceedings (2023) 307–312. https://doi.org/10.1109/ICETA61311.2023.10343978.

[79] H. Ahmed, L. Devoto, The Potential of a Digital Twin in Surgery, Surg Innov 28 (2021) 509–510. https://doi.org/10.1177/1553350620975896.

[80] M. Cellina, M. Cè, M. Alì, G. Irmici, S. Ibba, E. Caloro, D. Fazzini, G. Oliva, S. Papa, Digital Twins: The New Frontier for Personalized Medicine?, Applied Sciences (Switzerland) 13 (2023). https://doi.org/10.3390/app13137940.

[81] Materialise and Siemens Healthineers syngo.via Partnership, (n.d.). https://www.materialise.com/en/news/press-releases/materialise-and-siemens-healthineers-syngovia-partnership (accessed October 5, 2024).

[82] Materialise, Siemens, Philips, Stratasys, 3D Systems: Medical 3D Printing Partnerships and Products Introduced at 2017 RSNA Annual Meeting - 3DPrint.com | The Voice of 3D Printing / Additive Manufacturing, (n.d.). https://3dprint.com/195331/rsna-3d-printing-announcements/ (accessed October 5, 2024).

[83] G.E. Daoud, D.L. Pezzutti, C.J. Dolatowski, R.L. Carrau, M. Pancake, E. Herderick, K.K. VanKoevering, Establishing a point-of-care additive manufacturing workflow for clinical use, J Mater Res 36 (2021) 3761–3780. https://doi.org/10.1557/s43578-021-00270-x.

[84] B.G. Beitler, P.F. Abraham, A.R. Glennon, S.M. Tommasini, L.L. Lattanza, J.M. Morris, D.H. Wiznia, Interpretation of regulatory factors for 3D printing at hospitals and medical centers, or at the point of care, 3D Print Med 8 (2022) 7. https://doi.org/10.1186/s41205-022-00134-y.

[85] G. Biglino, C. Hopfner, J. Lindhardt, F. Moscato, J. Munuera, G. Oberoi, A. Tel, A.V. Esteve, Perspectives on medical 3D printing at the point-of-care from the new European 3D Printing Special Interest Group, 3D Print Med 9 (2023) 14. https://doi.org/10.1186/s41205-022-00167-3.

[86] L. Risse, G. Kullmer, Application of engineering methods in the planning process of surgical treatments, J 3D Print Med 5 (2021) 111–121. https://doi.org/10.2217/3dp-2020-0020.

[87] C.T. Wu, T.C. Lu, C.S. Chan, T.C. Lin, Patient-Specific Three-Dimensional Printing Guide for Single-Stage Skull Bone Tumor Surgery: Novel Software Workflow with Manufacturing of Prefabricated Jigs for Bone Resection and Reconstruction, World Neurosurg 147 (2021) e416–e427. https://doi.org/10.1016/j.wneu.2020.12.072.

[88] L. Frizziero, G.M. Santi, A. Liverani, V. Giuseppetti, G. Trisolino, E. Maredi, S. Stilli, Paediatric orthopaedic surgery with 3D printing: Improvements and cost reduction, Symmetry (Basel) 11 (2019) 1317. https://doi.org/10.3390/sym11101317.

[89] D. Ostaș, O. Almășan, R.R. Ileșan, V. Andrei, F.M. Thieringer, M. Hedeșiu, H. Rotar, Point-of-Care Virtual Surgical Planning and 3D Printing in Oral and Cranio-Maxillofacial Surgery: A Narrative Review, J Clin Med 11 (2022) 6625. https://doi.org/10.3390/jcm11226625.

[90] F. Osti, G.M. Santi, M. Neri, A. Liverani, L. Frizziero, S. Stilli, E. Maredi, P. Zarantonello, G. Gallone, S. Stallone, G. Trisolino, CT conversion workflow for intraoperative usage of bony models: From DICOM data to 3D printed models, Applied Sciences (Switzerland) 9 (2019) 708. https://doi.org/10.3390/app9040708.

[91] L. Frizziero, A. Liverani, G. Donnici, F. Osti, M. Neri, E. Maredi, G. Trisolino, S. Stilli, New methodology for diagnosis of orthopedic diseases through additive manufacturing models, Symmetry (Basel) 11 (2019) 542. https://doi.org/10.3390/sym11040542.

[92] M. Zhang, M. Lei, J. Zhang, H. Li, F. Lin, Y. Chen, J. Chen, M. Xiao, Feasibility study of three-dimensional printing knee model using the ultra-low-dose CT scan for preoperative planning and simulated surgery, Insights Imaging 13 (2022) 151. https://doi.org/10.1186/s13244-022-01291-8.

[93] S.M. Stieger-Vanegas, K.F. Scollan, Development of three-dimensional (3D) cardiac models from computed tomography angiography, Journal of Veterinary Cardiology 51 (2024) 195–206. https://doi.org/10.1016/j.jvc.2023.11.017.

[94] L.J. Lo, H.H. Lin, Applications of three-dimensional imaging techniques in craniomaxillofacial surgery: A literature review, Biomed J 46 (2023). https://doi.org/10.1016/J.BJ.2023.100615.

[95] G. Trisolino, A. Depaoli, G.C. Menozzi, L. Lerma, M. Di Gennaro, C. Quinto, L. Vivarelli, D. Dallari, G. Rocca, Virtual Surgical Planning and Patient-Specific Instruments for Correcting Lower Limb Deformities in Pediatric Patients: Preliminary Results from the In-Office 3D Printing Point of Care, J Pers Med 13 (2023) 1664. https://doi.org/10.3390/jpm13121664.

[96] G.C. Menozzi, A. Depaoli, M. Ramella, G. Alessandri, L. Frizziero, A. De Rosa, F. Soncini, V. Sassoli, G. Rocca, G. Trisolino, High-Temperature Polylactic Acid Proves Reliable and Safe for Manufacturing 3D-

Printed Patient-Specific Instruments in Pediatric Orthopedics—Results from over 80 Personalized Devices Employed in 47 Surgeries, Polymers (Basel) 16 (2024) 1216. https://doi.org/10.3390/polym16091216.

[97] G.C. Menozzi, A. Depaoli, M. Ramella, G. Alessandri, L. Frizziero, A. Liverani, G. Rocca, G. Trisolino, Side-to-Side Flipping Wedge Osteotomy: Virtual Surgical Planning Suggested an Innovative One-Stage Procedure for Aligning Both Knees in "Windswept Deformity," J Pers Med 13 (2023) 1538. https://doi.org/10.3390/jpm13111538.

[98] A. Depaoli, G.C. Menozzi, G.L. Di Gennaro, M. Ramella, G. Alessandri, L. Frizziero, A. Liverani, D. Martinelli, G. Rocca, G. Trisolino, The Flipping-Wedge Osteotomy: How 3D Virtual Surgical Planning (VSP) Suggested a Simple and Promising Type of Osteotomy in Pediatric Post-Traumatic Forearm Deformity, J Pers Med 13 (2023) 549. https://doi.org/10.3390/jpm13030549.

[99] G. Alessandri, L. Frizziero, G.M. Santi, A. Liverani, D. Dallari, L. Vivarelli, G.L. Di Gennaro, D. Antonioli, G.C. Menozzi, A. Depaoli, G. Rocca, G. Trisolino, Virtual Surgical Planning, 3D-Printing and Customized Bone Allograft for Acute Correction of Severe Genu Varum in Children, J Pers Med 12 (2022) 2051. https://doi.org/10.3390/jpm12122051.

[100] L. Frizziero, G. Trisolino, G.M. Santi, G. Alessandri, S. Agazzani, A. Liverani, G.C. Menozzi, G.L. Di Gennaro, G.M.G. Farella, A. Abbruzzese, P. Spinnato, L. Berti, M.G. Benedetti, Computer-Aided Surgical Simulation through Digital Dynamic 3D Skeletal Segments for Correcting Torsional Deformities of the Lower Limbs in Children with Cerebral Palsy, Applied Sciences (Switzerland) 12 (2022) 7918. https://doi.org/10.3390/app12157918.

[101] G. Alessandri, G.M. Santi, L. Frizziero, A. Liverani, 3D Printing Methods in Medicine: The Case of an Aortic Section, in: Lecture Notes in Mechanical Engineering, Springer Science and Business Media Deutschland GmbH, 2024: pp. 138–145. https://doi.org/10.1007/978-3-031-52075-4_17.

[102] G.M. Santi, G. Alessandri, L. Frizziero, A. Loforte, G. Folesani, L. Botta, D. Pacini, 3D Reconstruction and 3D Printing of Sections of the Aortic Arch, in: Proceedings of the International Conference on Industrial Engineering and Operations Management, IEOM Society International, Michigan, USA, 2022: pp. 1363–1369. https://doi.org/10.46254/EU05.20220271.

[103] A. De Rosa, G. Alessandri, E. Pignatelli, G.C. Menozzi, G. Trisolino, L. Frizziero, Exploring Virtual Reality Surgical Planning Applications in Paediatric Orthopaedics: A Preliminary Case Study, in: Lecture Notes in Computer Science (Including Subseries Lecture Notes in Artificial Intelligence and Lecture Notes in Bioinformatics), Springer Science and Business Media Deutschland GmbH, 2024: pp. 289–297. https://doi.org/10.1007/978-3-031-71704-8_23.